Expression, purification and biochemical analysis of Zea mays cytochrome b561 and its site-directed mutants

Md. Motiur Rahman

(Degree)
博士（理学）

(Date of Degree)
2008-09-25

(Date of Publication)
2009-09-30

(Resource Type)
doctoral thesis

(Report Number)
甲4440

(URL)
https://hdl.handle.net/20.500.14094/D1004440

Doctoral Dissertation

Expression, purification and biochemical analysis of *Zea mays* cytochrome b_{561} and its site-directed mutants

July, 2008

Graduate School of Science and Technology
Kobe University

Md. Motiur Rahman

Doctoral Dissertation

Expression, purification and biochemical analysis of *Zea mays* cytochrome b_{561} and its site-directed mutants

トウモロコシ cytochrome b_{561} とその部位特異的変異体の発現、精製と生化学的解析

July, 2008

Graduate School of Science and Technology

Kobe University

Md. Motiur Rahman

TABLE OF CONTENTS

ABBREVIATIONS

DBH	Dopamine β-hydroxylase
PAM	Peptidylglycine α-amidating monooxygenase
AsA	Ascorbic acid, ascorbate
MDA	Monodehydroascorbic acid, monodehydroascorbate
CGCytb	Chromaffin granule cytochrome b_{561}
NADH	Nicotinamide adenine dinucleotide
NADPH	Nicotinamide adenine dinucleotide phosphate
EPR	Electron paramagnetic resonance
HALS	Highly anisotropic low-spin
PM	Plasma membrane
BLAST	Basic local alignment search tool
PSI-BLAST	Position specific-iterated BLAST
TMD	Transmembrane domain
DoH	Dopamine β-hydroxylase homology
SDR2	Stromal cell-derived receptor 2
DCytb	Duodenal cytochrome b_{561}
LCytb	Lysosomal cytochrome b_{561}
TSCytb	Tumor suppressor cytochrome b_{561}
TCytb	Tonoplast cytochrome b_{561}
DEPC	Diethylpyrocarbonate
MALDI-TOF	Matrix assisted laser desorption/ionization-time of flight
SDS-PAGE	Sodium dodecyl sulphate-polyacrylamide gel electrophoresis
β-OG	n-octyl-β-D-glucoside
PVDF	Polyvinylidene difluoride
HRP	Horseradish peroxidase

AOX	Alcohol oxidase promoter
YNB	Yeast Nitrogen Base w/o amino acids
YPDS	Yeast Extract Peptone Dextrose medium with sorbitol
BMGY	Buffered complex medium containing glycerol
BMMY	Buffered complex medium containing methanol
EDTA	Ethylenediaminetetraacetic acid
PMSF	Phenylmethylsulfonyl fluoride
TMHs	Transmembrane α-helices
CHCA	α-Cyano-4-hydroxycinnamic acid
TFA	Trifluoroacetic acid

Chapter 1

Literature review on the studies of transmembrane electron transfer reaction catalyzed by cytochrome b_{561} and the aims of my study

1-1. History of cytochrome b_{561} study

Cytochrome b_{561} in chromaffin granule membrane: Cytochrome b_{561}, first discovered in chromaffin vesicles of bovine adrenal medulla (*1*) and, later, found to be distributed in many neuroendocrine tissues (*2-7*), is structurally and functionally very different from other cytochromes such as cytochromes b_5 and P-450 (*8*) and was proposed to be the most likely candidate for a transmembrane electron carrier in the neuroendocrine vesicles (*9*). A cytochrome b_{561} has also been spectrophotometrically identified in noradrenaline storage vesicles from bovine splenic nerves (*10*) and in the membranes of serotonin dense core vesicles in porcine platelets, which have an embryologically distinct origin from those of the adrenal catecholamine-synthesizing cells (*11*). Later, the cytochrome was purified in octaethylene glycol dodecylether by ammonium sulphate fractionation followed by aminohexyl-Sepharose hydrophobic column chromatography (*12*). This procedure yielded a single protein band with an apparent molecular weight of 22,000 on sodium dodecyl sulphate-polyacrylamide gel electrophoresis (SDS-PAGE). Its isoelectric point was estimated as 6.2 and was suggested to be identical to the major granule membrane component, chromomembrin B. Cytochrome b_{561} was also purified by preparative gel electrophoresis in the presence of Triton X-100 (*13*) and its molecular weight was determined to be 20,500 by sedimentation studies (*14*). Later, it was reported that cytochrome b_{561} could be reduced by ascorbic acid (AsA) very rapidly (*8, 15, 16*). The adrenal medulla is the central core of the adrenal gland, surrounded by the adrenal cortex. In higher animals, the chromaffin cells in the adrenal medulla are the body's main source of the catecholamine hormones (neurotransmitters) such as adrenaline and noradrenaline, which are stored in neurosecretory vesicles in sub-molar concentrations. In the neurosecretory vesicles,

biosynthesis of these neurotransmitters is performed by a group of enzymes containing a copper ion in each of the active center. Dopamine β-hydroxylase (DBH) catalyzes the hydroxylation of dopamine and tyramine to noradrenaline and octopamine, respectively, in the chromaffin vesicles of adrenal medulla. On the other hand, peptidylglycine α-amidating monooxygenase (PAM) enzyme converts the C-terminal carboxyl group of various neuropeptides and prohormones, such as vasopressin and oxytocin, to an amide group during processing in the neuroendocrine secretory vesicles. These enzymes require two electron equivalents for the reduction of the chelating copper and for the activation of a molecular dioxygen, and utilize ascorbic acid (AsA) as an electron donor of the reaction (*17-20*). In the neuroendocrine vesicles, AsA is present in millimolar concentrations but not enough concentrations for the enzymatic reactions. For example, the AsA concentration in chromaffin vesicles is about 22 mM (*21*), whereas the concentration of the product (norepinephrine and epinephrine) is 550 mM (*22*), meaning that the catecholamine / AsA ratio in chromaffin vesicles is about 25:1. Therefore, the intravesicular AsA must be re-generated and re-used many times. Upon the biological oxidation of AsA for supplying electron equivalents to the catalytic center of the enzyme inside the neuroendocrine secretory vesicles (*23*), AsA is converted to monodehydroascorbic acid (MDA) radical via monovalent oxidation rather than divalent oxidation to form dehydroascorbate. Furthermore, since there is no transmembrane transporter for AsA in the chromaffin vesicle membranes (*24*), it has been postulated that cytochrome b_{561} has an important role as a transmembrane electron carrier which conveys a reducing equivalent from the extravesicular AsA to the intravesicular MDA radical (*24-32*). The pH gradient across the chromaffin vesicles membrane generated by V-type proton motive ATPase might create a thermodynamic

force driving this transmembrane electron flow. This is because the midpoint reduction potential of AsA is pH dependent (*33*) being 90 mV higher in the intravesicular pH (5.5) than in the cytosolic pH (7.0). Since the midpoint potential of cytochrome b_{561} does not depend on pH (*34*), AsA should reduce the cytochrome more readily at higher pH. On the other hand, MDA radical should oxidize it more readily at lower pH (*34*). Later, an identical form of cytochrome b_{561} was found to be present as an integral component of both chromaffin vesicles from adrenal medulla and neurosecretory vesicles from posterior pituitary based on the spectrophotometric and immunological techniques (*35*). Thus, cytochrome b_{561} is very unique in the physiological functions, in the electron transfer mechanism, and in the tissue-specificity than any other cytochromes which have ever known. To reveal these characteristic natures in a molecular level, purification of cytochrome b_{561} protein might be absolutely required. Cytochrome b_{561} was purified from bovine adrenal medulla for the first time by Silsand and Flatmark (*13*). However, their procedure had some problems in the purity and the stability of the protein. Later, many other procedures had been introduced for the purification of this protein, using Triton X-100, Nonidet P-40, sodium cholate, and β-octyl glucoside as a solubilizing detergent (*12, 13, 35-40*). However, no one had ever succeeded to analyze the detailed properties of the cytochrome b_{561} in the highly purified state. Very recently, Tsubaki *et al.* have succeeded in establishing a new purification procedure of cytochrome b_{561} from bovine adrenal chromaffin vesicles, which included β-octyl glucoside as a detergent and ω-aminooctyl Sepharose 4B resin in the hydrophobic column chromatography step (*41*). The purity and stability of their sample was much more superior to those of previous ones.

Biochemical properties of bovine chromaffin granule cytochrome b_{561}:

Chromaffin granule cytochrome b_{561} (CGCytb) was identified 35 years ago for the first time in the bovine adrenal chromaffin granules (*42*). So far, CGCytb is still the best characterized member among the cytochrome b_{561} protein family. Although the X-ray crystal structure data are not available for any of the members of cytochromes b_{561}, their biochemical and biophysical properties have been studied to some extent using various techniques. Different from most of other *b*-type cytochromes, cytochromes b_{561} were readily and quickly reducible with AsA, but not with NADH or NADPH (*43, 44*). The purified cytochrome b_{561} in reduced form showed α, β, and Soret (or γ-peak) absorption maxima at 561, 530, and 427 nm, respectively (*44, 45*). The redox potential of cytochromes b_{561} was atypically high (between +120 mV and +160 mV) (*44, 46, 47*). Previously, some investigators suggested that cytochromes b_{561} contained only one heme group *per* protein molecule or that cytochrome b_{561} proteins form a dimer coordinated by three heme prosthetic groups (*48, 49*). However, redox titration and electron paramagnetic resonance (EPR) studies of the purified cytochromes b_{561} in our lab and other groups strongly supported the presence of two heme centers in a protein molecule, with slightly different redox potentials, and located on each side of the membranes (*41, 44, 45*). EPR spectra of the purified bovine cytochrome b_{561} in the oxidized state showed the presence of two distinct heme *b* centers, with a usual low-spin EPR signal (g_z=3.14) and a highly anisotropic low-spin EPR signal (g_z=3.70) (*41*). Recent EPR spectra of the purified *Zea mays* cytochrome b_{561} in the oxidized state showed the presence of two heme centers with distinct EPR signals (g_z=3.69 and g_z=3.21) (*50*). On the other hand, Burbaev *et al.* (*51*) reported that the intact chromaffin vesicle membranes from bovine adrenal medulla showed three different EPR signals

derived from the ferric form of cytochrome b_{561}. A typical g_z signal from the low-spin cytochrome b_{561} observed at g～3 actually comprised of a high potential component with g_z=3.14 and a low potential one with g_z=3.11. In addition, a highly temperature sensitive low-spin heme signal at g_z=3.7 was observed. The g_z values of the usual low-spin signals were very similar to those of microsomal cytochrome b_5 (g_z=3.05, g_y=2.22, and g_x=1.41) (*52*), chloroplast cytochrome b_{559} (g_z=2.94, g_y=2.27, and g_x=1.54) (*53*), and the cytochrome *b* component of *bo*-type ubiquinol oxidase (g_z=2.98, g_y=2.26, and g_x=1.45) (*54*), all of which are known to have bisimidazole ligands. The other EPR species showed a HALS-type (a highly anisotropic low–spin) signal (g_z=3.70), having a lower redox potential than the other, and a temperature-sensitive character. These properties were very similar to cytochromes *b* (b_{566}, g_z=3.75; b_{562}, g_z=3.45) of the mitochondrial complex III (*55, 56*) and chloroplast cytochrome b_6 (b_{563}, g_z= 3.5) (*57*). Presence of two independent heme *b* centers in cytochrome b_{561} was supported by the observation of two potentiometrically different forms (midpoint potentials, +170 mV and +70 mV, respectively) of cytochrome b_{561} determined by an optical potentiometric technique (*34*). It had not been understood for a long time why the *b*-type heme center with identical bis-imidazole coordination structure could produce two distinct g_z signals. But this question was solved later by the X-ray crystal structure of bovine mitochondrial complex III determined by Iwata *et al.* in1998 (*58*). In 2005, Takeuchi *et al.* reported that when either of two Cys residues near the intravesicular heme center of bovine cytochrome b_{561} was modified with 4,4'-dithiopyridine, only the usual low-spin signal with g_z=3.14 was affected in the EPR spectra (*59*). Thus, the two g_z signals (g_z=3.69 and g_z=3.14) were assignable to the cytosolic heme and the intravesicular heme, respectively. Moreover, in 1998, Kobayashi *et al.* succeeded in observing the fast electron transfer

reaction from intravesicular ferrous heme of bovine cytochrome b_{561} to MDA radical, in millisecond order just after the generation of MDA radical in the AsA solution by using a pulse radiolysis technique (*60*). Following the electron donation to MDA radical, the electron acceptance reaction of the oxidized heme from AsA was observed in a slower time domain. When the MDA radical concentration dependency was examined, only one equivalent of electron residing in the fully reduced heme centers of cytochrome b_{561} was used for the rapid reduction with MDA radical (*60*). Thus, it was speculated that three steps of electron transfer reactions occurring in bovine cytochrome b_{561}: (1) cytosolic AsA to the cytosolic heme center, (2) from the cytosolic heme center to the intravesicular heme center, (3) from the intravesicular heme center to intravesicular MDA radical. Recently it was observed that heterologously expressed *Zea mays* cytochrome b_{561} had an efficient electron donating ability to MDA radical (Nakanishi *et al.* unpublished) as found for bovine cytochrome b_{561}. Srivastava *et al.* (*9*) reconstituted the purified cytochrome b_{561} into phospholipid vesicles for the first time and reported that these AsA-loaded vesicles would reduce external cytochrome *c*. Surprisingly, however, the turnover number measured for cytochrome b_{561} in the reconstituted system is approximately 100 times greater than that observed in the native membranes (*61*). In 2003, Seike *et al.* succeeded in the reconstitution of purified bovine cytochrome b_{561} into AsA-loaded proteoliposomes but in a reverse orientation (*62*). Further, they showed that cytochrome b_{561} in AsA-loaded vesicle membranes could supply electron equivalents to support the extravesicular DBH activity without the addition of any mediators, but that this activity was enhanced significantly by the addition of ferricyanide (*62*).

Stopped-flow analysis of bovine cytochrome b_{561}: The reaction kinetics

between cytochrome b_{561} and AsA or MDA radical has been studied in some details using chromaffin vesicles (*63*) and their ghosts (*36-38, 42, 64, 65*). It was reported that the reduction of oxidized cytochrome b_{561} in chromaffin vesicles by external AsA exhibited the Michaelis-Menten kinetics with the apparent K_m of around 300 μM (*42, 63*) or 4 mM (*65*). However, no detailed study had been reported for the reaction of AsA with purified cytochrome b_{561}, except for our pulse radiolysis studies (*60*). In 2003, Takigami *et al.* reported the stopped-flow analysis of bovine cytochrome b_{561} in the detergent solubilized state for the first time (*66*). The time course of the reduction of oxidized cytochrome b_{561} with AsA could not be fitted with a single exponential function but with a linear combination of at least four single exponential equations (*66*). This result indicated that the two hemes *b* prosthetic groups in cytochrome b_{561} must be involved in the different electron transfer reactions with AsA and MDA radical, respectively. The fastest phase of the four components in the reduction process was assigned to the electron donation from AsA to heme *b* on the extravesicular side of bovine cytochrome b_{561}. The apparent K_s=2.2 mM for AsA at pH 6.0 was obtained from the transient phase kinetics analysis of the fastest phase, which might adopt a two-step bi-uni sequential ordered mechanism (*66*). In addition, in an acidic pH ($<$5.5), a clear time-lag in the electron transfer from AsA to the oxidized heme center was observed. This result might indicate that a key amino acid residue(s) with pK_a around 5-6 might be present at the substrate binding site to interact with a bound AsA molecule. Very recently, stopped-flow analyses for the site-directed mutants of *Zea mays* cytochrome b_{561} was conducted and confirmed the importance of the conserved Lys^{83} residue. In the analysis, both K83D and K83E mutants showed a significant decrease in the electron accepting rate from AsA, although their final heme reduction levels were almost the

same with that of the wild-type protein (Nakanishi *et al.,* unpublished data).

Inhibition of the electron transfer reaction from AsA by DEPC: Njus and Kelly reported previously that the treatment of cytochrome b_{561} in intact chromaffin vesicles with dietylpyrocarbonate (DEPC), a histidyl imidazole group-specific reagent, inhibited its reduction by external AsA and this inhibition was reversed by addition of hydroxylamine (*67*). On the basis of their observation, they proposed that a His residue is involved in the reaction between AsA and cytochrome b_{561}. Later, Tsubaki *et al.* (*68*) found that the electron accepting ability of the purified bovine cytochrome b_{561} from AsA was selectively inhibited by the treatment with DEPC (*69*). However the electron donating activity from reduced heme *b* center to MDA radical was retained after the treatment. MALDI-TOF mass analyses revealed that two fully conserved His residues (His^{88} and His^{161}, the heme axial ligands on the cytosolic side) and one well-conserved Lys residue (Lys^{83}) were the major modification sites (*68*). Further, they found that the electron accepting ability from AsA could be protected by the presence of AsA during the DEPC-treatment, suggesting the presence of an AsA-binding site on the cytosolic side (*70*). Since DEPC attacks the deprotonated nitrogen atom of an imidazole group (*69*), it is postulated that the non-coordinated nitrogen atom of the coordinating imidazole group of the cytosolic heme center might be specifically *N*-carbethoxylated. This specific *N*-carbethoxylation might be directly coupled to the inhibition of electron acceptance of the cytosolic heme center from AsA.

Cytochrome b_{561} residing in plant plasma membranes: Presence of *b*-type cytochromes in higher plant PM (plasma membrane) was first reported by Brain *et al.* (*71*) and Jesaitis *et al.* (*72*). After the discovery of the presence of *b*-type cytochromes in the PM of higher plants, characterization studies were performed to obtain a more

detailed description and identification of the cytochrome species. AsA-reducible cytochromes with a wavelength maximum near 561 nm and a typical high redox potential (E_0' around +140 mV) were found to be ubiquitous in PM preparations from different plant species and tissues (*47, 73*). This cytochrome, named as cytochrome b_{561} from the wavelength maximum of its α-band, was purified to homogeneity from plasma membranes isolated from bean hypocotyls and was shown to be a heme-containing glycoprotein with a molecular mass of approximately 55 kDa (*74*). The involvement of a *b*-type cytochrome, analogous to the one described above, in the transmembrane electron transport in the PM vesicles has been documented (*75*). AsA could reduce cytochrome b_{561} on the cytosolic side of the membranes while MDA could oxidize it on the apoplastic side. Thus, PM cytochrome b_{561} was proposed to constitute a simple transmembrane electron transfer system to regenerate extracellular AsA in plants (*76*). In agreement with this electron-transfer activity, redox titrations of PM cytochrome b_{561} indicated the presence of two distinct heme centers *per* polypeptide (*74*).

Recently, a new method using two anion exchange chromatographic steps (Mono-Q columns) was successfully employed for the partial purification of an AsA-reducible *b*-type cytochrome from etiolated beans hypocotyls PM (*74, 77, 78*). After a single freeze-thaw cycle and consecutive ultracentrifugation of the phase-partition-purified PM vesicles, solubilization of the PM proteins was conducted with 1% (v/v) Triton X-100R (2 mg per mg protein) as a solubilizing detergent. However, the physiological functions of the partially purified protein from plants still remained unknown. A number of properties of the cytochrome b_{561} in plasma membranes raised a particular interest of many investigators. First, PM-cytochromes b_{561} from various plant species tested so far showed very similar standard redox

potentials (E_0') each other. Second, the plant PM-cytochrome b_{561} could transfer electrons from a cytoplasmic electron donor to an extracellular electron acceptor. Third, the PM-cytochrome b_{561} showed some homology to a mammalian protein present in the chromaffin granule membranes with similar E_0', α-band maxima, and the electron transport characteristics. All these results seemed to indicate that these proteins constitute a new protein family within the class of *b*-type cytochromes and are present at least in the kingdoms of plants and animals (*79*).

Cytochrome b_{561} family proteins: The cDNA cloning of cytochrome b_{561} from bovine adrenal medulla was succeeded and sequenced in 1984 (*40*). Later, BLAST (basic local alignment search tool) and PSI-BLAST (position specific iterated BLAST) were conducted to obtain better insights on the structure and function of cytochrome b_{561} family proteins (*80-82*). In the meantime, cytochromes b_{561} were identified in a large number of eukaryotes, but were absent in prokaryotes. A group of different forms of membrane bound *b*-type diheme cytochromes, named as cytochrome b_{561}, were also found in bacteria (*83, 84*). However, these proteins did not share the sequence homology with the authentic "cytochrome b_{561} family", which is the subject of my Ph.D. dissertation, and were expected to have a completely different architecture in the coordination of two heme prosthetic groups.

Most eukaryotic species contain multiple forms of cytochrome b_{561}. For example, six homologues in human, seven in mouse, six in *C. elegans,* and 16 in plant, *A. thaliana.* All members share well-conserved features (Fig. 1-1). Namely, all sequences contain six putative transmembrane domains (TMDs), with TMD 2-5 being more conserved and being known as the "core cyt b561 domain". All have four completely-conserved His residues (His^{54}, His^{88}, His^{122}, and His^{161}, based on the

numbering of bovine cytochrome b_{561}) within the core TMD 2-5. The first and third His residues in the TMD2 and TMD4, respectively, were suggested to coordinate one heme on the electron-donating side of the protein (Fig. 1-2). The second and fourth His residues in the TMD3 and TMD5, respectively, were suggested to coordinate the second heme on the electron-accepting side of the protein. In addition, there were two well-conserved motifs "SLHSW" and "ALLVYRVF", being suggested to have roles for the bindings to MDA radical and AsA, respectively, on either side of the protein (*85*). However, these predictions await conclusive experimental proof. The two conserved motifs showed some variations in the sub-families of cytochrome b_{561} (Fig. 1-1), indicating the possible functional diversity of the b_{561} proteins (*81*).

Several other forms of mammalian cytochromes b_{561} were identified; namely one located in the duodenal brush-border membrane, duodenal cytochrome b_{561} (DCytb) (*86*) and one located in macrophage lysosomes, lysosomal cytochrome b_{561} (LCytb) (*87*). DCytb was also found in human erythrocyte membranes where it may function as a MDA radical reductase (*88*). All three mammalian cytochromes b_{561}, DCytb, CGCytb, and LCytb, showed AsA-dependent *trans*-membrane ferrireductase activity when expressed in yeast cells (*89*). A one form of plant cytochrome b_{561} was recently reported as a constituent of the tonoplast membrane with a *trans*-membrane ferrireductase activity (*90*). The observation that cytochromes b_{561} may be involved in the iron metabolism has opened new perspectives for their physiological functions. Another interesting member of the cytochrome b_{561} family is TSCytb (tumor suppressor cytochrome b_{561}) encoded by the human gene *101F6*, which has been identified as a candidate tumor suppressor factor since this gene was found to be located in the frequently-deleted region (found in lung and breast cancers) of human chromosome

3p21.3 (*91, 92*). Indeed, forced over-expression of wild-type *101F6* protein in human lung cancer cell lines significantly inhibited tumor cell growth by induction of apoptosis and alteration of cell cycle processes. However, the molecular mechanism underlying these effects is still unclear (*93*). In several plant and animal species, a new form of cytochrome b_{561} has been identified. These forms contained the "cytochrome b561-like core domain" in connection with other unrelated domains. These 'fusion proteins' frequently contain the dopamine β-hydroylase homology (DoH) domain as well (*94*). One such example is SDR2 (stromal cell-derived receptor 2) protein in mammals, which had been shown to have a ferric reductase activity when expressed in *Xenopus oocytes* (*95*).

Cytochromes b_{561} are widespread in plants as well and, further, there are multiple homologues being expressed in many of plant species (*81, 83*). The plant cytochrome b_{561} sequences all contain the conserved features described above for animal species. The physiological roles of plant cytochrome b_{561}, which might be apparently different from those of animal cytochrome b_{561}, since plants have no neuroendocrine vesicles, has become a one of the most important aims to be clarified in my study. Genome analysis showed that there are sixteen putative cytochrome b_{561} isoforms in *A. thaliana*; one of which has already been over-expressed in yeast (*Saccharomyces serevisiae*) cells and the recombinant protein has been characterized to some extent (*43*). One form of *A. thaliana* cytochrome b_{561} protein (TCytb) was found to be localized in the tonoplast membranes, which was found to be AsA-reduicible having absorbance characteristics similar to those of chromaffin granule cytochrome b_{561}. Indication for the presence of cytochrome b_{561} in plant tonoplast membranes was also obtained by examining the AsA-reducible *b*-type cytochromes in the

tonoplast-enriched bean membrane fractions (*43*). Recently, one form of cytochrome b_{561} from maize, *Zea mays*, was successfully over-expressed in yeast cells *Pichia pastoris* in our group. Biochemical and biophysical analyses of the purified sample showed that the heterologously expressed protein was in a fully-functional form (Nakanishi *et al.* unpublished).

Due to the high abundance of a single form of cytochrome b_{561} in the chromaffin granules membrane and relative easiness of its purification, CGCytb has been well-characterized. However, other forms of cytochrome b_{561}, particularly plant cytochromes b_{561}, are much less abundant and, in most cases, their tissue and subcellular localization is still not well understood. Therefore, to conduct the studies on their biochemical properties in more details, generation of a recombinant form of plant cytochrome b_{561} and its efficient purification might be highly desired.

Possible roles and locations of plant cytochromes b_{561}: There are two proposals being raised as the possible locations of plant cytochromes b_{561}; either in the cell membrane (or plasma membranes) or in the vacuole membranes (tonoplast membranes). In both cases, cytochrome b_{561} catalyzes transmembrane electron transfer reaction and is likely to use cytosolic ascorbate (AsA) as a source of the electron equivalents (*67, 80*).

The cell membranes are found in all cells and contain a wide variety of biological molecules, primarily proteins and lipids, which are involved in a vast array of cellular processes such as cell adhesion, ion channel conductance, cell signaling, and most importantly transport of various nutrients including iron. One likely role of plant cytochrome b_{561} is participation in the transport of iron into the cytosolic side in collaboration with a ferrous ion transporter residing in the cell membranes. In this case,

cytochromes b_{561} are postulated to work as a ferrireductase and are located in the cell membranes (*90*). One such example was shown previously for Dcytb in higher animals. In this case, electron equivalent from cytosolic AsA might be used to reduce the extracellular ferric ion, after the transmembrane electron transfer. The other possibility is such electron equivalents might be used for the regeneration of AsA from MDA radical. Such regeneration of AsA might be essential for some enzymatic reactions being present outside of the cell membranes, in which AsA is employed as the electron donating substrates.

Most mature plant cells have one or several vacuoles that typically occupy more than 30% of the total cell volume, and that can occupy as much as 90% of the volume for certain cell types and conditions (*96*). Each vacuole is surrounded by a membrane called as "tonoplast". Vacuoles house large amounts of a liquid called cell sap, composed of water, various enzymes, inorganic ions (like K^+ and Cl^-), salts (such as Ca^{2+}), and other substances, including toxic byproducts removed from the cytosol to avoid interference with metabolism (*97-99*). Transport of protons (H^+) from cytosol to vacuole aids in keeping cytoplasmic pH stable, while making the vacuolar interior more acidic, allowing various degradative enzymes inside to act properly. Although having a large central vacuole is the most common case, the size and number of vacuoles may vary in different tissues and stages of development.

One important role of plant vacuole is the storage of various metal ions, particularly, iron and copper, which might be very toxic if excess amounts of these ions reside in cytosolic fraction causing an oxidative damage to various cytosolic enzymes and molecules by forming the reactive oxygen species (ROS). Once stored in the vacuoles, however, the ferrous iron could be easily oxidized in the acidic condition.

Therefore, when such iron was required in the cytosol fraction or in other cell organelle, the ferric iron must be reduced back and be transported into cytosol via ferrous ion transporter(s) residing in the vacuole membranes. Accordingly, cytochrome b_{561} residing in the tonoplast membranes has such a role as a transmembrane ferric reductase, again, utilizing cytosolic AsA as a source of electron equivalents.

***Possible membrane topology of cytochrome b_{561}*:** Most membrane proteins follow a predictable topological organization pattern and, therefore, cytochrome b_{561} is also likely to follow this rule. Since cytochrome b_{561} has six consecutive hydrophobic α-helices with intervening short hydrophilic loops, it might be expected that anti-parallel transmembrane α-helices (TMHs) would be buried within the membranes and hydrophilic loops alternate between a cytoplasmic and extracytoplasmic location. Since there was strong evidence that the NH_2-terminus of bovine cytochrome b_{561} was located on the cytoplasmic side, the COOH-terminus should be also facing cytoplasmic side, as noted above. The topology of our six-transmembrane helices models for both bovine (Fig. 1-2) and *Zea may* cytochromes b_{561} is based on these considerations. If the cytochromes were located on the plasma membranes, "extracytoplasmic" means the out side of the cell; whereas if the cytochromes were residing in the vacuole membranes, it means the intravesicular side. Thus, the extracytoplasmic side and the intravesicular side are topologically identical and, therefore, the direction of the electron transfer in both membranes will be topologically identical employing cytosolic AsA as the source of electron equivalents.

Possible signal and sorting sequences of cytochrome b_{561}: Majority of the membrane proteins with a multipass transmembrane structure on organelles of the secretory pathway are synthesized on membrane-bound ribosomes and are

co-translationally integrated into the endoplasmic reticulum (ER) membrane, where they acquire unique topology (*100*). The code to the final topology of a membrane protein is concealed within its amino acid sequence and is deciphered during the insertion of the polypeptide chain into the membranes. There are many properties of the nascent polypeptide chain that contribute to establishing the topology (*101, 102*). The most prominent topological signals within the membrane polypeptides are the NH_2-terminal segments of ~20 amino acids with an overall hydrophobic character (the "signal sequence" or the "signal peptide"). The hydrophobic region of a signal sequence emerging from the free ribosome is recognized by a signal recognition particle (SRP), and then the ribosome-nascent chain complex is targeted onto the ER membrane. Upon binding to the SRP receptor on the ER membranes, SRP releases the signal sequence and the translation continued on the membrane bound ribosome (*103*). When the nascent polypeptide chain is fed into the translocon in the ER membranes, the hydrophobic segments form α -helical structure (TMHs) and are folded into the membranes laterally, while the hydrophilic parts remain in the cytoplasm or are translocated to the other side of the membranes. At this critical occasion, the topogenic process is determined mainly by the hydrophobic segments and the so-called topogenic sequences. The signal sequence and the type II signal anchor sequence initiate the translocation of the following C-terminal side, while the type I signal anchor sequence translocates the preceding N-terminal side (*104,105*). The translocation that is initiated by the signal sequence or the type II signal-anchor sequence is stopped by the following hydrophobic segment, the so-called stop-transfer sequence. Thus, the topogenic properties of the transmembrane segment should directly correlate with the final topology of each membrane protein (*106,107*).

Such signal sequences are not so relevant, however, in the amino acid sequences of cytochromes b_{561}. Therefore, it might be expected that the first transmembrane helix of the cytochrome is likely to serve as a start-transfer sequence. Since there are more positive-charged amino acid residues immediately preceding the hydrophobic core in most of the cytochrome b_{561} sequence, the NH_2-terminal sequence remained on the cytosolic side. Until the subsequent stop-transfer sequence to be recognized by the translocon apparatus, the translocation continues. In this way, six transmembrane helices might function in alteration as start-transfer and stop-transfer sequences and finally the COOH-terminal sequence remained on the cytosolic side. After the integration into the ER membranes, plant cytochrome b_{561} molecules must be transported to their destination, either to the plasma membrane or to the vacuole membranes, by the vesicular transport mechanism. For the transport of the cargo proteins to the target organelle to be occurred, each transmembrane protein should have a sorting signal(s) within the cytosolic domains of the molecules. Such sorting signals specific to plant vacuoles are named as “vacuolar sorting determinant” (VSD), and are categorized as ssVSD (sequence-specific VSD) and ctVSD (COOH-terminal VSD) (*108*). The former has NPIRL consensus sequence, whereas the latter has no consensus sequence but constituting with a rather hydrophobic amino acid residues. However, again, in the sequences of various plant cytochrome b_{561}, neither of them was identified yet. Although the elucidation of molecular mechanisms for cellular transport of transmembrane protein including cytochrome b_{561} by the unidentified signal sequence or sorting signals might be a very attractive target, it was not pursued in my Ph.D. study and is waiting for a clarification by future studies.

1-2. Aims of the study

Aims of my Ph. D. study: The aim of my study was elucidation of the AsA-specific transmembrane electron transfer mechanism catalyzed by cytochrome b_{561} in a molecular level. The purification of plant cytochromes b_{561}, however, had been a very difficult task in the past. Indeed, there has been scarce information regarding the nature of plant cytochromes b_{561}. Recently, however, our group has succeeded in the construction of the heterologous expression system for *Zea mays* cytochrome b_{561}. Fusion proteins by adding an affinity tag (6xHis-tag) moiety to the recombinant proteins are frequently formed and are expressed in order to simplify the purification steps. Affinity chromatography is a powerful purification method where usually only one-step might be enough to obtain the expressed protein in the purified state in high homogeneity. Following this molecular biological strategy, we modified the *Zea mays* cytochrome b_{561} cDNA with a 6xHis-tag sequence at the position corresponding to the C-terminal end of the *Zea mays* cytochrome b_{561} protein. The 6xHis-tag moiety can be used as target for the Ni-NTA agarose chromatography. Elucidation of the physiological role of plant cytochrome b_{561}, which might be distinctly different from those of animal cytochrome b_{561}, was the target to be clarified during my Ph.D. study. Further, clarification of the underlying electron transfer mechanism from the putative substrate, AsA, to the heme center was another target of my Ph.D. study. For these purpose, I employed the site-directed mutagenesis study for the recombinant *Zea mays* cytochrome b_{561} protein.

Organization of thesis: The introductory chapter, Chapter 1, provides the necessary background for conducting the research on cytochromes b_{561}, particularly from animals and plants species.

We have succeeded in the purification of heterologously expressed 6x His-tagged *Zea mays* cytochrome b_{561} in *Pichia pastoris* cells. In Chapter 2, I described the development and optimization of the expression systems for the recombinant *Zea mays* cytochrome b_{561} in *Pichia pastoris* yeast cells. Then, I also described the procedures for the purification of the 6xHis-tagged recombinant protein. Surprisingly, presence of the 6xHis-tag moiety at the COOH-terminus of the protein influenced significantly on its expression levels. Purification of the *Zea mays* cytochrome b_{561} from our expression system yielded a protein sample with very similar physico-chemical properties to those of yeast recombinant CGCytb and bovine CGCytb in the detergent-solubilized state. Therefore, our new system offers a great improvement in the yield and other advantages over existing insect and yeast cell systems for the production the recombinant cytochrome b_{561} for the detailed studies on their structure and functions.

We also have performed extensive site-directed mutagenesis studies on *Zea mays* cytochrome b_{561} to clarify the underlying molecular mechanism of the AsA-specific electron transfer reaction in cytochrome b_{561}. In Chapter 3, I described a part of such results obtained from the site-directed mutagenesis study. In my Ph. D. study, I have conducted a mutagenesis study with a particular interest on the two conserved amino acid residues (Arg^{72} and Tyr^{71}) residing in the putative AsA-binding sequence. Changing the positive charge at the Arg^{72} residue to a neutral or a negative one did not affect significantly on the final heme reduction level when AsA was used as a reductant. However, characteristic pH-dependent initial time-lag upon the electron acceptance from AsA in an acidic pH region was almost completely lost for R72A and R72E mutants. In the case of Tyr^{71} mutants (Y71A and Y71F), we did not observe any

significant influences on the final heme reduction level with AsA as a reductant. However, the mutations at Tyr^{71} residue did affect significantly on the characteristic pH-dependent initial time-lag.

In Chapter 4, I conclude the results of my Ph.D. study with a short summary of my research efforts and several suggestions for the future works in the field of cytochrome b_{561} study.

1-3. References

1. Spiro, M. J., and Ball, E. G. (1961) Studies on respiratory enzymes of the adrenal gland. I. The medulla, *J. Biol. Chem.* **256**, 225-230.
2. Hortnagl, H., Winkler, H., and Lochs, H. (1973) Immunological studies on a membrane protein (chromomembrin B) of catecholamine-storing vesicles, *J. Neurochem*. **20**, 977-985.
3. Hagn, C., Klein, R. L., Fischer-Colbrie, R., Douglas, B. H., and Winkler, H. (1986) An immunological characterization of five common antigens of chromaffin granules and of large dense-cored vesicles of sympathetic nerve, *Neurosci. Lett*. **67**, 295-300.
4. Pruss, R. M., and Shepard, E. A. (1987) Cytochrome b_{561} can be detected in many neuroendocrine tissues using a specific monoclonal antibody, *Neuroscience*. **22**, 149-157.
5. Weiler, R., Cidon, S., Gershon, M. D., Tamir, H., Hogue-angeletti, R., and Winkler, H. (1989) Adrenal chromaffin granules and secretory granules from thyroid parafollicular cells have several common antigens, *FEBS Lett*. **257**, 457-459.
6. Mackin, R. B., Jones, D. P., and Noe, B. D., (1986) Islet secretory granules contain cytochrome b_{561}, *Diabetes*. **35**, 881-885.
7. Fried, G. (1978) Cytochrome *b*-561 in sympathetic nerve terminal vesicles from rat vas deferens, *Biochim. Biophys. Acta*. **507**, 175-177.
8. Ichikawa, Y., and Yamano, T. (1965) Cytochrome 559 in the microsomes of the adrenal medulla, *Biochem. Biophys. Res. Commun*. **20**, 263-268.
9. Srivastava, M., Duong, L. T., and Fleming, P. J. (1984) Cytochrome b_{561} catalyzes transmembrane electron transfer, *J. Biol. Chem*. **259**, 8072-8075.
10. Flatmark, T., Lagercrantz, H., Terland, O., Helle, K. B., and Stjarne, L. (1971)

Electron carriers of the noradrenaline storage vesicles from bovine splenic nerves, *Biochim. Biophys. Acta*. **245**, 249-252.

11. Johnson, R. G., and Scarpa, A. (1981) The electron transport chain of serotonin-dense granules of platelets, *J. Biol. Chem*. **256**, 11966-11969.
12. Apps, D. K., Pryde, J. G., and Phillips, J. H. (1980) Cytochrome b_{561} is identical with chromomembrin B, a major polypeptide of chromaffin granule membranes, *Neuroscience*. **5**, 2279-2287.
13. Silsand, T., and Flatmark, T. (1974) Purification of cytochrome *b*-561. An integral heme protein of the adrenal chromaffin granule membrane, *Biochim. Biophys. Acta*. **359**, 257-266.
14. Flatmark, T., and Gronberg, M. (1981) Cytochrome *b*-561 of the bovine adrenal chromaffin granules. Molecular weight and hydrodynamic properties in micellar solutions of triton X-100, *Biochem. Biophys. Res. Commun*. **99**, 292-301.
15. Hollenbeck, R. A., Giachetti, A., and Peterson, J. A. (1975) Studies on cytochrome b_{561} in amine storage granules, *Biochem. Pharmacol*. **24**, 1049-1051.
16. Terland, O., and Flatmark, T. (1988) Oxidoreductage activities of chromaffin granule ghosts isolated from the bovine adrenal medulla, *Biochim. Biophys. Acta*. **597**, 318-330.
17. Levin, E. Y., Levenberg, B., and Kaufman, S. (1960) The enzymatic conversion of 3, 4-dihydroxyphenylethylamine to norepinephrine, *J. Biol. Chem*. **235**, 2080-2086.
18. Levin, E. Y., and Kaufman, S. (1961) Studies on the enzyme catalyzing the conversion of 3, 4-dihydroxyphenylethylamine to norepinephrine, *J. Biol. Chem*. **236**, 2043-2049.
19. Bradbury, A. F., Finnie, M. D. A., and Smyth, D. G. (1982) Mechanism of

C-terminal amide formation by pituitary enzymes, *Nature*, **298**, 686-688.

20. Eipper, B. A., Mains, R. E., and Glembotski, C. C. (1980) Identification in pituitary tissue of a peptide alpha-amidation activity that acts on glycine-extended peptides and requires molecular oxygen, copper, and ascorbic acid, *Proc. Natl. Acad. Sci. U. S. A.* **80**, 5144-5148.
21. Ingebretsen, O. C., Terland, O., and Flatmark, T. (1980) Subcellular distribution of ascorbate in bovine adrenal medulla. Evidence for accumulation in chromaffin granules against a concentration gradient, *Biochim. Biophys. Acta*. **628**, 182-189.
22. Phillips, J. H. (1982) Dynamic aspects of chromaffin granule structure, *Neuroscience*. **7**, 1595-1609.
23. Stewart, L. C., and Klinman, J. P. (1998) Dopamine β–hydroxylase of adrenal chromaffin granules: structure and function, *Annu. Rev. Biochem*. **57**, 551-592.
24. Beers, M. F., Johnson, R. G., and Scarpa, A. (1986) Evidence for an ascorbate shuttle for the transfer of reducing equivalents across chromaffin granule membranes, *J. Biol. Chem*. **261**, 2529-2535.
25. Njus, D., Knoth, J., Cook, C., and Kelly, P. M. (1983) Electron transfer across the chromaffin granule membrane, *J. Biol. Chem*. **258**, 27-30.
26. Diliberto, E. J., Jr, Heckman, G. D., and Daniels, A. J. (1983) Characterization of ascorbic acid transport by adrenomedullary chromaffin cells. Evidence for Na^+–dependent co-transport, *J. Biol. Chem*. **258**, 12886-12894.
27. Levine, M., Morita, K., and Pollard, H. (1985) Enhancement of norepinephrine biosynthesis by ascorbic acid in cultured bovine chromaffin cells, *J. Biol. Chem*. **260**, 12942-12947.
28. Russell, J. T., Levine, M., and Njus, D. (1985) Electron transfer across posterior

pituitary neurosecretory vesicle membranes, *J. Biol. Chem*. **260**, 226-231.

29. Njus, D., Kelley, P. M., and Harnadek, G. J. (1986) Bioenergetics of secretory vesicles, *Biochim. Biophys. Acta*. **853**, 237-265.
30. Menniti, F. S., Knoth, J., Diliberto, E. J., and Jr, Heckman, G. D. (1986) Role of ascorbic acid in dopamine beta-hydroxylation. The endogenous enzyme cofactor and putative electron donor for cofactor regeneration, *J. Biol. Chem*. **261**, 16901-16908.
31. Wakefield, L. M., Cass, A. E. G., and Radda, G. K. (1986a) Functional coupling between enzymes of the chromaffin granule membrane, *J. Biol. Chem*. **261**, 9739-9745.
32. Wakefield, L. M., Cass, A. E. G., and Radda, G. K. (1986b) Electron transfer across the cromaffin granule membrane. Use of EPR to demonstrate reduction of intravesicular ascorbate radical by the extravesicular mitochondrial NADH: ascorbate radical oxidoreductase, *J. Biol. Chem*. **261**, 9746-9752.
33. Iyanagi, T., Yamazaki, I., and Anan, K. F. (1984) One-electron oxidation-reduction properties of ascorbic acid, *Biochim. Biophys. Acta*. **806**, 255-261.
34. Apps, D. K., Boisclair, M. D., Gavine, F. S., and Pettigrew, G., W. (1984) Unusual redox behaviour of cytochrome *b*-561 from bovine chromaffin granule membranes, *Biochim. Biophys. Acta*. **764**, 8-16.
35. Duong, L. T., Fleming, P. J., and Russell, J. T. (1984) An identical cytochrome b_{561} is present in bovine adrenal chromaffin vesicles and posterior pituitary neurosecretory vesicles, *J. Biol. Chem*. **259**, 4885-4889.
36. Kelley, P. M., and Njus D. (1988) A kinetic analysis of electron transport across chromaffin vesicle membranes, *J. Biol. Chem*. **263**, 3799-3804.
37. Kelley, P.M., Jalukar, V., and Njus, D. (1990) Rate of electron transfer between

cytochrome b_{561} and extravesicular ascorbic acid, *J. Biol. Chem*. **265**, 19409-19413.

38. Jalukar, V., Kelley, P. M., and Njus, D. (1991) Reaction of ascorbic acid with cytochrome b_{561} concerted electron and proton transfer, *J. Biol. Chem*. **266**, 6878-6882.
39. Duong, L. T., and Fleming, P. J. (1982) Isolation and properties of cytochrome b_{561} from bovine adrenal chromaffin granules, *J. Biol. Chem*. **257**, 8561-8564.
40. Wakefield, L. M., Cass, A. E. G., and Radda, G. K. (1984) Isolation of a membrane protein by chromatofocusing: cytochrome *b*-561 of the adrenal chromaffin granule, *J. Biochem. Biophys. Methods*. **9**, 331-341.
41. Tsubaki, M., Nakayama,M., Okuyama, E., Ichikawa, Y., and Hori, H. (1997) Existence of two heme *b* centers in cytochrome b_{561} from bovine adrenal chromaffin vesicles as revealed by a new purification procedure and EPR spectroscopy, *J. Biol. Chem*. **272**, 23206-23210.
42. Flatmark, T., and Terland, O. (1971) Cytochrome b_{561} of the bovine adrenal chromaffin granules. A high potential *b*-type cytochrome, *Biochim. Biophys. Acta*. **253**, 487-491.
43. Griesen, D., Su, D., Berczi, A., and Asard, H. (2004) Localization of an ascorbate reducible cytochrome b_{561} in the plant tonoplast, *Plant Physiol*. **134**, 726-734.
44. Berczi, A., Su, D., Lakshminarasimhan, M., Vargas, A., and Asard, H. (2005) Heterologous expression and site-directed mutagenesis of an ascorbate-reducible cytochrome b_{561}, *Arch. Biochem. Biophys*. **443**, 82-92.
45. Liu, W., Kamensky, Y., Kakkar, R., Foley, E., Kulmacz, R. J., and Palmer, G. (2005) Purification and characterization of bovine adrenal cytochrome b_{561} expressed in insect and yeast cell systems, *Protein. Expr. Purif*. **40**, 429-439.

46. Takeuchi, F., Hori, H., Obayashi, E., Shiro, Y., and Tsubaki, M. (2004) Properties of two distinctheme centers of cytochrome b_{561} from bovine chromaffin vesicles studied EPR, resonance Raman, and ascorbate reduction assay, *J. Biochem*. (Tokyo) **135**, 53-64.

47. Asard, H., Venken, M., Caubergs, R., Reijnders, W., Oltmann, F. L., and De Greef, J. A. (1989) *b*-Type Cytochromes in Higher Plant Plasma Membranes, *Plant Physiol*. **90**, 1077-1083.

48. Kamensky, Y. A., and Palmer, G. (2001) Chromaffin granule membranes contain at least three heme centers: direct evidence from EPR and absorption spectroscopy, *FEBS. Lett*. **491**, 119-122.

49. Srivastava, M. (1996) Xenopus cytochrome b_{561}: molecular confirmation of a general five transmembrane structure and developmental regulation at the gastrula stage, *DNA Cell Biol*. **15**, 1075-1080.

50. Nakanishi, N., Rahman, M. M., Kobayashi, K., Hori, H., Hase, T., Park, S.-Y., and Tsubaki, M. (2008) Site-directed mutagenesis analysis on the ascorbate-specific transmembrane electron transfer reactions catalyzed by *Zea mays* cytochrome b_{561}, *Biochemistry (to be submitted).*

51. Burbaev, D. S., Moroz, I. A., Kamenskiy, Y. A., and Konstantinov, A. A. (1991) Several forms of chromaffin granule cytochrom b_{561} revealed by EPR spectroscopy, *FEBS Lett*. **283**, 97-99.

52. Ikeda, M., Iizuka, T., Takako, H., and Hagihara, B. (1974) Studies on the heme environment of oxidized cytochrome b_5, *Biochim. Biophys. Acta*. **336**, 15-24.

53. Babcock, G. T., Widger, W. R., Cramer, W. A., Oertling, W. A., and Metz, J. G. (1985) Axial ligands of chloroplast cytochrome *b*-559: Identification and

requirement for a heme-crosslinked polypeptide structure, *Biochemistry*. **24**, 3638-3645.

54. Tsubaki, M., Mogi, T., Anraku, Y., and Hori, H. (1993) Structure of the heme-copper binuclear center of the cytochrome *bo* complex of *Escherichia coli*: EPR and Fourier transform infrared spectroscopic studies, *Biochemistry*. **32**, 6065-6072.
55. Orme-Johnson, N. R., Hansen, R. E., and Beinert, H. (1971) EPR studies of the cytochrome *b*-c_1 segment of the mitochondrial electron transfer system, *Biochem. Biophys. Res. Commun*. **45**, 871-878.
56. Salerno, J. C. (1984) Cytochrome electron spin resonance line shapes, ligand fields, and components stoichiometry in ubiquinol-cytochrome *c* oxidoreductase, *J. Biol. Chem*. **259**, 2331-2336.
57. Bergstrom, J., Andreasson, L.-E, and Pettigrew, G. W. (1983) The EPR spectrum of cytochrome *b*-563 in the cytochrome *bf* complex from spinach, *FEBS Lett*. **164**, 71-74.
58. Iwata, S., Lee, J. W., Okada, K., Lee, J. K., Iwata, M., Rasmussen, B., Link, T. A., Ramaswamy, S., and Jap, B. K. (1998) Complete structure of the 11-subunit bovine mitochondrial cytochrome *bc*$_1$ complex, *Science*. **281**, 64-71.
59. Takeuchi, F., Hori, H., and Tsubaki, M. (2005) Selective perturbation of the intravesicular heme center of cytochrome b_{561} by cysteinyl modification with 4, 4'-dithiodipyridine, *J. Biochem*. **138**, 751-762.
60. Kobayashi, K., Tsubaki, M., and Tagawa, S. (1998) Distinct role of two heme centers for transmembrane electron transfer in cytochrome b_{561} from bovine adrenal chromaffin vesicles as revealed by pulse radiolysis, *J. Biol. Chem*. **273**, 16038-16042.

61. Harnadek, G. J., Ries, E. A., and Njus, D. (1985) Rate of transmembrane electron transfer in cromaffin-vesicle ghosts, *Biochemistry*. **24**, 2640-2644.

62. Seike, Y., Takeuchi, F., and Tsubaki, M. (2003) Reversely-oriented cytochrome b_{561} in reconstituted vesicles catalyzes transmembrane electron transfer and supports extravesicular dopamine β-hydroxylase activity, *J. Biochem*. **134**, 859-867.

63. Dhariwal, K. R., Shirvan, M., and Lavine, M. (1991) Ascorbic acid regeneration in chromaffin granule: in situ kinetics, *J. Biol. Chem*. **266**, 5384-5387.

64. Kipp, B. H., Kelly, P. M., and Njus, D. (2001) Evidence for an essential histidine residue in the ascorbate-binding site of cytochrome b_{561}, *Biochemistry*. **40**, 3931-3937.

65. Njus, D., Wigle, M., Kelley, P. M., Kipp, B. H., and Schlegel, H. B. (2001) Mechanism of ascorbic acid oxidation by cytochrome b_{561}, *Biochemistry*. **40**, 11905-11911.

66. Takigami, T., Takeuchi, F., Nakagawa, M., Hase, T., and Tsubaki, M. (2003) Stopped-flow analyses on the reaction of ascorbate with cytochrome b_{561} purified from bovine chromaffin vesicle membranes, *Biochemistry*. **42**, 8110-8118.

67. Njus, D., and Kelley, P. M. (1993) The secretory-vesicle ascorbate-regenerating system: a chain of concerted $H^+/e^{(-)}$-transfer reactions, *Biochim. Biophys. Acta*. **1144**, 235-248.

68. Tsubaki, M., Kobayashi, K., Ichise, T., Takeuchi, F., and Tagawa, S. (2000) Dietyl pyrocarbonate modification abolishes fast electron accepting ability of cytochrome b_{561} from ascorbate but does not influence electron donation to monodehydroascorbate radical: identification of the modification sites by mass spectrometric analysis, *Biochemistry*. **39**, 3276-3282.

69. Miles, E. W. (1977) Modification of histidyl residues in proteins by dietylpyrocarbonate, *Methods Enzymol*. **47**, 431-442.

70. Takeuchi, F., Kobayashi, K., Tagawa, S., and Tsubaki, M. (2001) Ascorbate inhibits the carbethoxylation of two histidyl and one tyrosyl residues indispensable for the transmembrane electron transfer reaction of cytochrom b_{561}, *Biochemistry*. **40**, 4067-4076.

71. Brain, R. D., Freeberg, J. A., Weiss, C. V., and Briggs, W. R. (1977) Blue light-induced absorbance changes in membrane fraction from corn and Neurospora, *Plant Physiol*. **59**, 948-952.

72. Jesaitis, A. J., Heners, P. R., Hertel, R., and Briggs, W. R. (1977) Characterization of a membrane fraction containing a *b*-type cytochrome, *Plant Physiol*. **59**, 941-947.

73. Askerlund, P., Larsson, C., and Widell, S. (1989) Cytochromes of plant plasma membranes. Characterization by absorbance difference spectrophotometry and redox titration, *Physiologia Plantarum*. **76**, 123-134.

74. Trost, P., Berczi, A., Sparla, F., Sponza, G., Marzadori, B., Asard, H., and Pupillo, P. (2000) Purification of cytochrome *b*-561 from bean hypocotyls plasma membrane. Evidence for the presence of two heme centers, *Biochim. Biophys. Acta*. **1468**, 1-5.

75. Asard, H., Horemans, N., and Caubergs, R. J. (1992) Transmembrane electron transport in ascorbate loaded plasma membrane vesicles from higher plants involves a *b*-type cytochrome, *FEBS Lett*. **306**, 143-146.

76. Horemans, N., Asard, H., and Caubergs, R. J. (1994) The role of ascorbate free radical as an electron acceptor to cytochrome *b*-mediated trans-plasma membrane electron transport in higher plants, *Plant Physiol*. **104**, 1455-1458.

77. Scagliarini, S., Rotino, L., Baurle, I., Asard, H., Pupillo, P., and Trost, P. (1998)

Initial purification study of the cytochrome b_{561} of bean hypocotyls plasma membrane, *Protoplasma*. **205**, 66-73.

78. Berczi, A., Luthje, S., and Asard, H. (2001) *b*-Type cytochromes in plasma membranes of *Phaseolus vulgaris* hypocotyls, *Arabidopsis thaliana* and *Zea mays* roots, *Protoplasma*. **217**, 50-55.
79. Asard, H., Terol-Alcayde, J., Preger, V., Del Favero, J., Verelst, W., Sparla, F., Perez-Alonso, M., and Trost, P. (2000) *Arabidopsis thaliana* sequence analysis confirms the presence of cyt *b*-561 in plants: evidence for a novel protein family, *Plant Physiol. Biochem*. **38**, 905-912.
80. Asard, H., Kapila, J., Verelst, W., and Berczi, A. (2001) Higher-plant plasma membrane cytochrome b_{561}: a protein in search of a function, *Protoplasma*. **217**, 77-93.
81. Tsubaki, M., Takeuchi, F., and Nakanishi, N. (2005) Cytochrome b_{561} protein family: Expanding role and versatile transmembrane electron transfer abilities as predicted by a new classification system and protein sequence motif analyses, *Biochim. Biophys. Acta*. **1753**, 174-190.
82. Verelst, W., and Asard, H. (2003) A phylogenetic study of cytochrome b_{561} proteins, *Genome Biol*. **4**, R38.
83. Meek, L., and Arp, D. J. (2000) The hydrogenase cytochrome *b* heme ligands of *Azotobacter vinelandii* are required for full H_2 oxidation capability, *J. Bacteriol*. **182**, 3429-3436.
84. Murakami, H., Kita, K., and Anraku, Y. (1986) Purification and properties of a diheme cytochrome b_{561} of the *Escherichia coli* respiratory chain, *J. Biol. Chem*. **261**, 548-551.

85. Okuyama, E., Yamamoto, R., Ichikawa, Y., and Tsubaki, M. (1998) Structural basis for the electron transfer across the cromaffin vesicle membrane catalyzed by cytochrome b_{561}: Analyses of cDNA nucleotide sequences and visible absorption spectra, *Biochim. Biophys. Acta*. **1383**, 269-278.

86. Mckie, A. T., Barrow D., Latunde-Dada, G. O., Rolfs, A., Sager, G., Mudaly, E., Mudaly, M., Richardson, C., Barlow, D., Bomford, A., Peters, T. J., Raja, K. B., Shirali, S., Hediger, M. A., Farzaneh, F., and Simpson, R. J. (2001) An iron-regulated ferric reductase associated with the absorption of dietary iron, *Science*. **291**, 1755-1759.

87. Zhang, D. L., Su, D., Berczi, A., Vargas, A., and Asard, H. (2006) An ascorbate-reducible cytochrome b_{561} is localized in macrophage lysosomes, *Biochim. Biophys. Acta*. **1760**, 1903-1913.

88. Su, D., May, J. M., Koury, M. J., and Asard, H. (2006) Human erythrocyte membranes contain a cytochrome b_{561} that may be involved in extracellular ascorbate recycling, *J. Biol. Chem*. **281**, 39852-39859.

89. Su, D., and Asard, H. (2006) Three mammalian cytochromes b_{561} are ascorbate dependent ferrireductases, *FEBS J*. **273**, 3722-3734.

90. Berczi, A., Su, D., and Asard, H. (2007) An Arabidopsis cytochrome b_{561} with trans-membrane ferrireductase capability, *FEBS Lett*. **581**, 1505-1508.

91. Sekido, Y., Ahmadian, M., Wistuba, I. I., Latif, F., Bader, S., Wei, M. H., Duh, F. M., Gazdar, A. F., Lerman, M. I., and Minna, J. D. (1998) Cloning of a breast cancer homozygous deletion junction narrows the region of search for a 3p21.3 tumor suppressor gene, *Oncogene*. **16**, 3151-3157.

92. Ji, L., Nishizaki, M., Gao, B., Burbee, D., Kondo, M., Kamibayashi, C., Xu, K., Yen,

N., Atkinson, E. N., Fang, B., Lerman, M. I., Roth, J. A., and Minna, J. D. (2002) Expression of several genes in the human chromosome 3p21.3 homozygous deletion region by an adenovirus vector results in tumor suppressor activities *in vitro* and *in vivo*, *Cancer Res*. **62**, 2715-2720.

93. Ohtani, S., Ueda, K., Jayachandran, G., Xu, K., Minna, J. D., Roth, J., and Ji, L. (2007) Tumor suppressor *101F6* and ascorbate synergistically and selectively inhibit non-small cell lung cancer growth by caspase-independent apoptosis and autophagy, *Cancer Res*. **67**, 6293-6303.
94. Ponting, C. P. (2001) Domain homologues of dopamine beta-hydroxylase and ferric reductase: roles for iron metabolism in neurodegenerative disorders, *Hum. Mol. Genet*. **10**, 1853-1858.
95. Vargas, J. D., Herpers, B., McKie, A. T., Gledhill, S., McDonnell, J., van den Heuvel, M., Davies, K. E., and Ponting, C. P. (2003) Stromal cell-derived receptor 2 and cytochrome b_{561} are functional ferric reductases, *Biochim. Biophys. Acta*. **1651**, 116-123.
96. Taiz, L. (1992) The plant vacuole, *J. Exp. Biol*. **172**, 113-122.
97. Boller, T., and Wiemken, A. (1986) Dynamics of vacuolar compartmentation, *Annu. Rev. Physiol*. **37**, 137-164.
98. Matile, P. (1987) The sap of plant cells, *New Phytol*. **105**, 1-26.
99. Wink, M. (1993) The plant vacuole: a multifunctional compartment, *J. Exp. Botany*. **44**, 231-246.
100. Sakaguchi, M. (1997) Eukaryotic protein secretion, *Curr. Opin. Biotech*. **8**, 595-601.
101. White, S. H., and von Heijne, G. (2005) Transmembrane helices before, during,

and after insertion. *Curr. Opin. Struct Biol*. **15**, 378-386.

102. Higy, M., Junne, T., and Spiess, M. (2004) Topogenesis of membrane proteins at the endoplasmic reticulum, *Biochemistry*. **43**, 12716-12722.

103. Walter, P., and Johnson, A. E. (1994) Signal sequence recognition and protein targeting to the endoplasmic reticulum membrane, *Annu. Rev. Cell Biol*. **10**, 87-119.

104. Sakaguchi, M., Hachiya, N., Mihara, K., and Omura, T. (1992) Mitochondrial porin can be translocated across both endoplasmic reticulum and mitochondrial membranes, *J. Biochem*. **112**, 243-248.

105. High, S., and Dobberstein, B. (1992) Mechanisms that determine the transmembrane disposition of proteins, *Curr. Opin. Cell Biol*. **4**, 581-586.

106. Ota, K., Sakaguchi, Hamasaki, N., and Mihara, K. (1998) Assessment of topogenic functions of anticipated transmembrane segments of human band 3, *J. Biol. Chem*. **273**, 28286-28291.

107. Ota, K., Sakaguchi, M., von Heijne, G., Hamasaki, N., and Mihara, K. (1998) Forced transmembrane orientation of hydrophilic polypeptide segments in multispanning membrane proteins, *Mol. Cell*. **2**, 495-503.

108. Chrispeels, M. J., and Raikhel N. V. (1992) Short peptide domains target proteins to vacuoles, *Cell*. **68**, 613-616.

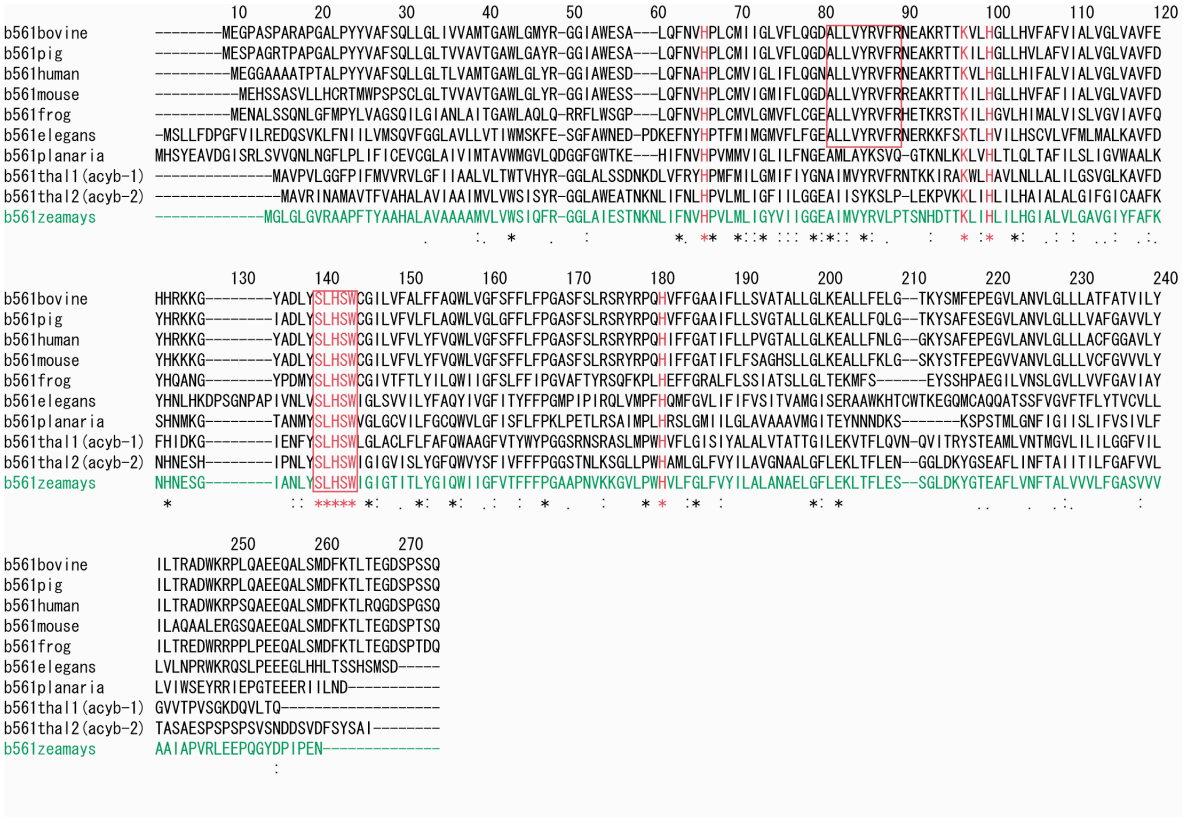

Figure 1-1. Multiple alignment of *Zea mays* cytochrome b_{561} amino acid sequence with those of animal and plant cytochromes b_{561}. Below the aligned sequences, 27 totally-conserved amino acid residues including 4 His residues, potential axial ligands for the two heme prosthetic groups, were indicated by an asterisk. Additionally, the "SLHSW" and the "ALLVYRVFR" sequences were also indicated by a box, respectively. Amino acid sequence of cytochromes b_{561} from bovine, pig, human, mouse, frog, *C. elegans*, planaria, *Arabidopsis thaliana*, and *Zea mays* were aligned.

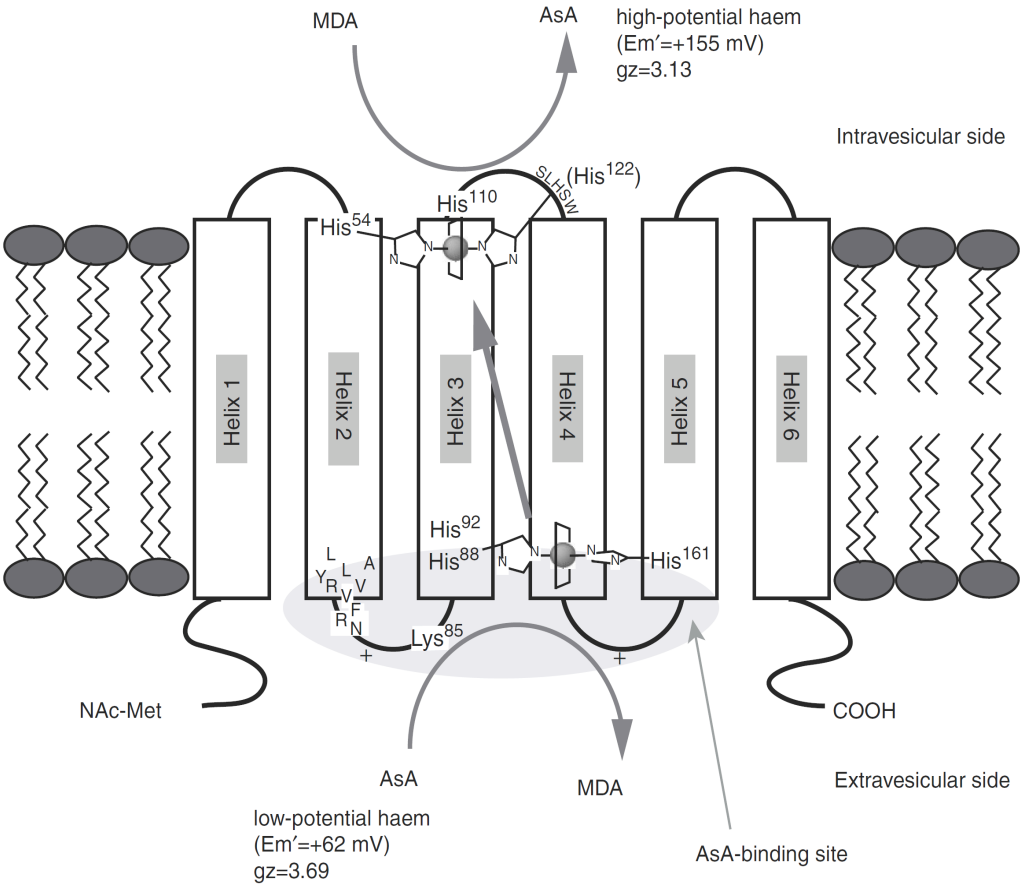

Figure 1-2. Structural model of bovine cytochrome b_{561}. Two well-conserved motifs "ALLVYRVFR" and "SLHSW" and five conserved His residues (His^{54}, His^{88}, His^{110}, His^{122} and His^{161} are indicated based on the model. His^{54} and His^{122} are the heme axial ligands on the intravesicular side, whereas His^{88} and His^{161} are the heme axial ligands on the cytosolic side. The heme *b* on the cytosolic side has a function for the electron acceptance from AsA; on the other hand, the heme *b* on the intravesicular side may donate electron equivalent to MDA radical to reproduce AsA.

Chapter 2

Purification and biochemical analyses of *Zea mays* cytochrome b_{561} heterologously expressed in *Pichia pastoris*

2-1. Abstract

Cytochromes b_{561} constitute a novel class of transmembrane electron transport proteins present in large variety of eukaryotic cells, with a number of highly relevant common structural features including the six hydrophobic transmembrane α-helices and the two heme ligation sites. Of particular interest is the presence of a number of plant homologues that encode proteins having possible ascorbate and monodehydroascorbate radical-binding sites proposed previously for mammalian cytochromes b_{561}. In the present study, we conducted a molecular cloning of cytochrome b_{561} cDNA from corn plant, *Zea mays,* its functional heterologous expression in yeast *Pichia pastoris,* its purification, and its biochemical analyses. The purified recombinant *Zea mays* cytochrome b_{561} protein (WTZMb_{561}-H_6) showed characteristic visible absorption peaks very similar to those of bovine cytochrome b_{561}. The results from a stopped-flow analysis indicated that *Zea mays* cytochrome b_{561} utilizes ascorbate and possibly, monodehydroascorbate radical as a physiological electron donor and acceptor, respectively. Pre-treatment of the purified *Zea mays* cytochrome b_{561} with dietylpyrocarbonate in the oxidized form caused a drastic inhibition of the electron transfer from ascorbate and such inhibition was protected by the presence of ascorbate during the treatment with diethylpyrocarbonate. These results suggested that plant cytochrome b_{561} might perform an ascorbate-related transmembrane electron transfer reaction by utilizing a very similar molecular mechanism with that of bovine cytochrome b_{561}. Our new system offers an improvement in the yield and other advantages over existing insect and yeast cell systems for the producing the recombinant cytochrome ZMb_{561} for the studies on the structure and functions.

2-2. Introduction

During the past twenty-five years, evidence has accumulated on the presence of a specific high-potential ascorbate-reducible *b*-type cytochrome in the plasma membranes of higher plants. This cytochrome is named cytochrome b_{561} according to the wavelength maximum of its α-band in the reduced form. More recent evidence suggested that this protein is homologous to a *b*-type cytochrome present in chromaffin granules of neuroendocrine cells of higher animals. These cytochromes b_{561} probably constitute a novel class of transmembrane electron transport proteins present in large variety of eukaryotic cells (*1*). Of particular interest is the recent discovery of a number of plant genes that show striking homologies to the genes encoding for the mammalian neuroendocrine cytochrome b_{561}. A number of highly relevant structural features, including six hydrophobic transmembrane α-helices, heme ligation sites, and possible ascorbate (AsA) and monodehydroascorbate (MDA) radical-binding sites (*2*), are almost perfectly conserved in all these proteins. It is our most requisite to understand the physiological roles of plant cytochrome b_{561} and its molecular mechanism operative for the transmembrane electron transfer in the biomembranes.

Purification of plant cytochromes b_{561}, however, seemed a very difficult task in the past. Indeed, there has been scarce information regarding the nature of plant cytochromes b_{561}. We decided to exploit a heterologous expression system to study plant cytochromes b_{561}. The use of the methyltrophic yeast, *Pichia pastoris,* as a cellular host for the expression of recombinant proteins has become increasingly popular in recent days. *Pichia pastoris* is much easier to genetically manipulate and to culture than mammalian cells and can be grown to high cell densities under the control of alcohol oxidase (AOX1) promoter. In the present study, we have succeeded in constructing the

heterologous expression system of His-tagged *Zea mays* cytochrome b_{561} protein in *Pichia pastoris* cells. Detailed studies on its biochemical characterization of the purified sample are also reported.

2-3. Materials and methods

Preparation of Zea mays b_{561}/pPICZB construct and expression of recombinant Zea mays cytochrome b_{561} in yeast Pichia pastoris cells: *Pichia pastoris* expression kit were purchased from Invitrogen (Carlsbad, CA). For the construction of 6xHis-tagged *Zea mays* cytochrome b_{561}/pPICZB plasmid (Invitrogen, Carlsbad, CA), the *Zea mays* cytochrome b_{561}/pBluescript II SK(+) plasmid which contains the full length *Zea mays* b_{561} cDNA (AB182641) was used as the template to amplify the b_{561} gene by PCR, with using following two primers; PPMb561s (sense primer), 5'-ACGGAATTCG AATCCATGGG GCTTGGC-3'; PPHMb561a (anti-sense primer), 5'-TTTCTAGATC AGTGGTGGTG GTGGTGG TGG TTTTCTGGAA-3'. The sense primer introduced an *EcoR*I site upstream of the initiation codon (underlined). The former anti-sense primer introduced a hexa-histidine (6xHis) sequence before, and an *Xba*I site immediately after, the stop codon, resulting in the expression of the recombinant *Zea mays* cytochrome b_{561} protein having a C-terminal 6xHis-tag (WT-ZMb_{561}-H_6; in which the C-terminal part of the deduced amino acid sequence was ^{211}GASVVVAAIAPVRLEEPQGYDPIPENHHHHHH^{242} in its C-terminal region). The PCR amplified product was digested with *EcoR*I and *Xba*I, purified by agarose gel electrophoresis, inserted into an expression cassette of the pPICZB vector under the control of the inducible alcohol oxidase promoter (AOX1) and the resulting plasmid

was used to transform *E. coli* XL1-Blue competent cells. The transformants were screened for proper insertion of the 6xHis-tagged *Zea mays* cytochrome b_{561} gene. The resulting construct, designated as pPICZB-ZMb_{561}-His_6, was verified by restriction digestion analyses and by DNA sequencing (Applied Biosystems, Foster City, CA). The transformation of *Pichia pastoris* cell was performed according to the manufacture's procedure (Invitrogen, Carlsbad, CA). The pPICZB-ZMb_{561}-H_6 construct (10 μg) was linerized with *Pme*I, and was transformed into *Pichia pastoris* GS115 competent cells (His^-, Mut^+) (Invitrogen, Carlsbad, CA) to give a methanol-inducible *Zea mays* cytochrome b_{561} protein expression. The transformants were selected on YPDS plates containing zeocin (100 μg/mL). Genomic DNA from *Pichia pastoris* integrants was extracted and PCR analysis was conducted to confirm the presence of the *Zea mays* cytochrome b_{561} gene at the AOX1 locus, using primers in the AOX1 promoter. To produce starter cultures, a single colony of *Pichia pastoris* GS115/pPICZB-WTZMb_{561}-His_6 was inoculated in 25 mL of buffer glycerol complex (BMGY) medium and was cultured at 30°C with shaking at 225 rpm overnight. The cells were then transferred into 225 mL of BMGYH medium (1.34 % yeast nitrogen base, 1 % yeast extract, 2 % peptone, 0.1 M potassium phosphate buffer, pH 6.1, 1 % glycerol, 0.4 μg biotin/mL, and 0.04 mg histidine/mL) containing zeocin (25 μg/mL) and cultivation was continued under the same condition. When OD_{600} of the culture reached to 3.0, the cells were collected by centrifugation at 5,000 rpm for 5 min at room temperature. The pelleted cells were suspended in 250 mL of BMMYH medium (BMGYH medium without glycerol but with 1.0 % (v/v) methanol) supplemented with Δ-ALA (0.5 mM) and hemin (40 μM). The cell culture was continued at 30°C for 96 h with shaking at 225 rpm and, in every 12h, 100 % methanol solution was added to the

culture to make the final methanol concentration of 1 % (v/v) to maintain the induction of the protein expression.

Preparation of Pichia pastoris microsomal fraction: The cultured cells were centrifuged at 5,000 rpm for 5 min at room temperature. The pelleted cells were suspended with buffer A (50 mM potassium-phosphate buffer, pH 6.0, 2.0 M sorbitol, 0.1 mM dithiothreitol, 0.1 mM EDTA). To the suspension, zymolyase (from *Arthrobacter luteus*) (Seikagaku Corp., Tokyo, Japan) was directly added to 0.5 mg/mL and the mixture was incubated for 3h at 30°C with shaking at 240 rpm. The mixture was centrifuged at 5,000 rpm for 10 min at 4°C. The pellets were re-suspended with buffer B (50 mM potassium-phosphate buffer, pH 7.0, 0.65 M sorbitol, 0.1 mM dithiothreitol, 0.1 mM EDTA, 1.0 mM PMSF). Then, the suspension was sonicated with an Astrason S3000 ultrasonic processor (Misonix Inc., Farmingdale, NY) at 48 W (with duty cycle of 50 %) for 3.0 min on ice and, then, was centrifuged at 10,000 rpm for 10 min at 4°C. The supernatant was ultracentrifuged at 30,000 rpm for 60 min at 4°C. The resultant pellet was re-suspended with 50 mM potassium-phosphate buffer, pH 7.0, containing 10 %(w/v) glycerol. This yeast microsomal fraction was saved in −80°C until use.

Solubilization of microsomal membranes and purification of the recombinant Zea mays cytochrome b_{561} protein: The recombinant 6xHis-tagged WTZMb_{561} protein expressed in *Pichia pastoris* cells was readily solubilized from microsomal membrane fractions with 1.0% (w/v) n-octyl-β-D-glucoside (β-OG) in 50 mM potassium-phosphate buffer (pH 7.0), 10% (v/v) glycerol and 1 mM AsA, on ice with stirring for 3h. The detergent-solubilized solution containing the cytochrome was concentrated using a Millipore ultrafiltration apparatus (membrane MWCO=30,000; Millipore, Billerica, MA) and then applied to a DEAE-Sepharose CL-6B (Amersham

Biosciences, GE Healthcare Bio-sciences) ion-exchange column that had been pre-equilibrated with 35 mM potassium-phosphate (pH 7.0) buffer. The adsorbed cytochrome in the column was eluted with 35 mM potassium-phosphate (pH 7.0) buffer containing 1 % β-OG and 1 mM AsA. After the analyses with SDS-PAGE and with measuring the absorbance at 425 nm, active fractions were collected, combined and concentrated. The concentrated sample was supplemented with 300 mM NaCl and 10 mM imidazole and was applied to a 5 ml volume of Ni^{2+}-NTA agarose (QIAGEN, Hilden, Germany) column that had been pre-equilibrated with buffer A (50 mM potassium-phosphate buffer, pH 7.0, containing 1 % β-OG , 10 % glycerol, 300 mM NaCl, and 1 mM AsA) containing 10 mM imidazole. The column was then washed with 20 bed volumes of buffer A containing 20 mM imidazole. The His-tagged protein was then eluted with buffer A containing 250 mM imidazole. The eluate was concentrated with a Millipore ultrafiltration apparatus (membrane MWCO=30,000; Millipore, Billerica, MA) and imidazole was removed by gel filtration on a PD-10 column (Amersham Bioscience) equilibrated with 50 mM potassium-phosphate (pH 7.0) buffer containing 1 % β-OG.

Biochemical analyses of the purified recombinant Zea mays cytochrome b_{561}: The concentration of the purified cytochrome b_{561} was determined by using a millimolar extinction coefficient of 27.7 $mM^{-1}cm^{-1}$ (*3*). For immunoblotting, unstained protein were transferred electrophoretically onto a nitrocellulose membrane and probed with rabbit anti-C-terminal peptide of *Zea mays* b_{561} antibodies (1:1000) (Takara-Bio, Ohtsu, Japan). Visualization of immunoreactive bands was done using horseradish peroxidase (HRP)-conjugated secondary antibodies, 4-chloro-1-napthol, and diluted hydrogen peroxide. NH_2-terminal amino acid sequence of the purified 6xHis-tagged WTZMb_{561}

in the gel was analyzed as follows. Proteins in the gel were electro-blotted onto a PVDF membrane (sequi-Blot, 0.2 μm. Bio-Rad, USA). The Ponceau S-stained protein band on the PVDF membrane was cut using a clean razor and was directly analyzed with an ABI protein sequencer (Model492; Applied Biosystem, USA) up to 10 cycles. Mass spectrometric analyses were conducted with a Voyager DE Pro mass spectrophotometer (Applied Biosystems, Foster City, CA) using a 20kV accelerating voltage. The mass spectra were acquired by adding the individual spectrum from 256 laser shots. For peptide analysis the samples were run in reflector mode. The recombinant wild-type protein (WTZMb_{561}-H_6) was digested either with TPCK-treated trypsin (0.01 mg/mL) or *Staphylococcus aureus* V8 protease (0.01 mg/mL), respectively. After 48h of incubation at room temperature, the peptide solutions were diluted 1:9 (v/v) with a matrix solution (α -cyano-4-hydroxycinamic acid (Aldrich, Gillingham, England), 50 mg/ml in 50% acetonitrile in 0.3% TFA). The mixtures (typically, 1.0 μL) were deposited on the sample plate, allowed to air-dry, and analyzed. The search of the corresponding fragments in the amino acid sequence of *Zea mays* b_{561} was conducted using GPMAW (v 6.11) (Lighthouse Data, Odense M, Denmark).

Stopped-flow spectroscopic measurements of the recombinant Zea mays cytochrome b_{561}: Rapid kinetic measurements were carried out using an RSP-100-03DR stopped-flow rapid-scan spectrometer (UNISOKU Co. Ltd., Osaka, Japan), as previously described (*4*). One chamber of the apparatus contained the oxidized form of WTZMb_{561} (2.0 μm or indicated in the text) in 50 mM sodium acetate (pH 5.0), 50 mM potassium-phosphate (pH 6.0) or 50 mM potassium-phosphate (pH 7.0) buffer containing 1.0 % n-octyl-β-glucoside. The other chamber contained a test concentration of sodium ascorbate (AsA) (2, 4, 8, 16 mM) in the same buffer. The temperature of both

chambers and the sample holder was maintained at 20°C by connecting to a thermo-bath (Tokyo Rikakikai Co. Ltd., Model NCB-1200; Tokyo, Japan). The mixing was carried out with a 1:1 (v/v) ratio. Heme reduction of cytochrome b_{561} was followed spectrophotometrically either by absorbance change at 427 nm using a photomultiplier (single wavelength mode) or by multiple wavelengths (rapid scan mode; ～360～640 nm) using a photodiode array (512 channels). Data points were collected in every 120 msec (with 1-msec exposure time) for 1 min. The time-courses of the absorbance change at 427 nm were fitted by use of a non-linear least-squares method of a built-in software of the apparatus (or "Igor" software, v. 6.03) with a single (or a linear combination of) exponential decay equations.

2-4. Results and discussion

***Properties of the recombinant Zea mays cytochrome b_{561}*:** The recombinant 6xHis-tagged WTZMb_{561} (WTZMb_{561}-His_6) was expressed successfully under the control of the methanol-inducible promoter (AOX) in yeast *Pichia pastoris* cells. The purified WTZMb_{561}-His_6 showed characteristics visible absorption spectra with absorption peaks at 414 nm for the oxidized form and at 561, 529, and 427 nm for the dithionite-reduced form (Fig. 2-1), which were very similar to those of bovine neuroendocrine cytochrome b_{561} (*3*). The SDS-PAGE (Fig. 2-2) and Western blotting (Fig. 2-3) of the purified sample showed a single protein band at 26.2 kDa. MALDI-TOF mass spectrum of the intact *Zea mays* cytochrome b_{561} (WTZMb_{561}-His_6) in the presence of 1 % β-OG was directly analyzed in a linear mode. The spectrum showed a clear [$M+H^+$] peak at 26,176.9 (m/z), slightly lower than the theoretical value

of 26,247.84 (Fig. 2-4). MALDI-TOF mass spectrometric analyses on the tryptic and V8-protease peptides of the recombinant WTZMb_{561}-His_6 showed many partially cleaved polypeptides (Fig. 2-5A and 2-5B). We identified most of the polypeptides and found that there was no undesirable mutation being introduced. The NH_2-terminal amino acid sequencing (10 cycles) of the purified WTZMb_{561}-His_6 showed a sequence of GLGLGVRAAP, corresponding to the authentic sequence of ZMb_{561} gene. MALDI-TOF-MS analyses of the digested peptides of WTZMb_{561}-His_6 also confirmed that the Met residue at the initiation site was removed.

Electron transfer activity of the recombinant Zea mays cytochrome b_{561}: The purified WTZMb_{561}-His_6 protein showed a rapid electron acceptance from AsA with a final reduction level of ～80 % when examined spectrophotometrically by a manual mixing method. Further, we found that the rapid electron accepting ability of WTZMb_{561}-His_6 from AsA was inhibited significantly upon the treatment with dietylpyrocarbonate (DEPC) in the oxidized state, as found previously for bovine neuroendocrine cytochrome b_{561} (*5, 6, 7*). The modification sites with DEPC were analyzed by MALDI-TOF mass spectrometry and were found as the two His axial heme ligands and one conserved Lys residue, very similar to the results for bovine cytochrome b_{561} (*6, 7*). These results suggested that plant cytochromes b_{561} utilize AsA as physiological electron donor in a very similar mechanism as found in bovine neuroendocrine cytochrome b_{561} (*8*).

Stopped-flow analyses of Zea mays cytochrome b_{561}: The electron acceptance reaction of oxidized WT-ZMb_{561}-H_6 was further analyzed by stopped-flow spectrometry (Fig. 2-6). The absorbance change at 427 nm after mixing of oxidized form of WT-ZMb_{561}-H_6 (final 1μM) with AsA (final 2 mM) was presented against time scale.

The result showed that, in initial phase of the electron acceptance from AsA, the heme reduction rate of WT-ZMb_{561}-H_6 was much slower at pH 5.0 than that measured at pH 7.0, as observed for bovine cytochrome b_{561} (*7*) and for WT-ZMb_{561} (*9*).

2-5. Conclusion

In conclusion, our new expression system offers a great improvement in the yield and the quality and other advantages over the existing insect and yeast cell systems for producing the recombinant WTZMb_{561}. This system was also found to be very suitable for the production of various site-directed mutants for the studies on the structure and functions of cytochrome b_{561}.

2-6. References

1. Tsubaki, M., Takeuchi, F., and Nakanishi, N. (2005) Cytochrome b_{561} protein family: Expanding role and versatile transmembrane electron transfer abilities as predicted by a new classification system and protein sequence motif analyses, *Biochim. Biophys. Acta*. **1753**, 174-190.
2. Okuyama, E., Yamamoto, R., Ichikawa, Y., and Tsubaki, M. (1998) Structural basis for the electron transfer across the chromaffin vesicle membrane catalysed by cytochrome b_{561}: Analyses of cDNA nucleotide sequences and visible absorption spectra, *Biochim. Biophys. Acta*. **1383**, 269-278.
3. Tsubaki, M., Nakayama, M., Okuyama, E., Ichikawa, Y., and Hori, H. (1997) Existence of two heme *b* centers in cytochrome b_{561} from bovine adrenal chromaffin vesicles as revealed by a new purification procedure and EPR spectroscopy, *J. Biol. Chem*. **272**, 23206-23210.
4. Takeuchi, F., Hori, H., and Tsubaki, M. (2005) Selective perturbation of the intravesicular heme center of cytochrome b_{561} by cysteinyl modification with 4, 4'-dithiodipyridine. *J. Biochem*. **138**, 751-762.
5. Tsubaki, M., Kobayashi, K., Ichise, T., Takeuchi, F., and Tagawa, S. (2000) Diethyl pyrocarbonate modification abolishes fast electron accepting ability of cytochrome b_{561} from ascorbate but does not influence electron donation to monodehydroascorbate radical: identification of the modification sites by mass spectrometric analysis, *Biochemistry*. **39**, 3276-3284.
6. Takeuchi, F., Kobayashi, K., Tagawa, S., and Tsubaki, M. (2001) Ascorbate inhibits the carbethoxylation of two histidyl and one tyrosyl residues indispensable for the transmembrane electron transfer reaction of cytochrome b_{561}, *Biochemistry*. **40**,

4067-4076.

7. Takigami, T., Takeuchi, F., Nakagawa, M., Hase, T., and Tsubaki, M. (2003) Stopped-flow analyses on the reaction of ascorbate with cytochrome b_{561} purified from bivine chromaffin vesicle membranes, *Biochemistry*. **42**, 8110-8118.
8. Nakanishi, N., Takeuchi, F., and Tsubaki, M. (2007) Histidine cycle mechanism for the concerted proton/electron transfer from ascorbate to the cytosolic heme *b* center of cytochrome b_{561}: A unique machinery for the biological transmembrane electron transfer, *J. Biochem.* **142**, 553-560.
9. Nakanishi, N., Rahman, M. M., Takigami, T., Kobayashi, K., Hori, H., Hase, T., Park, S.-Y., and Tsubaki, M. (2008) Functional expression of *Zea mays* cytochrome b_{561} in yeast *Pichia pastoris*: Properties of an ascorbate-specific plant transmembrane electron transfer protein, *Biochemistry (submitted)*.

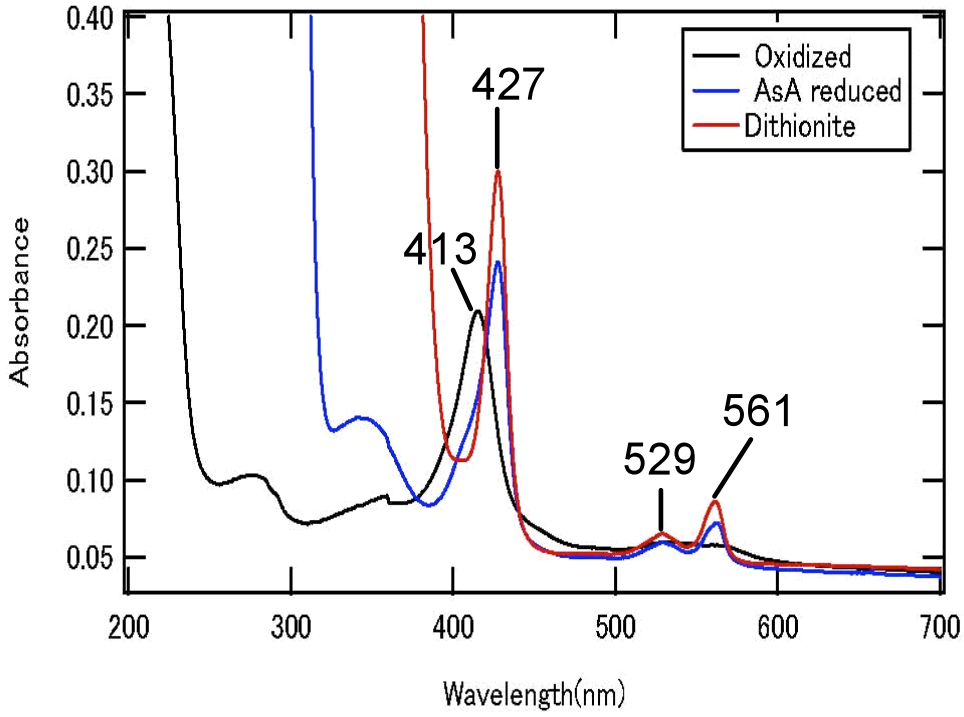

Figure 2-1. Visible absorption spectra of the purified recombinant *Zea mays* cytochrome b_{561} (WTZMb_{561}-H$_6$). Spectrometric analysis was carried out using a Shimadzu UV2400 spectrometer (Shimadzu, Kyoto, Japan). Oxidized form, AsA-reduced form, dithionite-reduced from are presented (Protein concentration was 0.742 μM in 50 mM potassium-phosphate buffer pH 7.0 containing 1% β-OG).

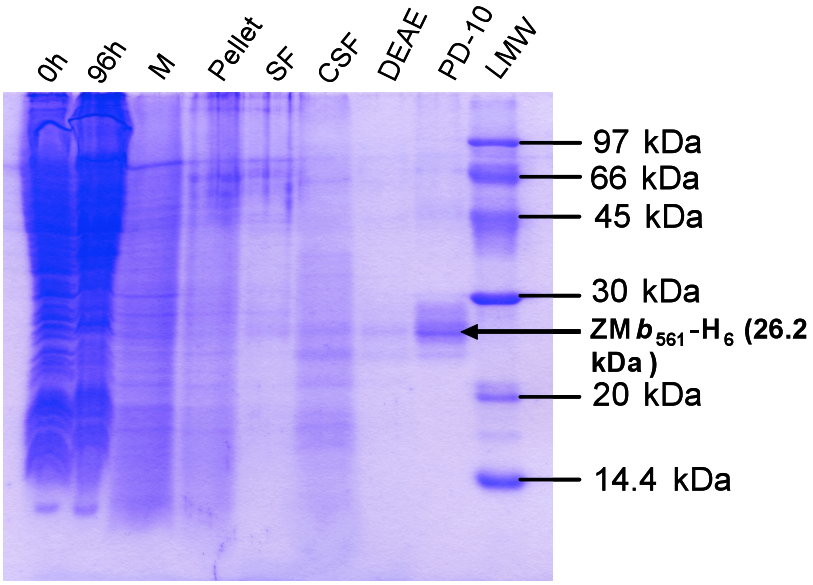

Figure 2-2. SDS-PAGE analysis on the solubilization and purification of the recombinant *Zea mays* cytochrome b_{561} heterologously-expressed in yeast *Pichia pastoris* cells. 0h, before the induction with MeOH (final 1.0 %); M, microsomal fraction (10 μg); Pellet, pellet fraction after the solubilization with β-OG (1.0 %); SF, supernatant fraction after the solubilization with β-OG (10 μg); CSF, concentrated supernatant fraction (10 μg); DEAE, partially purified fraction after the DEAE-Sepharose column chromatography (10 μg); PD-10, final form after the Ni^{2+}-NTA agarose column and PD-10 column chromatography (2 μg); LMW, low molecular weight markers.

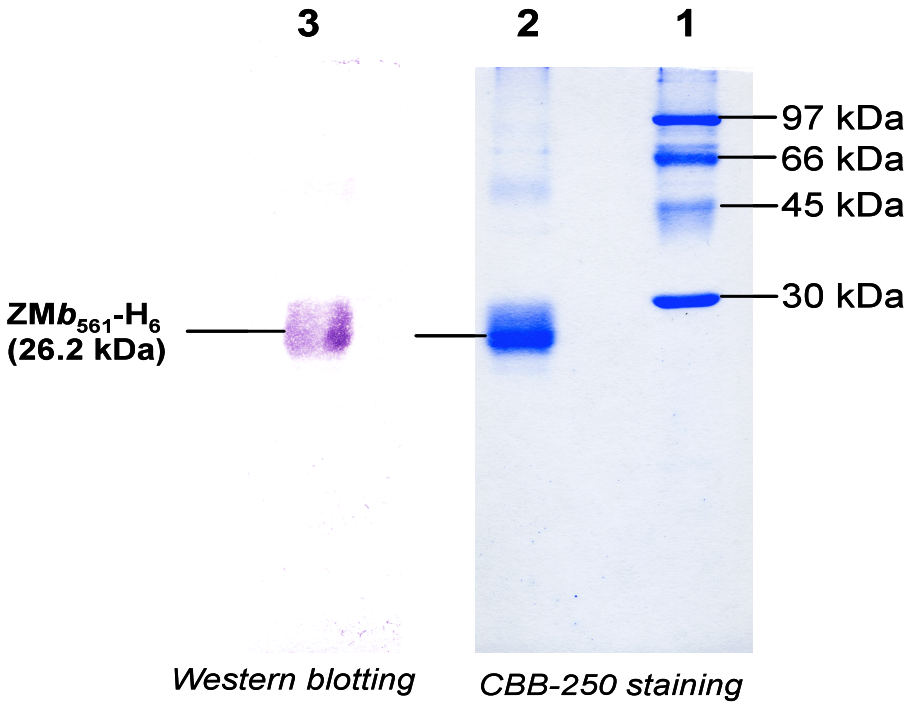

Figure 2-3. SDS-PAGE and Western blotting analyses of the purified recombinant *Zea mays* cytochrome b_{561} (WTZMb_{561}-H_6). SDS-PAGE was conducted on a 15 % gel. After the electrophoresis, the gel was stained with CBB-R250. A part of the gel was cut and the gel was electro-blotted onto a nitrocellulose membrane. The membrane was treated with a 100 × diluted primary antibody (anti-C-terminal *Zea mays* b_{561} peptide rabbit IgG antibody) and then with a 1000 × diluted HRP-conjugated anti-rabbit IgG antibody. The staining of the protein band was conducted with 4-chloro-1-napthol and hydrogen peroxide. Lane 1, LMW marker, lanes 2, 3, purified WTZMb_{561}-H_6 (2.0 μg of protein).

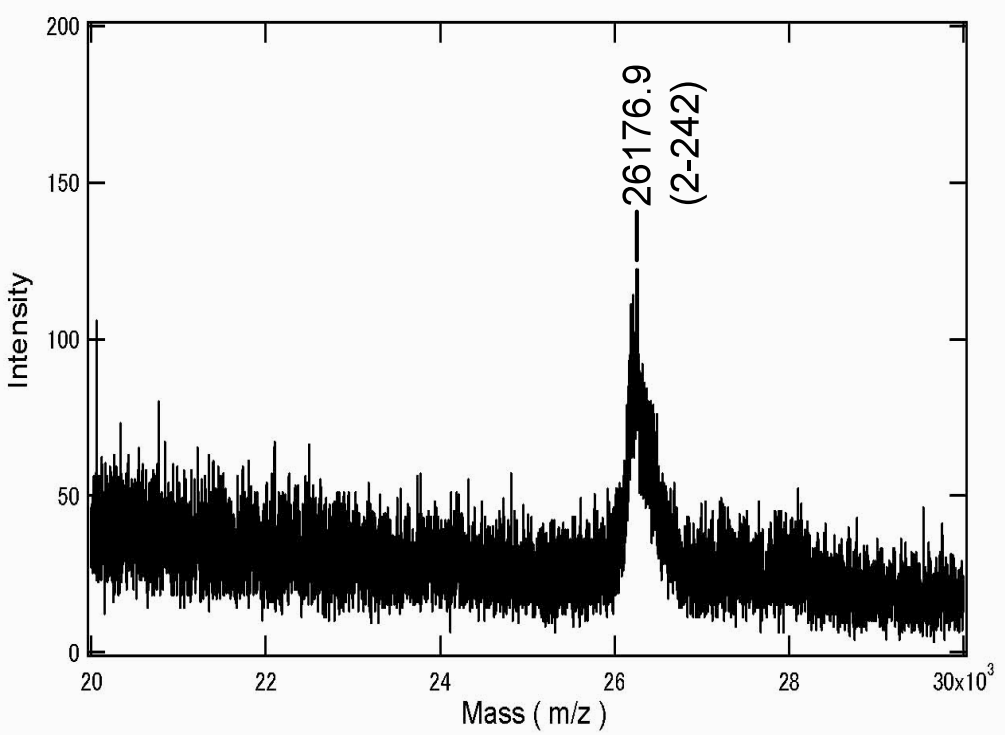

Figure 2-4. MALDI-TOF mass analysis of the purified recombinant *Zea mays* cytochrome b_{561} (WTZMb_{561}-H_6). Mass spectrometric analysis was carried out on a Voyager DE Pro mass spectrometer (Applied Biosystem, Foster City, CA) using a 20 kV accelerating voltage. The mass spectrum was acquired in a linear mode by adding the individual spectrum from 256 laser shots. The protein solutions were diluted 1:9 (v/v) with a matrix solution, 3,5-dimethoxy-4-hydroxycinnamic acid (Aldrich, Gillingham, England), 50 mg/ml in 30 % acetonitrile in 0.3 % TFA.

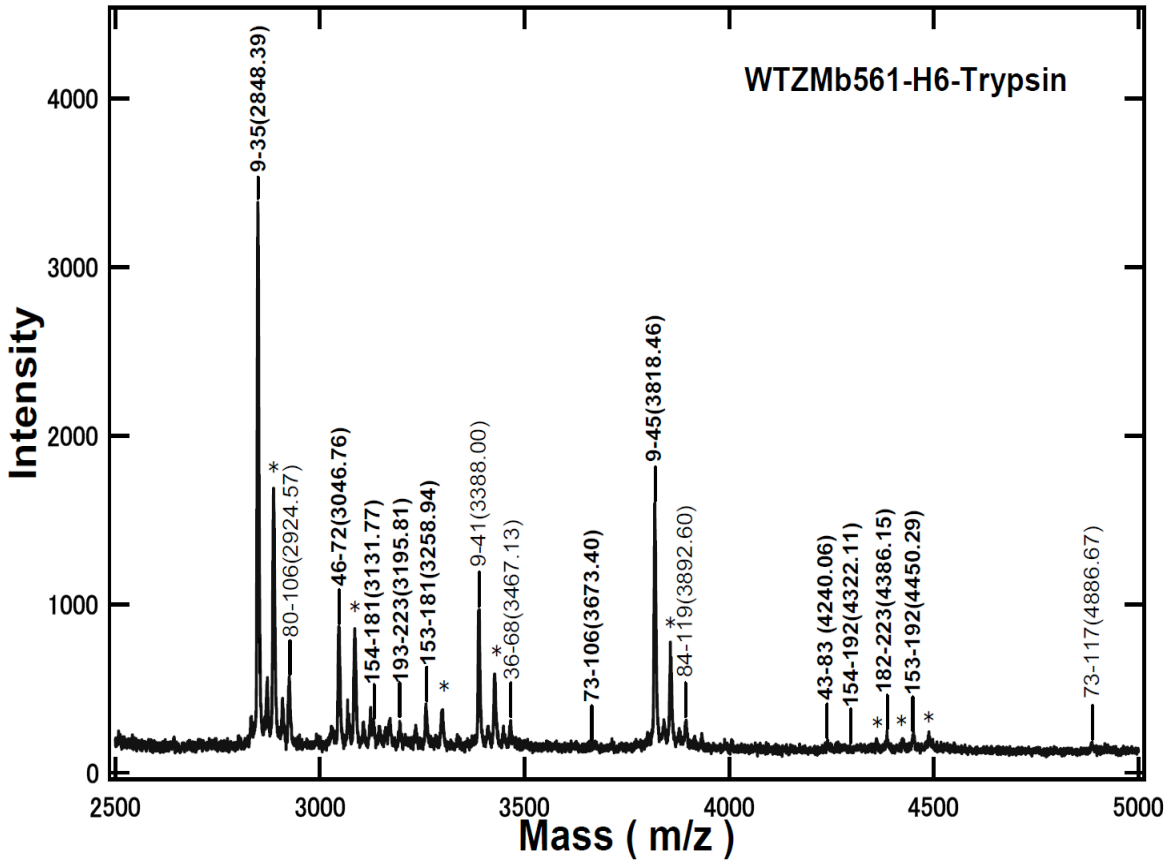

Figure 2-5A. MALDI-TOF-mass spectrum of trypsin-cleaved peptides from WT-ZMb_{561}-H_6. Mass spectrum of WT-ZMb_{561}-H_6 after the treatment with TPCK-treated trypsin was shown in the region from 2500 to 5000 m/z. Authentically-cleaved peptides by trypsin are indicated in boldface. Peaks indicated by asterisk (*) are due to the K^+ ion form [M+K^+] of the molecular ion.

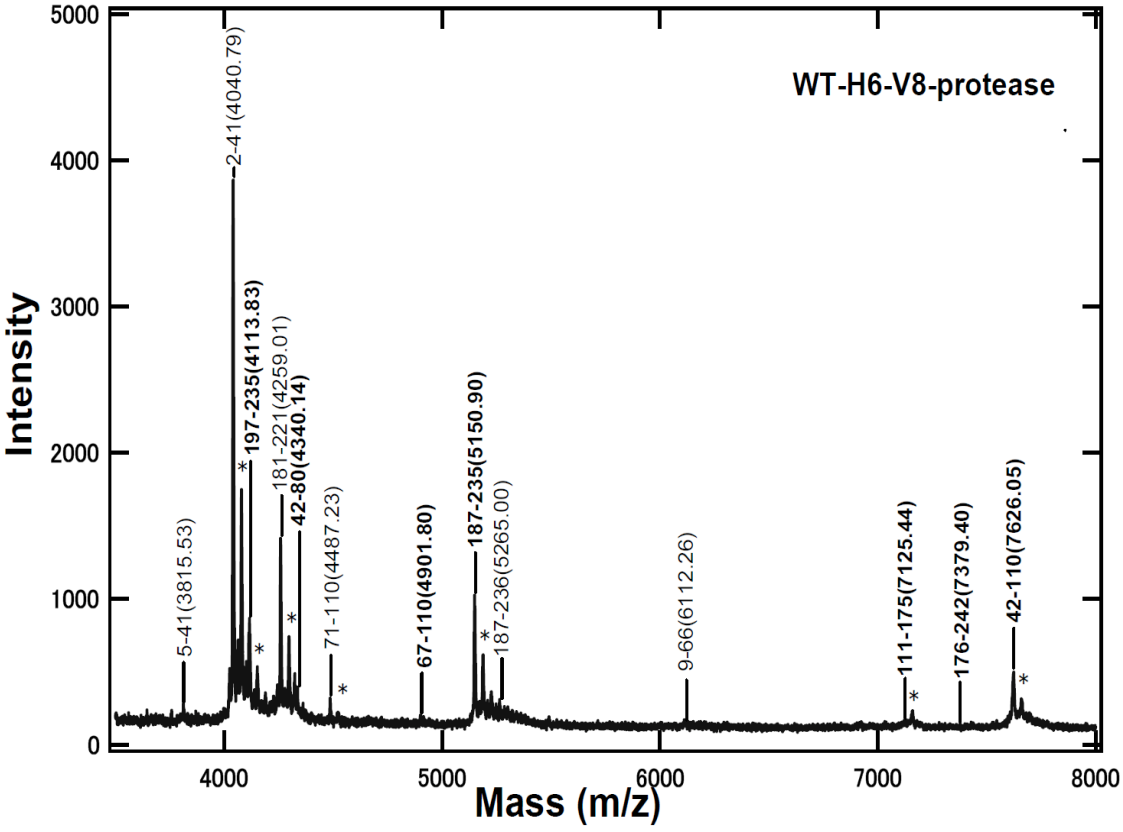

Figure 2-5B. MALDI-TOF-mass spectrum of the V8-protease-cleaved peptides from WT-ZMb_{561}-H_6. Mass spectrum of WT-ZMb_{561}-H_6 after the treatment with V8-protease was shown in the region from 3500 to 8000 m/z. Authentically-cleaved peptides by V8-protease are indicated in boldface. Peaks indicated by asterisk (*) are due to the K^+ ion form [M+K^+] of the molecular ion.

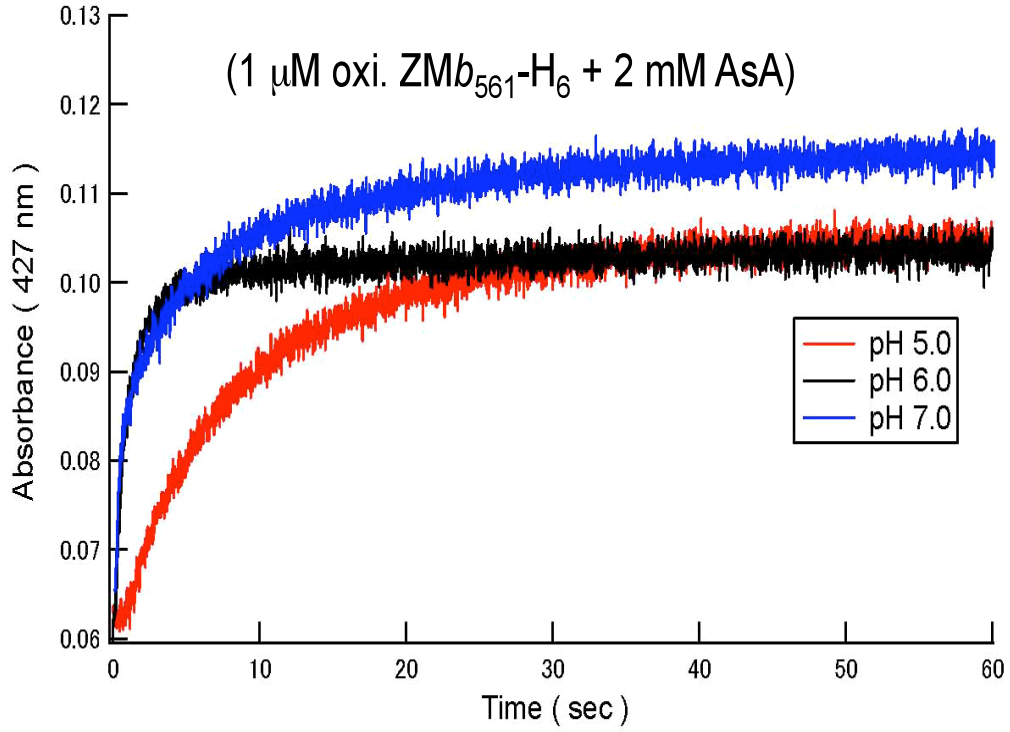

Figure 2-6. Stopped-flow analysis on the electron transfer from AsA to the purified WT-ZMb_{561}-H_6 at three different pH. The electron accepting reaction of the oxidized WT-ZMb_{561}-H_6 was measured at 427 nm by stopped-flow spectrometry using the solution mixing system with a 1:1 volume ratio. The absorbance changes were plotted against the time in a linear time scale from 0 to 60 sec. Buffer conditions are described in the text.

Chapter 3

Roles of conserved Arg^{72} and Tyr^{71} in the ascorbate-specific transmembrane electron transfer reactions catalyzed by *Zea mays* cytochrome b_{561}

3-1. Abstract

Cytochromes b_{561}, a novel class of transmembrane electron transport proteins residing in large variety of eukaryotic cells, have a number of common structural architecture with the six hydrophobic transmembrane α-helices bundle and two heme ligation sites. Our recent studies on a recombinant *Zea mays* cytochrome b_{561}, which was produced by a heterologous expression system using yeast *Pichia pastoris* cells, suggested that the "concerted proton/electron transfer mechanism", which was hypothesized to be operative in bovine cytochrome b_{561} upon electron acceptance from ascorbate, was likely to be functioning in plant cytochromes b_{561} as well and that the conserved Lys^{83} residue on a cytosolic loop had very important roles for the binding of ascorbate and the electron transfer from it. In the present study, we conducted a site-directed mutagenesis study on the conserved Arg^{72} and Tyr^{71} residues residing in the same loop with that of Lys^{83}. Changes of a positive charge at the Arg^{72} residue did not affect significantly on the final heme reduction level with ascorbate as a reductant. However, the characteristic pH-dependent initial time-lag upon electron acceptance from ascorbate in an acidic pH region was almost completely lost for R72A and R72E mutants. Substitution of Tyr^{71} residue with Ala or Phe did show some influences on the final heme reduction level and affect on the pH-dependent initial time-lag causing an acceleration of the electron transfer, particularly at a lower pH. These observations were interpreted as the existence of some specific interactions of Tyr^{71} and Arg^{72} residues with the bound substrate. However, their mechanistic roles were distinctly different from that of Lys^{83} and might be related for expelling monodehydroascorbate radical from the substrate-binding site to prevent the reverse electron flow.

3-2. Introduction

The plasma membranes (PM) of higher plants contain an ascorbate-reducible, high-potential (E'_o= ~ +140 mV) *b*-type cytochrome, named cytochrome b_{561} due to it's α-band maximum at 561 nm in the reduced form. Presence of the *b*-type cytochromes in the plasma membranes of higher plants has long been demonstrated in a variety of plant species and in different tissues (*1-6*).

The availability of the primary sequences of cytochrome b_{561} from bovine adrenal gland chromaffin cells and from other animal species has recently resulted in the identification of many homologous sequences in plant as well (*7, 8*). Further extensive studies found that cytochrome b_{561}-like genes distribute in nearly all the organisms including invertebrates (insects, nematodes, platheminthes, tunicates), vertebrates (mammals, amphibians), fungi, and plants (monocots, dicots, and gymnosperms) (*5*). Presence of cytochrome b_{561} in a wide variety of species indicates the general importance of this class of proteins in eukaryotic cell functions. Members of the cytochrome b_{561} family are characterized by a number of common structural features, including six hydrophobic transmembrane α-helices, four totally conserved His residues, possibly coordinating two heme prosthetic groups (*9-16*). Further, putative substrate-binding sites for ascorbate (AsA) and monodehydroascorbate (MDA) radical are almost perfectly conserved among the members of animal and plant cytochrome b_{561} subfamilies (*9-16*). The strict conservation of these essential structural features suggests that the mode of action and physiological functions of these membrane proteins may be very similar each other.

Purification of plant cytochrome b_{561}, however, was found to be a very difficult task in the past (*1-6*). Indeed, there has been scarce information regarding the nature of

plant cytochrome b_{561}. However, recent progress on plant cytochromes b_{561} study suggested that they also utilize AsA as a physiological electron donating substrate (*15, 17-19*) to supply electron equivalents *via* transmembrane electron transfer to other reactions operative on the opposite side of the membranes (*20*). To perform this unique transmembrane electron transfer, two heme *b* prosthetic groups are each locating near the two highly-conserved sequences (the putative AsA-binding sequence on the cytosolic side and the putative MDA radical-binding sequence on the intravesicular side) (*7, 10*). This molecular architecture is consistent with a view that cytosolic heme *b* center has a role to receive an electron equivalent from cytosolic AsA and, after the intramolecular transmembrane electron transfer, the reduced heme center on the opposite side of the membranes donates the electron equivalent to MDA radical. In the case of neuroendocrine bovine cytochrome b_{561}, this postulation was verified using various biochemical and biophysical techniques (*11, 12, 21-23*).

For plant cytochrome b_{561}, however, there have been only a few detailed studies being conducted, although a form of *Arabidopsis* cytochrome b_{561} was reported to have reductase activities for ferric-chelates when expressed in *Saccharomyces cerevisiae* cells (*15*). For the putative physiological functions of plant cytochrome b_{561}, two possibilities might be raised. As one possible role, it might utilize AsA as the physiological substrate on the cytosolic side to re-generate AsA on the other side of membranes, as found for neuroendocrine cytochrome b_{561} in animals (*24-26*). Such re-generated AsA on the other side of biomembranes might be used for cell growth and cell division and/or coupling to other redox proteins (*5, 19*). The other possibility is that plant cytochrome b_{561} might work as a transmembrane ferrireductase to reduce ferric ion to ferrous state (*15*) and have an indirect role for the cellular iron absorption, as

proposed for Dcytb, a homolog of cytochrome b_{561} identified in the duodenal plasma membrane (*27*). Indeed, it was shown that a member of cytochrome b_{561} family had a ferrireductase activity more or less (*14, 28*). However, since the sub-cellular and tissue-specific localization of plant cytochrome b_{561} was still not completely understood (*6, 17-19, 29, 30*), it might be too early to make conclusive arguments. For the better understanding of the exact physiological role of this unique plant membrane protein, more detailed studies concerning the biochemical nature and molecular mechanism of transmembrane electron transfer reaction might be required.

Recently, we have succeeded in the construction of a heterologous expression system for *Zea mays* cytochrome b_{561} (Fig. 3-1) using methyltrophic yeast *Pichia pastoris* cells, established its purification procedure, and opened a new way for the detailed biochemical and biophysical analyses of plant cytochrome b_{561} (*20*). Our analysis using stopped-flow and pulse radiolysis techniques showed that purified wild-type *Zea mays* cytochrome b_{561} (WT-ZMb_{561}) protein had significant abilities for the electron acceptance from AsA and the electron donation to MDA radical (*20*). Further, our comparative study on WT-ZMb_{561} with bovine cytochrome b_{561} using a site-specific chemical modification technique demonstrated that the “concerted proton/electron transfer mechanism”, which was hypothesized to be operative in bovine cytochrome b_{561} upon electron acceptance from AsA (*31*), was likely to be operative in *Zea mays* cytochrome b_{561} as well (*20*). In our more recent study, we performed a site-directed mutagenesis study on this cytochrome b_{561} with particular interests on the conserved amino acid residues residing in the putative AsA and MDA radical binding sites (*32*). Three site-directed mutants, K83A, K83E, and K83D, showed a significant decrease in their electron accepting abilities from AsA both in the initial electron

transfer rate and in the final reduction level, indicating that Lys^{83} has a very important role for the binding of and electron transfer from AsA (*32*).

In the present study, we focused on two amino acid residues (Tyr^{71} and Arg^{72}) with a high conservation among the sequences of plant and animal cytochrome b_{561} as the targets for a detailed site-directed mutagenesis study (Fig. 3-1). Although these residues are locating on a cytosolic loop connecting the hydrophobic α-helices (helices 2 and 3) and are likely to have some roles for the electron acceptance from AsA rather than structural integrity of the cytochrome itself, their exact roles and mechanisms in the electron transfer reactions have scarcely been understood.

The first target residue, Tyr^{71} (corresponding to Tyr^{73} of bovine cytochrome b_{561}), is locating on the same loop with that of the Lys^{83} residue and is within a part of "motif1" (*7*) and putative "AsA-binding sequence" (*10*) (Fig. 3-1). Since the conservation of this Tyr residue is very high and is one of a few aromatic residues close to the cytosolic heme center, it might be very reasonable to assume having very important roles for the electron accepting reaction from AsA. To investigate the role of conserved aromatic side-chain group, we constructed and expressed two site-directed mutants, namely, Y71A-H_6 and Y71F-H_6.

The second and more important target residue in the present study was Arg^{72}, which is locating next to the Tyr^{71} residue in the same loop and is within a part of "motif1" (*7*) and putative "AsA-binding sequence" (*10*). More importantly, the positive-charge of this side-chain group might be participating in the direct interaction with AsA molecule, in collaboration with other positively-charged residues including Lys^{83} (*32*), which might have a guiding role upon the approach of AsA molecule to the substrate-binding site on the cytosolic side (Fig. 3-1). Further, AsA-dependent reduction

level assay on the site-directed mutants R72A of recombinant mouse cytochrome b_{561} in the yeast membrane fraction (*13*) and of recombinant bovine cytochrome b_{561} in purified state (*33*) indicated the importance of the positive-charge for the high-affinity AsA-binding. However, for the recombinant *Arabidopsis thaliana* cytochrome b_{561}, its K70A mutant (the corresponding position to the Arg^{72} of *Zea mays* cytochrome b_{561} was replaced with Lys residue in the *Arabidopsis* cytochrome b_{561}) in yeast microsomal membranes did not show any such effect (*34*). To solve these apparently contradictory results, we decided to construct three site-directed mutants, namely, R72A-H_6, R72D-H_6, and R72E-H_6.

To investigate the physiological and mechanistic roles of these conserved residues on the cytosolic side for the electron transfer reactions catalyzed by *Zea mays* cytochrome b_{561}, we performed detailed biochemical and biophysical analyses on each of the site-directed mutants in a highly purified state.

3-3. Materials and methods

Site-directed mutagenesis: The cloned full-length *Zea mays* cytochrome b_{561} (AB182641; DDBJ/EMBL/GenBank) was ligated into *EcoR*I-*Xba*I site of pPICZB vector, as described previously (*20*). We further introduced a hexa-histidine (6xHis) sequence at the 3' end of the *Zea mays* cytochrome b_{561} gene (*20*). The resulting expression vector, pPICZB-WTZMb_{561}-H_6, could express the recombinant *Zea mays* cytochrome b_{561} protein with a C-terminal hexa-histidine sequence (WT-ZMb_{561}-H_6) (Fig. 3-1). The amino acid sequence of its C-terminal part was, therefore, ^{211}GASVVVAAIAPVRLEEPQGYDPIPENHHHHHH^{242}). Site-specific mutations were,

then, introduced using Quickchange II site-directed mutagenesis kit (Stratagene Corp., La Jolla, CA). All the primers, which were used for the mutagenesis, are listed in Table 3-1. Five site-specific mutants with a C-terminal 6xHis-tag moiety (R72A-H_6, R72D-H_6, R72E-H_6, Y71A-H_6, and Y71F-H_6) were, thus, constructed. These constructs were each confirmed by DNA sequencing using an ABI 3100 Genetic Analyzer (Applied Biosystems, Foster City, CA).

Expression of Zea mays cytochrome b_{561} mutants in yeast, Pichia pastoris, cells: The resulting pPICZB plasmids containing modified or mutated *Zea mays* cytochrome b_{561} gene were each linearized with *Pme*I and were used for the transformation of *Pichia pastoris* cell strain GS115 (His^-, Mut^+). The transformation was performed according to the manufacture's procedure (Invitrogen, Carlsbad, CA). The transformants were selected on YPDS plates containing zeocin (100 μg/mL). Genomic DNA from *Pichia pastoris* integrants was extracted and PCR analysis was conducted to confirm the presence of the *Zea mays* cytochrome b_{561} gene at the aox1 locus, using primers in the alcohol oxidase promoter. The expression and purification of *Zea mays* cytochrome b_{561} mutants were followed by the procedure as described in our previous studies (*20, 32*).

Solubilization of microsomal membranes and purification of Zea mays cytochrome b_{561} mutants: The expressed wild-type *Zea mays* cytochrome b_{561} and its mutants were purified as follows. Yeast microsomal membrane fractions containing *Zea mays* cytochrome b_{561} (or its mutants) were solubilized with 1.0 % (w/v) *n*-octyl-β-D-glucoside (Anatrace, Maumee, OH) in 50 mM potassium-phosphate buffer (pH 7.0), 10 % (v/v) glycerol and 1 mM AsA (Na-ascorbate, Wako Pure Chemical Industries, Ltd., Osaka, Japan). After stirring at 4°C for 3h, the solubilized extracts were centrifuged at

20,000 rpm for 20 min. The detergent-solubilized cytochrome was concentrated and applied to a DEAE-Sepharose CL-6B (Amersham Bioscience, GE Healthcare Bio-Sciences, Buckinghamshire, England) ion exchange column that had been pre-equilibrated with 35 mM potassium-phosphate (pH 7.0) buffer. The adsorbed cytochrome in the column was eluted with 35 mM potassium-phosphate (pH 7.0) containing 1% *n*-octyl-β-D-glucoside (β-OG) and 1 mM AsA. After the analyses with SDS-PAGE and with measuring absorbance at 425 nm, active fractions were collected, combined, and concentrated. The concentrated sample was supplemented with 300 mM NaCl and 10 mM imidazole, and was applied to a 5 ml Ni-NTA agarose (QIAGEN, Hilden, Germany) column that had been equilibrated with buffer A (50 mM potassium-phosphate buffer, pH 7.0, containing 1% β-OG, 10% glycerol, 300 mM NaCl, 10 mM imidazole and 1 mM AsA). The column was then washed with 20 bed volumes of buffer A containing 10 mM imidazole. The 6xHis-tagged protein was eluted with buffer A containing 240 mM imidazole. The eluate was concentrated with a Millipore ultrafiltration membranes MWCO=30,000 (Millipore, Billerica, MA) and imidazole was removed by gel filtration on a PD-10 mini-column (Amersham Bioscience, GE Healthcare Bio-Sciences, Buckinghamshire, England) equilibrated with 50 mM potassium-phosphate (pH 7.0) buffer containing 1% β-OG. SDS-PAGE analysis was performed using 15% gels according to the method of Laemmli (*35*). The concentration of the purified *Zea mays* cytochrome b_{561} mutant was determined spectrophotometrically using a difference extinction coefficient of 27.7 $mM^{-1}cm^{-1}$ at 561 nm *minus* 575 nm in the reduced state (*9*). Final protein concentration was determined by a modified Lowry method (*36*).

MALDI-TOF mass spectrometory: Mass spectrometric analyses were

conducted with a Voyager DE Pro mass spectrometer (Applied Biosystems, Foster City, CA) using a 20-kV accelerating voltage. The mass spectra were acquired by adding the individual spectrum from 256 laser shots. For peptide analysis the samples were run in a reflector mode. Other experimental conditions were essentially the same as in previously described (*11, 12, 20*). All the *Zea mays* cytochrome b_{561} mutant proteins (Y71A-H_6, Y71F-H_6, R72A-H_6, R72D-H_6, and R72E-H_6) and the recombinant wild-type protein (WT-ZMb_{561}-H_6) (~100 μM) were each digested either with TPCK-treated trypsin (0.01 mg/mL) or *Staphyrococcus aureus* V8 protease (0.01 mg/mL), respectively. After 48h of incubation at room temperature, the peptide solutions were diluted 1:9 (v/v) with a matrix solution (α-cyano-4-hydroxycinamic acid (Aldrich, Gillingham, England), 50 mg/ml in 50% acetonitrile in 0.3% TFA). The mixtures (typically, 1.0 μL) were deposited on the sample plate, allowed to air-dry, and analyzed. The search of the corresponding fragments in the amino acid sequence of *Zea mays* cytochrome b_{561} mutants was conducted using the program GPMAW (v 6.11) (Lighthouse Data, Odense M, Denmark).

AsA-reduction level assay: All six purified *Zea mays* cytochrome b_{561} mutants (Y71A-H_6, Y71F-H_6, R72A-H_6, R72D-H_6, and R72E-H_6) and the wild-type protein (WT-ZMb_{561}- H_6) were each diluted to 1 μM with 50 mM potassium-phosphate buffer (pH 7.0, 6.0) or 50 mM sodium acetate buffer (pH 5.0) each containing 1.0 % (w/v) *n*-octyl-β-glucoside. After 30 min of incubation at room temperature, UV-visible absorption spectra of the mutants in oxidized and dithionite-reduced states were measured in the region from 700 to 200 nm with a UV-2400PC spectrophotometer (Shimadzu Corp., Kyoto, Japan). For the AsA-reduced state of the mutants, the absorbance change at 425 nm was kept measured for 30 min after the addition of AsA

(10 mM) and, then, the spectra were recorded. The final reduction level with AsA as a reductant was calculated based on the dithionite-reduced form as the 100 % reduction level.

DEPC treatment of Zea mays cytochrome b_{561}: The oxidized WT-ZMb_{561}- H_6 and four purified *Zea mays* cytochrome b_{561} mutants (Y71A-H_6, R72A-H_6, R72D-H_6, R72E-H_6) solution was diluted to 10 μM with 50 mM potassium-phosphate buffer (pH 7.0) containing 1.0% (w/v) *n*-octyl-β-glucoside. The sample was treated with 0.5 mM diethylpyrocarbonate (DEPC) (Wako Pure Chemical Industries, Ltd., Osaka, Japan) for 30 min, as previously described (*11, 12, 20*). The DEPC-treated samples were gel-filtered through a PD-10 column equilibrated with 50 mM potassium-phosphate buffer (pH 7.0) containing 1.0 % (w/v) *n*-octyl-β-glucoside to remove the un-reacted DEPC. During the DEPC treatment, difference spectra in UV-visible region were recorded with a UV-2400PC spectrophotometer (Shimadzu Corp., Kyoto, Japan).

Stopped-flow analysis of the Zea mays b_{561} mutants: Rapid kinetic measurements were carried out using an RSP-1000-03DR stopped-flow spectrometer (UNISOKU, Osaka, Japan). Purified site-directed mutants (Y71A-H_6, Y71F-H_6, R72A-H_6, R72D-H_6, and R72E-H_6) and the recombinant wild-type protein (WT-ZMb_{561}-H_6) were each diluted to 2 μM with 50 mM potassium-phosphate buffer (pH 7.0, 6.0) or 50 mM sodium acetate buffer (pH 5.0) each containing 1.0 % (w/v) *n*-octyl-β-glucoside. After 30 min of incubation at room temperature, the protein solution and AsA solution were loaded into a different chamber of the apparatus, respectively. The temperature of both chambers was maintained at 20 °C by connecting to a thermo-bath. The mixing of the two solutions was carried out with a 1:1 volume ratio and the heme absorbance change at 427 nm due to the reduction with AsA was

recorded against time. Data points were collected in every 250 μsec for the measurements of time duration of 1 sec and in every 2.5 msec and 15 msec for the measurements of time duration of 10 sec and 60 sec, respectively. Both Igor Pro software (v. 6.03) and a built-in software of the stopped-flow apparatus were used for the data analyses. Other experimental conditions were described previously (*37*).

3-4. Results

Purification and MALDI-TOF mass spectrometric analyses of the site-directed mutants: The core procedure used for the purification of site-directed mutants in the present study was based on the Ni^{2+}-NTA agarose affinity chromatography by utilizing C-terminal hexa-histidine sequence. For the evaluation with various spectroscopic and biochemical techniques, we could obtain sufficient amounts of purified samples from the yeast microsomal fractions containing heterologously expressed *Zea mays* b_{561} protein.

To verify the introduction of site-specific mutation in the expressed protein, we conducted MALDI-TOF mass spectrometric analyses on the digested peptides for each of the mutants. In the case of wild-type protein (WT-ZMb_{561}-H_6), the identified region covered 9-242 residues for tryptic peptides and 2-235 residues for V8 protease peptides. In the case of Arg^{72} mutants (R72A-H_6, R72D-H_6, R72E-H_6), the identified region covered 9-242 residues for tryptic peptides and 2-235 residues for V8 protease peptides. Substitutions of Arg^{72} residue with Ala, Asp, and Glu were directly confirmed by the inability of cleavage with trypsin at this site and by the decreases of mass (85.1 for Ala; 41.1 for Asp; 27.1 for Glu) for the peptides containing the substitutions, respectively

(Tables 3-2 and 3-3). Typical examples are shown in Figure 3-2, where the V8-protease-cleved peptides of WT-ZMb_{561}-H_6, R72A-H_6, R72D-H_6, and R72E-H_6 were aligned in the region from 6500 to 8500 m/z to visualize the site-specific substitution of the Arg^{72} residue. Another example is shown in Figure 3-3, where the tryptic peptides of WT-ZMb_{561}-H_6, R72A-H_6, R72D-H_6, and R72E-H_6 were aligned in the region from 3000 to 4500 m/z to visualize the site-specific substitution of the Arg^{72} residue. For the case of Y71A-H_6, we identified tryptic peptides covering 9-223 residues and V8 protease peptides covering 2-235 residues, respectively. Substitution of the Tyr^{71} residue with Ala was directly confirmed in both samples by the decrease of mass (92.1) for the peptides containing the substitution (Tables 3-4 and 3-5 and Figures 3-4 and 3-5). In the case of Y71F-H_6, substitution of the Tyr^{71} residue with Phe was similarly confirmed in both V8 protease-treated and trypsin-treated samples by the decrease of mass (16.0) for the peptides containing the substitution (Figures 3-4 and 3-5). It must be noted that there was neither undesirable mutation being introduced nor any other type(s) of post-translational modification being occurred. In addition, we could not identify peptides containing the initiation Met residue for all the mutants examined, being consistent with the result of NH_2-terminal protein sequencing analyses for both WT-ZMb_{561}-H_6 (present study) and WT-ZMb_{561} (*20*).

Visible absorption spectra of purified Zea mays cytochrome b_{561} and its site-specific mutants: All of the purified recombinant wild-type protein (WT-ZMb_{561}-H_6) and its site-directed mutants (Y71A-H_6, Y71F-H_6, R72A-H_6, R72D-H_6, and R72E-H_6) showed characteristics visible absorption spectra with peaks at 414 nm for the oxidized form and at 561, 529, and 427 nm for the dithionite-reduced form. Figure 3-6 shows the spectra of R72A-H_6 mutant as a representative example (for

other mutants, spectra are not shown), very similar to those of wild-type cytochrome b_{561} (WT-ZMb_{561}) (*20*) and of bovine cytochrome b_{561} (*9*) both in oxidized and in sodium dithionite-reduced states. These results suggested that all the mutations introduced in the present study were not affecting the overall structure of the ZMb_{561} molecule or even the local structures around the immediate surroundings of the two heme *b* centers.

The pH-dependent behavior of the final reduction level: To evaluate the overall influences of the mutations introduced, we investigated the final heme reduction level with AsA (10 mM) as a reductant in different pH (Fig. 3-7). At pH 7.0, addition of AsA (10 mM) to the oxidized WT-ZMb_{561}-H_6 caused a quick reduction of heme *b* reaching the final reduction level of ~80%, as previously reported (*20*), being consistent with the notion that *Zea mays* cytochrome b_{561} utilize AsA as a physiological reductant in maize cells. Three site-directed mutants (R72A, R72D, and R72E) for the Arg^{72} residue, which is locating on the cytosolic side of the molecule, did not show any significant change in the final heme reduction level. Further, they did not show any significant pH-dependency.

On the other hand, Y71A-H_6 mutant showed a much lower heme reduction level than those of WTZMb_{561}-H_6 and slight pH-dependent changes in the electron transfer activity with AsA as a reductant. Y71F-H_6 mutant showed a very different property from those of WTZMb_{561}-H_6 and other mutants. It showed a very high reduction level at pH5.0, whereas at pH 6.0 and 7.0 its reduction level was somewhat low (45~50%) (Fig. 3-7).

Inhibition of the electron accepting ability of purified Zea mays cytochrome b_{561} and its site-specific mutants from AsA upon modification with DEPC: Previously

we used diethylpyrocarbonate (DEPC) for the studies on the electron transfer mechanism of cytochromes b_{561} (*11, 12, 20*). DEPC is well known as a chemical modification reagent possessing high selectivity toward a deprotonated nitrogen atom of an imidazole ring of His residues (*38*) and with a lesser reactivity to Lys, Tyr or other residues. When the DEPC treatment was done on the purified WT-ZMb_{561}-H_6 in oxidized state (DEPC : WT-ZMb_{561}-H_6 = 16 : 1), slight but clear absorbance changes in both UV and Soret regions occurred (Fig. 3-8A). The changes in the UV region around 240 nm was due to the *N*-carbethoxylation of the His residues (Fig. 3-8A, inset). Extent of the *N*-carbethoxylation was calculated based on the absorbance change at 240 nm (ΔA_{240}) using a molar extinction coefficient of 3.2 $mM^{-1}cm^{-1}$ for *N*-carbethoxylated histidine (*38*) and was found as 2.54 residues per molecule for WT-ZMb_{561}-H_6, and around 2.2 residues for the mutants irrespective to the positions of the site-directed mutation. The concerted progress in absorbance change at the Soret and UV regions (Fig. 3-8A) was consistent with the notion that the *N*-carbethoxylation of His residues occurred at or near the heme center. As observed for bovine cytochrome b_{561} (*11*) and WT-ZMb_{561} (*20*), we found that major modification sites with DEPC as His^{86}, His^{159}, and Lys^{83} (and non-conservative His^{17} with a slightly lower extent). Considering the total number of His residues in the deduced amino acid sequence of WT-ZMb_{561} (*20*) (8 residues) and the additional C-terminal His-tag moiety (6 residues), these small values indicated a site-specific *N*-carbethoxylation being occurred at the heme-cooridinating His residues (His^{86}, His^{159}) of *Zea mays* cytochrome b_{561}.

Interestingly, we found that the DEPC-treatment of *Zea mays* cytochrome b_{561} caused a significant inhibition of its electron acceptance ability from AsA both in the final reduction level (Fig. 3-8B) and in the apparent rate constant (Fig. 3-8C). As shown

in Figure 3-8B, visible absorption spectrum of the DEPC-pretreated WT-ZMb_{561}-H_6 after the addition of AsA (10 mM) showed no clear development of sharp peaks around α and β region; however, in the dithionite-reduced state, there were clear peaks at 561, 530, and 427 nm in the absorption spectrum, indicating full-reduction of the two heme centers. The final heme reduction level of the DEPC-treated *Zea mays* cytochrome b_{561} with AsA (10 mM) as a reductant was around 35% based on the absorption at 561 and 427 nm. This specific inhibition of the electron acceptance ability from AsA caused by the DEPC-modification had a very similar precedence for bovine cytochrome b_{561} (*11, 12*), as previously reported based on the analysis for WT-ZMb_{561} (*20*). Upon the DEPC treatment of four site-directed mutants (Y71A-H_6, R72A-H_6, R72D-H_6, and R72E-H_6), a similar inhibition of the electron acceptance from AsA (with 20~40% final heme reduction level and the slowed electron transfer rate) was observed at pH 7.0. A typical example was shown in Figure 3-8 (D) for Y71A-H_6, in which a significant inhibition of the electron transfer reaction from AsA by the DEPC-treatment was obvious. These observations suggested that the conserved Arg^{72} and Tyr^{71} residues are not directly related to the DEPC-modification-related inhibition of the electron transfer from AsA. Further, possible structural changes induced by these site-directed mutations did not affect significantly on the overall inhibition mechanism caused by the DEPC-modification.

Stopped-flow analyses of Zea mays cytochrome b_{561} and its site-specific mutants on the electron acceptance activity from AsA: The electron acceptance reaction of oxidized WT-ZMb_{561}-H_6 and its site-directed mutants were further analyzed by stopped-flow spectrometry (Fig. 3-9). The absorbance change at 427 nm after mixing of oxidized form of WT-ZMb_{561}-H_6 (final 1 μM) with AsA (final 2 mM) was presented

against time in logarithmic scale (Fig. 3-9A) as representative examples. The result showed that, in the initial phase of the electron acceptance from AsA, the heme reduction rate of WT-ZMb_{561}-H_6 was much slower at pH 5.0 than that measured at pH 7.0, as observed for bovine cytochrome b_{561} (*22*) and for WT-ZMb_{561} (*20*). On the other hand, such an initial time-lag at pH 5.0 was almost completely absent in R72A-H_6 (Fig. 3-9B) and R72E-H_6 (Fig. 3-9C) mutants. For the R72D-H_6 mutant, the initial time-lag at pH 5 still persisted but with a much reduced extent (Fig. 3-9D). It might be stressed that there were not so much pH dependency in the initial apparent rate constants for R72A and R72E mutants and these values were very similar to those of WT-ZMb_{561}-H_6 measured at pH 6.0.

The time-courses of the reduction process of both Y71A-H_6 and Y71F-H_6 mutants with AsA were also analyzed by stopped-flow spectrometry. In the case of Y71A-H_6, the initial time-lag at pH 5 was almost absent (Fig. 3-9E). Further, over all reduction process of Y71A-H_6 with AsA as a reductant was similar to (or even faster than) those of R72A-H_6 (Fig. 3-9B) and R72E-H_6 (Fig. 3-9C) mutants. Acceleration of the electron transfer from AsA at pH 5 was clearly seen for Y71F-H_6 mutant (Fig. 3-9F) in comparison with the time-courses of WT-ZMb_{561}-H_6 and the R72 mutants.

For clarification of these analyses based on the logarithmic time-scale plots, we also calculated the apparent rate constants (k_{app} (sec^{-1})) of the reduction processes corresponding to the plotted data in Figure 3-9. For the calculation, we assumed a single exponential decay for the initial 10 sec and 60 sec after the mixing with AsA for the simplicity. It is obvious from Table 3-6 that WT-ZMb_{561}-H_6 and R72D- H_6 showed much smaller k_{app} values at pH 5 compared to those of R72A- H_6, R72E-H_6, and Y71A-H_6 at pH 5. On the other hand, Y71F-H_6 showed distinctly large k_{app} values at pH

5, about 7~8 times larger than the corresponding values of WT-ZMb_{561}-H_6 and 3~4 times larger than those of R72A-H_6, R72E-H_6, and Y71A-H_6. Thus, we can conclude, from the data in Figure 3-9 and Table 3-6, that the substitution of Arg^{72} with Ala or Glu caused a significant suppression of the characteristic pH-dependent time-lag in the electron acceptance from AsA and, further more, substitution of Tyr^{71} with Phe caused a significant acceleration of the electron acceptance from AsA.

3-5. Discussion

Electrochemistry of AsA and its relation to the electron transfer to the heme center of cytochrome b_{561}: An AsA molecule has two acidic protons (pK_{a1}=4.04 and pK_{a2}=11.34) (*39*). Therefore, three species, ascorbic acid (H_2AsA), ascorbate monoanion ($HAsA^-$), and ascorbate dianion (AsA^{2-}), are present in solution, with the monoanion form as a predominant species at a physiological pH. On the other hand, MDA monoanion (MDA^-) radical, the one-electron oxidized form of AsA, is invariant in the pH range 0-13 and its protonated form is virtually non-existent under physiological conditions (*26, 39, 40*). Since the predominant monoanion form ($HAsA^-$) is not a good electron donor and the scarce dianion form (AsA^{2-}) is a much powerful electron donor, Njus and Kelley (*26*) postulated that cytochrome b_{561} has such a molecular mechanism to withdraw a proton from a monoanion form to facilitate the electron transfer to the heme iron ("concerted H^+/e^- transfer mechanism"). We extended their model to include the imidazole group of the cytosolic heme axial His ligand as such a site for the proton acceptance (*31*). Our model can explain reasonably (i) the high-affinity DEPC-modification of the cytosolic heme axial His reside (*11*), (ii)

specific inhibition of electron transfer from AsA by DEPC-modification (*11*), and (iii) protection of the imidazole *N*-carbethoxylation from DEPC by inclusion of AsA during the DEPC-treatment (*12*). In our previous (*20*) and present studies on the DEPC-modification of *Zea mays* cytochrome b_{561} showed that (i) there were three major modification sites (Lys^{83}, His^{86} and His^{159}), (ii) *N*-carbethoxylation of the heme axial ligands (His^{86} and His^{159}) caused the inhibition of electron transfer from AsA and (iii) inclusion of AsA during the treatment with DEPC protected the electron accepting ability from AsA. All these observations suggested strongly that the "concerted H^+/e^- transfer mechanism" at the cytosolic heme center (*31*) is operative in plant cytochrome b_{561} as well.

Possible roles of the highly conserved residues on the cytosolic side: From the considerations discussed in the previous section, we might expect four groups of amino acid residues that participate in the efficient electron acceptance from AsA on the cytosolic side; namely, (A) residues responsible for helping the approach of AsA to the AsA-binding site and for its recognition, (B) residues responsible for the stabilization of AsA at the AsA-binding site, which may also participate to provide a route for the electron transfer to the oxidized heme, (C) residues responsible for withdrawing and transferring a proton from AsA (from 2-OH), which may also have a role to provide a route for the electron transfer, and (D) residues responsible for expelling MDA radical from the AsA-binding site to prevent the reverse electron flow.

Previous site-specific chemical modification study on bovine cytochrome b_{561} using DEPC suggested the importance of Lys^{85} residue (corresponding to Lys^{83} of *Zea mays* cytochrome b_{561}) for the quick electron acceptance from AsA (*11, 12*). Indeed, Lys^{85} is well conserved among animal and plant cytochromes b_{561} (*10*). Our recent study

on WT-ZMb_{561} (*20*) (and present study on WT-ZMb_{561}-H_6) using a same strategy indicated that Lys^{83} had a similar high reactivity towards DEPC with that of Lys^{85} of bovine cytochrome b_{561} and such specific DEPC-modification at this Lys^{83} caused a significant retardation of the electron transfer from AsA. These results suggested an important role(s) of the conserved Lys^{83} residue in plant cytochrome b_{561} as well for the electron acceptance from AsA (*20*). Mechanistic role(s) of this positively-charged residue was further analyzed by three site-specific mutants, K83A, K83D, and K83E in our previous study (*32*). Stopped-flow analyses for these mutants showed that the duration of the initial time-lag was much longer than that of WT-ZMb_{561} in all the pH regions measured, causing a significant retardation of the electron transfer. These observations were consistent with the notion that a positive charge of the Lys^{83} residue in the physiological pH region would have an electrostatic interaction with a negatively-charged AsA molecule, as previously proposed (*22*). Thus, Lys^{83} residue can be classified clearly as group A.

In the present study, DEPC-treatment of WT-ZMb_{561}-H_6 and four site-specific mutants (Y71A-H_6, R72A-H_6, R72D-H_6, and R72E-H_6) showed similar inhibitory effects in their electron acceptance from AsA with that found for WT-ZMb_{561}. It might be noted further that DEPC-treatment of K83A mutant of *Zea mays* cytochrome b_{561} also showed a similar inhibition of the electron acceptance from AsA (Nakanishi *et al*., unpublished), in which only the heme axial His residue(s) were potential modification sites. These results suggested strongly that the specific *N*-carbethoxylation of the heme axial His residue(s) was the major cause of the inhibition of electron acceptance from AsA. Thus, based on our "concerted H^+/e^- transfer mechanism" at the cytosolic heme center (*31*), we could conclude that His^{86} residue might be classified as group C.

Possible mechanistic roles of Arg^{72}: Both Arg^{72} and Tyr^{71} residues are locating in the putative AsA-binding sequence, and they are well-conserved among the members of neuroendocrine and plant cytochrome b_{561} protein subfamilies. Particularly, Arg^{72} was proposed as an important residue for the interaction with AsA because of its positive charge and the high conservations (*13*). In the past, several X-ray crystal structures for the AsA-bound enzyme form were reported; such as ascorbate peroxidases (*41*), hyaluronate lyase (*42*), and mirosinase (*43*). In all of these structures, Arg residue seemed to have essential roles for the AsA-binding at the active sites (*44*), in which the side-chains of Arg residue were interacted with the 2-O and 3-O atoms (*41*), 1-O and 2-O atoms (*42*), 1-O and 2-O atoms (*43*) of the bound AsA molecule *via* hydrogen bonding, respectively.

Indeed, site-directed mutagenesis study on mouse recombinant CGCytb in the yeast membrane fraction indicated that mutation of Arg^{72} to Ala abolished high affinity heme reduction by AsA (*13*). Further, site-directed mutagenesis studies on LCytb showed that mutation of Arg^{67} (corresponding to Arg^{72}) to Ala resulted in an almost complete loss of the activity in the yeast cell-surface ferric reductase assay (*14*). However, present results on the Arg^{72} mutants did not support these observations and were not consistent with the notion that the Arg^{72} residue provides an electrostatic substrate-binding site for AsA to facilitate the electron transfer. Removal of the positive charge by substitution with Ala (R72A) or conversion to a negative-charged residue by substitution with Asp (R72E) did not cause any retardation of the electron transfer from AsA at all in a neutral pH when analyzed with stopped-flow spectrometry. More interestingly, the initial time-lag observed for bovine b_{561} (*22*) and WT-ZMb_{561} (*20*) (and in the present study for WT-ZMb_{561}-H_6) observed in an acidic pH (pH 5) was

completely lost in these mutants. However, for the R72D mutant, the initial time-lag was somewhat conserved and the apparent rate constants were still slower at pH 5 (Table 3-6). These results suggest that the Arg^{72} residue has a different mechanist role in the electron acceptance from that of Lys^{83}. In an acidic pH, the major $HAsA^-$ and the minor H_2AsA forms are in equilibrium and somehow the Arg^{72} residue stabilizes the bound AsA to shift the equilibrium in favoring the H_2AsA form, although this will not occur in the physiological conditions (the pH on the cytosolic side ~7). In this stabilized structure, a proton (of 2-OH group) could not be removed from AsA and, therefore, a significant initial time-lag might be observed. However, substitution of the positive side-chain with a neutral or a negative group might cause an easier release of a proton from the bound AsA leading to the faster electron transfer from AsA to the heme iron. In the case of R72D mutant, however, there was no such promoting effect for the proton release, possibly due to a shorter side-chain of Asp^{72} than that of Glu^{72} of R72E. If so, what is the physiological role of the stabilization of the bound AsA by the Arg^{72} residue in a lower pH region? The most-likely explanation is that the Arg^{72} residue may have a role to destabilize the binding of MDA monoanion (MDA^-) radical at the AsA-binding site to prevent the reverse electron flow. Fine discrimination between MDA monoanion (MDA^-) radical and ascorbate monoanion ($HAsA^-$) might be possible since the former has the unpaired electron spread over a highly conjugated tricarbonyl system (*45*) and is presumably much planar than the latter. It might be quite reasonable for bovine cytochrome b_{561} in the chromaffin vesicle membranes to have this kind of molecular mechanism since there are sufficient amounts of intravesicular (~10 mM) and cytosolic (~5 mM) AsA and, therefore, the cytochrome b_{561} is almost in the fully-reduced state and, accordingly, prevention of the reverse electron transfer might be a primary

importance. Such a molecular mechanism might be present in plant cytochromes b_{561} as well.

Possible mechanist roles of Tyr^{71}: In the present study for the two Tyr^{71} mutants, we did observe some significant influences of the mutations on the final heme reduction level with AsA as a reductant, but in a different way. Y71A-H_6 showed a lower heme reduction level than those of WTZMb_{561}-H_6. On the other hand, Y71F-H_6 mutant showed a very high reduction level at pH5.0, whereas at pH 6.0 and 7.0 its reduction level was much lower (45~50%) than that of WTZMb_{561}-H_6. Stopped-flow analysis of Y71A mutant did not show any drastic retardation in the electron acceptance from AsA in neutral pH. However, again, the characteristic initial time-lag was almost absent in an acidic pH. In the case of Y71F mutant, all the steps of the electron transfer from AsA seemed to be accelerated, particularly in a lower pH. These results indicated that the mechanistic role of the Tyr^{71} might be also very complex.

In our previous study, the EPR spectra of oxidized Y71A mutant measured at 5 and 15K showed that the low-spin species with the HALS character, which has been assigned to the cytosolic heme center, was actually composed of two species with slightly different g_z values (g_z=3.7 and 3.59) (*32*). This g_z signal (g_z=3.59) was not observed in those of oxidized WT-ZMb_{561} and K83A measured at 5 and 15K. On the other hand, the other low-spin species (g_z=3.2) assignable to the intravesicular heme center remained intact. These results suggested that the coordination structure of the cytosolic heme center was slightly perturbed upon the mutation of the Tyr^{71} residue and such an alteration might become apparent only in a low temperature. However, such slight changes would not affect the dynamic interaction of the cytosolic heme center with AsA and the electron acceptance ability from it at room temperature. Based on

these results, we concluded previously that Tyr^{71} would contribute to the structural role for the stability around the cytosolic heme center of cytochrome b_{561} rather than the direct interaction with AsA (*32*), despite of its rather high conservation in the amino acid sequences of many cytochromes b_{561} (*7, 10*).

Present result suggested, however, that the Tyr^{71} residue has an additional role for the electron acceptance from AsA but in a later stage of the reaction, possibly by destabilizing the bound MDA radical and driving it out from the substrate-binding site. In our proposed scenario, phenol –OH group of Tyr^{71} in collaboration with Arg^{72} residue might have specific interactions with the bound AsA in favoring the H_2AsA form and the release of 2-OH proton from the bound AsA might be inhibited in a lower pH. Indeed, such an example for the interaction between a Tyr residue and a bound AsA is proposed for a plant heme oxygenase (*44*). For a planar MDA radical without 2-OH group, the Tyr71 residue would not have any preference and the MDA radial might be released. Therefore, substitution of the Tyr^{71} residue with Ala will abolish such specific interactions in a lower pH leading to a prompt release of the proton leading to the faster electron transfer. Further, conversion to the hydrophobic environments would promote the release of MDA radical. This interpretation might be supported by the observation that the Y71A mutant showed a very similar property with that of the R72A mutant. Substitution of Tyr^{71} residue with a more hydrophobic Phe residue would enhance such promoting effect by changing the nature of the substrate-binding pocket. Indeed such promoting effect was verified in our present study. Thus, we propose that both Arg^{72} and Tyr^{71} residues can be classified as group D and have roles for expelling MDA radical from the AsA-binding site to prevent the reverse electron flow. To verify our present proposal,

however, a detailed structural data from X-ray crystallographic study might be necessary.

We are still in progress to clarify the mechanistic roles of other conservative residues, which might be working for the interactions with other possible redox partners on the cytosolic and intravesicular side of *Zea mays* cytochrome b_{561}. Further, some conserved residues locating within the hydrophobic α-helices, which might have some roles in the intramolecular electron transfer from the cytosolic heme to the intravesicular heme centers, are also our current targets. Such results will be reported in near future.

3-6. References

1. Asard, H., Venken, M., Caubergs, R., Reijnders, W., Oltmann, F. L., and De Greef, J. A. (1989) *b*-Type cytochromes in higher plant plasma membranes, *Plant Physiol*. **90**, 1077-1083.
2. Scagliarini, S., Rotino, L., Bäurle, I., Asard, H., Pupillo, P., and Trost, P. (1998) Intial purification study of the cytochrome b_{561} of bean hypocotyl plasm membrane, *Protoplasma*. **205**, 66-73.
3. Trost, P., Bèrczi, A., Sparla, F., Sponza, G., Marzadori, B., Asard, H., and Pupillo, P. (2000) Purification of cytochrome b_{561} from bean hypocotyls plasma membrane. Evidence for the presence of two heme centers, *Biochim. Biophys. Acta*. **1468**, 1-5.

4. Bérczi, A., Lüthje, S., and Asard, H. (2001) *b*-Type cytochromes in plasma membranes of *Phaseolus vulgaris* hypocotyls, *Arabidopsis thaliana* leaves, and *Zea mays* roots, *Protoplasma*, **217**, 50-55.
5. Asard, H., Kapila, J., Verelst, W., and Bérczi, A. (2001) Higher-plant plasma membrane cytochrome b_{561}: a protein in search of a function, *Protoplasma*. **217**, 77-93.
6. Bérczi, A., Caubergs, R. J., and Asard, H. (2003) Partial purification and characterization of an ascorbate-reducible *b*-type cytochrome from the plasma membrane of *Arabidopsis thaliana* leaves, *Protoplasma*. **221**, 47-56.
7. Tsubaki, M., Takeuchi, F., and Nakanishi, N. (2005) Cytochrome b_{561} protein family: Expanding roles and versatile transmembrane electron transfer abilities as predicted by a new classification system and protein sequence motif analyses, *Biochim. Biophys. Acta*. **1753**, 174-190.
8. Asard, H., Terol-Alcayde, J., Preger, V., Del Favero, J., Verelst, W., Sparla, F., Pérez-Alonso, M., and Trost, P. (2000) *Arabidopsis thaliana* sequence analysis confirms the presence of cyt *b*-561 in plants: Evidence for a novel protein family, *Plant Physiol. Biochem*. **38**, 905-912.
9. Tsubaki, M., Nakayama, M., Okuyama, E., Ichikawa, Y., and Hori, H. (1997) Existence of two heme *b* centers in cytochrome b_{561} from bovine adrenal chromaffin vesicles as revealed by a new purification procedure and EPR spectroscopy, *J. Biol. Chem*. **272**, 23206-23210.
10. Okuyama, E., Yamamoto, R., Ichikawa, Y., and Tsubaki, M. (1998) Structural basis for the electron transfer across the chromaffin vesicle membranes catalyzed by cytochrome b_{561}: Analyses of cDNA nucleotide sequences and visible absorption

spectra, *Biochim. Biophys. Acta*. **1383**, 269-278.

11. Tsubaki, M., Kobayashi, K., Ichise, T., Takeuchi, F., and Tagawa, S. (2000) Diethylpyrocarbonate-modification abolishes fast electron accepting ability of cytochrome b_{561} from ascorbate but does not influence on electron donation to monodehydroascorbate radical: Distinct roles of two heme centers for electron transfer across the chromaffin vesicle membranes, *Biochemistry*. **39**, 3276-3284.
12. Takeuchi, F., Kobayashi, K., Tagawa, S., and Tsubaki, M. (2001) Ascorbate inhibits the carbethoxylation of two histidyl and one tyrosyl residues indispensable for the transmembrane electron transfer reaction of cytochrome b_{561}, *Biochemistry*. **40**, 4067-4076.
13. Bérczi, A., Su, D., Lakshminarasimhan, M., Vargas, A., and Asard, H. (2005) Heterologous expression and site-directd mutagenesis of an ascorbate-reducible cytochrome b_{561}, *Arch. Biochem. Biophys*. **443**, 82-92.
14. Su, D., and Asard, H. (2006) Three mammalian cytochrome b_{561} are ascorbate-dependent ferrireductases, *FEBS J*. **273**, 3722-3734.
15. Bérczi, A., Su, D., and Asard, H. (2007) An *Arabidopsis* cytochrome b_{561} with *trans*-membrane ferrireductase capaility, *FEBS Lett*. **581**, 1505-1508.
16. Kamensky, Y., Liu, W., Tsai, A.-L., Kulmacz, R. J., and Palmer, G. (2007) The axial ligation and stoichiometry of heme centers in adrenal cytochrome b_{561}, *Biochemistry*. **46**, 8647-8658.
17. Griesen, D., Su, D., Bérczi, A., and Asard, H. (2004) Localization of an ascorbate-reducible cytochrome b_{561} in the plant tonoplast, *Plant Physiol*. **134**, 726-734.
18. Preger, V., Scagliarini, S., Pupillo, P., and Trost, P. (2005) Identification of an

ascorbate-dependent cytochrome *b* of the tonoplast membrane sharing biochemical features with members of the cytochrome b_{561} family, *Planta*. **220**, 365-375.

19. Nanasato, Y., Akashi, K., and Yokota, A. (2005) Co-expression of cytochrome b_{561} and ascorbate oxidase in leaves of wild watermelon under drought and high light conditions, *Plant Cell Physiol*. **46**, 1515-1524.
20. Nakanishi, N., Rahman, M. M., Takigami, T., Kobayashi, K., Hori, H., Hase, T., Park, S.-Y., and Tsubaki, M. (2008) Functional expression of *Zea mays* cytochrome b_{561} in yeast *Pichia pastoris:* Properties of an ascorbate-specific plant transmembrane electron transfer protein, *Biochemistry (submitted)*.
21. Kobayashi, K., Tsubaki, M., and Tagawa, S. (1998) Distinct roles of two heme centers for transmembrane electron transfer in cytochrome b_{561} from bovine adrenal chromaffin vesicles as revealed by pulse radiolysis, *J. Biol. Chem*. **273**, 16038-16042.
22. Takigami, T., Takeuchi, F., Nakagawa, M., Hase, T., and Tsubaki, M. (2003) Stopped-flow analyses on the reaction of ascorbate with cytochrome b_{561} purified from bovine chromaffin vesicle membranes, *Biochemistry*. **42**, 8110-8118.
23. Seike, Y., Takeuchi, F., and Tsubaki, M. (2003) Reversely-oriented cytochrome b_{561} in reconstituted vesicles catalyzes transmembrane electron transfer and supports the extravesicular dopamine β-hydroxylase activity, *J. Biochem*. **134**, 859-867.
24. Njus, D., Knoth, J., Cook, C., and Kelley, P. M. (1983) Electron transfer across the chromaffin granule membrane, *J. Biol. Chem*. **258**, 27-30.
25. Kelley, P. M., and Njus, D. (1986) Cytochrome b_{561} spectral changes associated with electron transfer in chromaffin-vesicle ghosts, *J. Biol. Chem*. **261**, 6429-6432.
26. Njus, D., and Kelley, P. M. (1993) The secretory-vesicle ascorbate-regenerating system: a chain of concerted H^+/e^--transfer reactions, *Biochim. Biophys. Acta*. **1144**,

235-248.

27. Mckie, A. T., Barrow, D., Latunde-Dada, G. O., Rolfs, A., Sager, G., Mudaly, E., Mudaly, M., Richardson, C., Barlow, D., Bomford, A., Peters, T. J., Raja, K. B., Shirali, S., Hediger, M. A., Farzaneh, F., and Simpson, R. J. (2001) An iron-regulated ferric reductase associated with the absorption of dietary iron, *Science*. **291**, 1755-1759.
28. Vargas, J. D., Herpers, B., Mckie, A. T., Gledhill, S., McDonnell, J., van der Heuvel, M., Davies, K. E., and Ponting, C. P. (2003) Stromal cell-derived receptor 2 and cytochrome b_{561} are functional ferric reductase, *Biochim. Biophys. Acta*. **1651**, 116-123.
29. Verelst, W., Kapila, J., de Almeida Engler, J., Stone, J. M., Caubergs, R. J., and Asard, H. (2004) Tissue-specific expression and developmental regulation of cytochrome b_{561} genes in *Arabidopsis thaliana* and *Raphanus sativus*, *Physiol. Planta*. **120**, 312-318.
30. Shimaoka, T., Ohnishi, M., Sazuka, T., Mitsuhashi, N., Hara-Nishimura, I., Shimazaki, K.-I., Maeshima, M., Yokota, A., Tomizawa, K.-I., and Mimura, T. (2004) Isolation of intact vacuoles and proteomic analysis of tonoplast from suspension-cultured cells of *Arabidopsis thaliana*, *Plant Cell Physiol*. **45**, 672-683.
31. Nakanishi, N., Takeuchi, F., and Tsubaki, M. (2007) Histidine cycle mechanism for the concerted proton/electron transfer from ascorbate to the cytosolic heme *b* center of cytochrome b_{561}: A unique machinery for the biological transmembrane electron transfer, *J. Biochem*. **142**, 553-560.
32. Nakanishi, N., Rahman, M. M., Kobayashi, K., Hori, H., Hase, T., Park, S.-Y., and Tsubaki, M. (2008) Site-directed mutagenesis analysis on the transmembrane electron transfer reactions catalyzed by *Zea mays* cytochrome b_{561}, *Biochemistry (to be*

submitted).

33. Lakshminarasimhan, M., Bérczi, A., and Asard, H. (2006) Substrate-dependent reduction of a recombinant chromaffin granule Cyt-*b*561 and its R72A mutant, *Acta Biol. Szeged*. **50**, 61-65.
34. Bérczi, A., and Asard, H. (2006) Characterization of an ascorbate-reducible cytochrome b_{561} by site-directed mutagenesis, *Acta Biol. Szeged*. **50**, 55-59.
35. Laemmli, U. K. (1970) Cleavage of structural proteins during the assembly of the head of bacteriophage T_4, *Nature*. **227**, 680-685.
36. Markwell, M. A. K., Haas, S. M., Tolbert, N. E., and Bieber, L. L. (1981) Protein determination in membrane and lipoprotein sampled: Manual and automated procedures, *Methods Enzymol*. **72**, 296-303.
37. Takeuchi, F., Hori, H., and Tsubaki, M. (2005) Selective perturbation of the intravesicular heme center of cytochrome b_{561} by cysteinyl modification with 4, 4'-dithiodipyridine, *J. Biochem*. **138**, 751-762.
38. Miles, E. W. (1977) Modification of histidyl residues in proteins by diethylpyrocarbonate, *Methods Enzymol*. **47**, 431-442.
39. Williams, N. H., and Yandell, J. K. (1982) Outer-sphere electron-transfer reactions of ascorbate anions, *Aust. J. Chem. 35*, 1133-1144.
40. Creutz, C. (1981) The complexities of ascorbate as a reducing agent, *Inorg. Chem*. **20**, 4449-4452.
41. Sharp, K. H., Mewies, M., Moody, P. C. E., and Raven, E. L. (2003) Crystal structure of the ascorbate peroxidase-ascorbate complex, *Nat. Struct. Biol*. **10**, 303-307.
42. Li, S., Taylor, K. B., Kelly, S. J., and Jedrzejas, M. J. (2001) Vitamin C inhibits the enzymatic activity of *Streptococcus pneumoniae* hyaluronate lyase, *J. Biol. Chem*. **276**,

15125-15130.

43. Burmeister, W. P., Cottaz, S., Rollin, P., Vasella, A., and Henrissat, B. (2000) High resolution X-ray crystallography shows that ascorbate is a cofactor for myrosinase and substrates for the function of the catalytic base, *J. Biol. Chem*. **275**, 39385-39393.
44. Linley, P. J., Landsberger, M., Kohchi, T., Cooper, J. B., and Terry, M. J. (2006) The molecular basis of heme oxygenase deficiency in the *pcd1* mutant of pea, *FEBS J*. **273**, 2594-2606.
45. Laroff, G. P., Fessenden, R. W., and Schuler, R. H. (1972) The electron spin resonance spectra of radical intermediates in the oxidation of ascorbic acid and related substances, *J. Am. Chem. Soc*. **94**, 9062-9073.

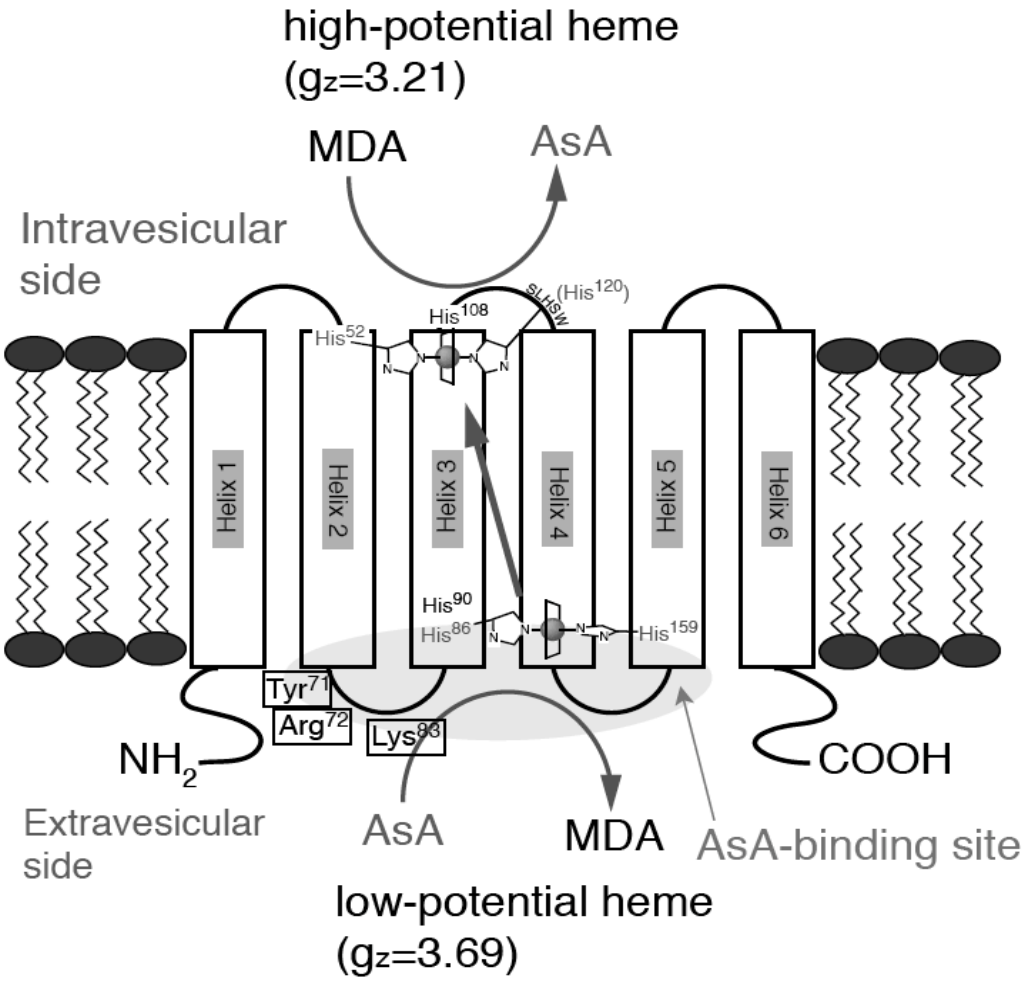

Figure 3-1. The six-transmembrane helices model of *Zea mays* cytochrome b_{561}. *Zea mays* cytochrome b_{561} is considered to have six transmembrane helices and two hemes *b* centers. Two hemes are located on the intravesicular and extravesicular side, respectively, with different EPR characters as indicated based on (*20*). The two well-conserved sequences (ALLVYRVFR, SLHSW) found initially in animal species were predicted as a part of the AsA- and MDA radical-binding site, respectively (*10*). The latter is also well-conserved in plant species and is indicated in a loop connecting helix 3 and 5. On the other hand, the former sequence residing in a loop connecting helix 2 and 3 is partially conserved in plant species. However, both Tyr^{71} and Arg^{72} residues in the sequence are well-conserved and are expected to have important roles for the electron acceptance from AsA together with the well-conserved Lys^{83} residue (*32*).

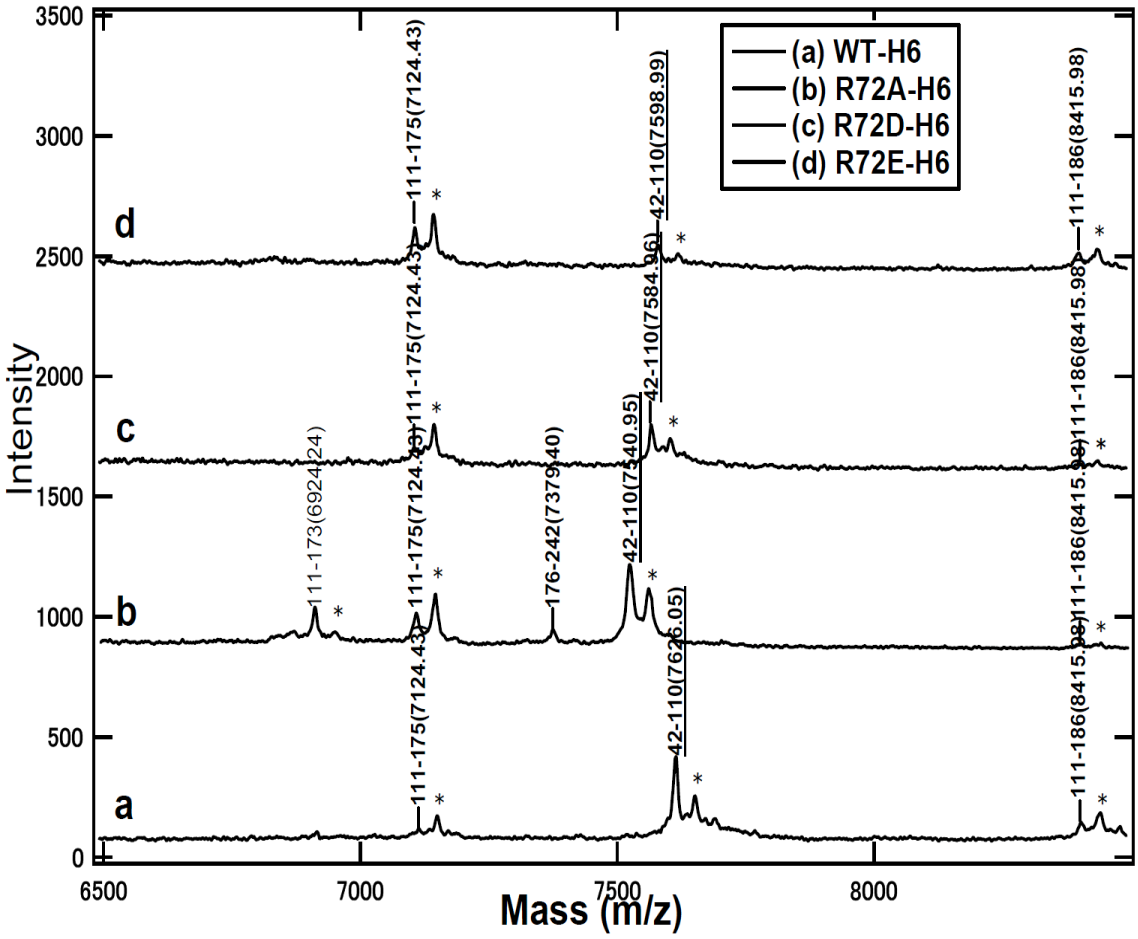

Figure 3-2. Comparison of MALDI-TOF-mass spectra of V8-protease-cleaved peptides from WT-ZMb_{561}-H_6, R72A-H_6, R72D-H_6, and R72E-H_6. Mass spectra of WT-ZMb_{561}-H_6, R72A-H_6, R72D-H_6, and R72E-H_6 being aligned in the region from 6500 to 8500 m/z to visualize the site-specific substitution of the Arg^{72} residue. The peptides containing the mutation site were indicated as underlined. Authentically-cleaved peptides by V8-protease are indicated in boldface. Peaks indicated by asterisk (*) are due to the K^+ ion form $[M+K^+]$ of the molecular ion.

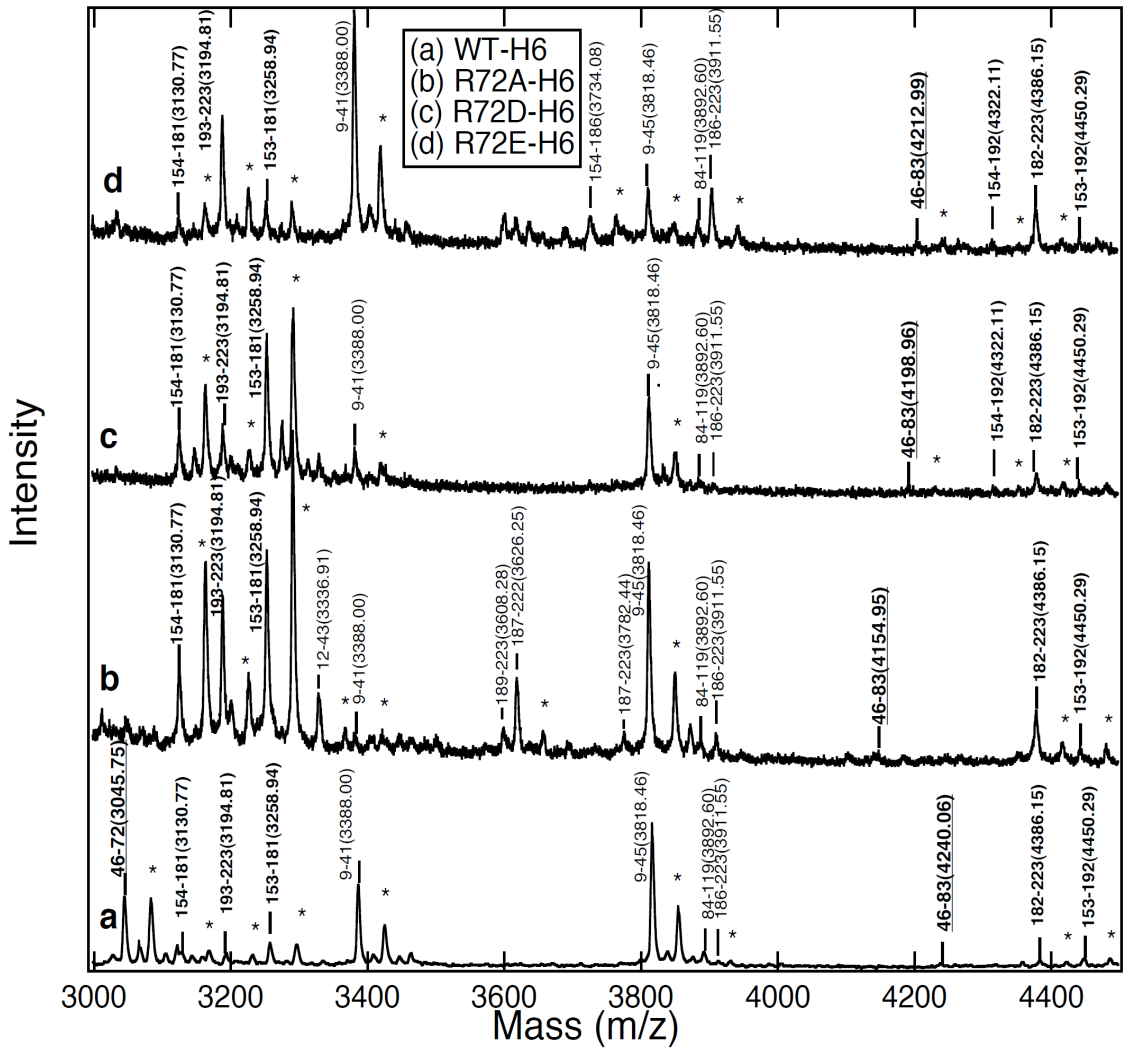

Figure 3-3. Comparison of MALDI-TOF-mass spectra of tryptic peptides obtained from WT-ZM*b*$_{561}$-H$_6$, R72A-H$_6$, R72D-H$_6$, and R72E-H$_6$. Mass spectra of WT-ZM*b*$_{561}$-H$_6$, R72A-H$_6$, R72D-H$_6$, and R72E-H$_6$ being aligned in the region from 3000 to 4500 m/z to visualize the site-specific substitution of the Arg^{72} residue. The peptides containing the mutation site were indicated as underlined. Authentically-cleaved peptides by TPCK-treated trypsin are indicated in boldface. Peaks indicated by asterisk (*) are due to the K^+ ion form [M+K^+] of the molecular ion.

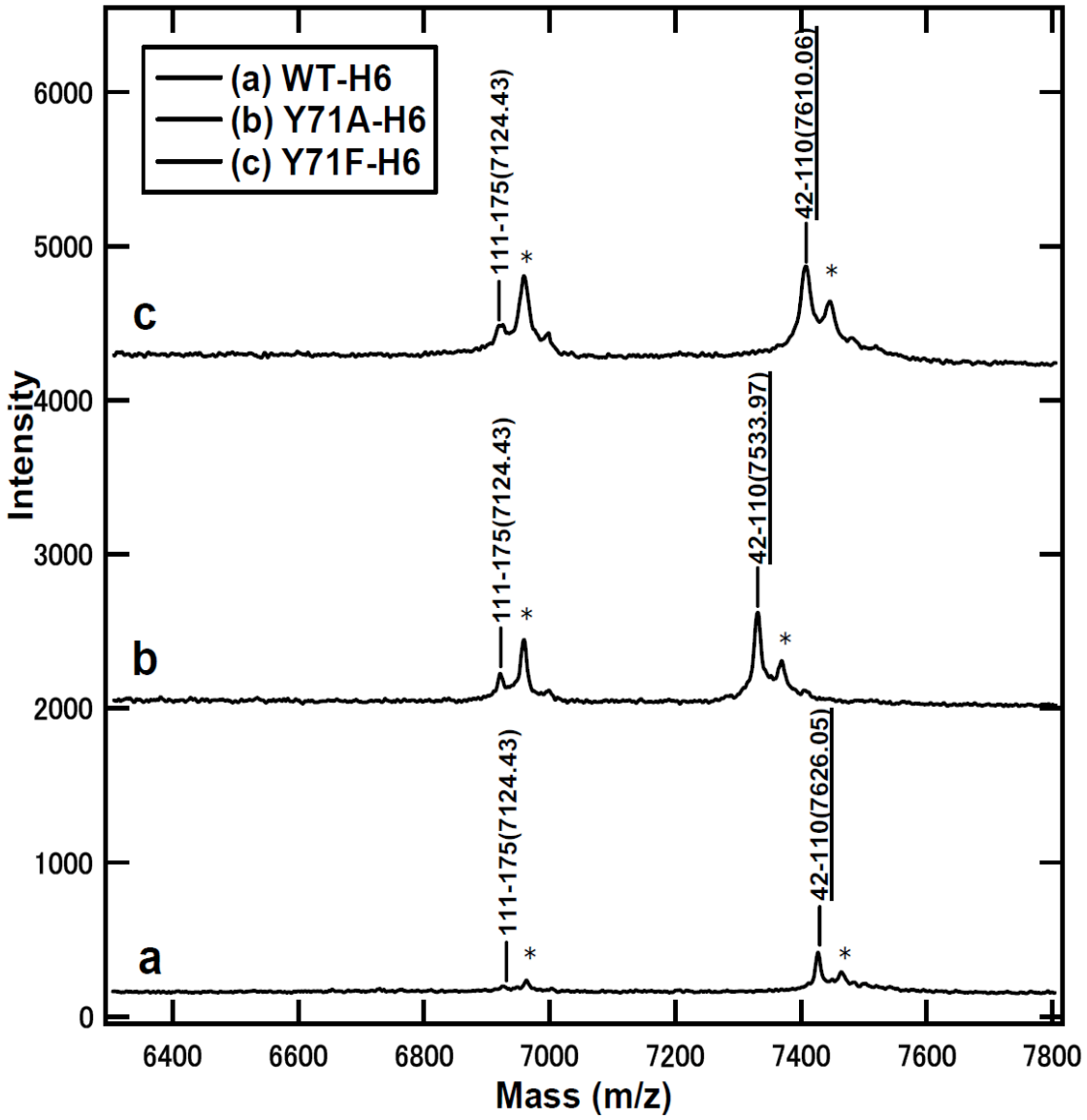

Figure 3-4. Comparison of MALDI-TOF-mass spectra of V8 protease-cleaved peptides from WT-ZM*b*$_{561}$-H$_6$, Y71A-H$_6$, and Y71F-H$_6$. Mass spectra of WT-ZM*b*$_{561}$-H$_6$, Y71A-H$_6$, and Y71F-H$_6$ being aligned in the region from 6300 to 7800 m/z to visualize the site-specific substitution of the Tyr^{71} residue. The peptides containing mutation were indicated as underlined. Authentically-cleaved peptides by V8-protease are indicated in boldface. Peaks indicated by asterisk (*) are due to the K^+ ion form [M+K^+] of the molecular ion.

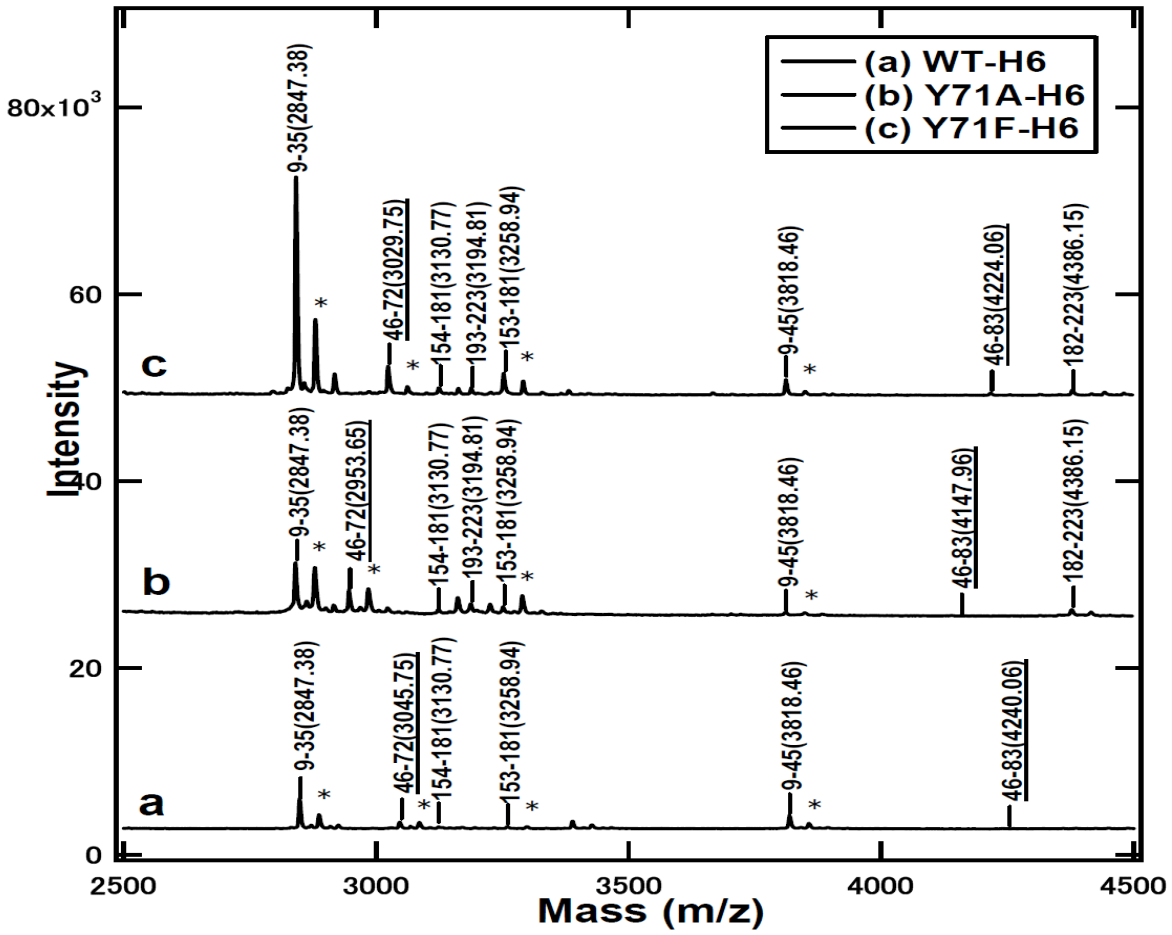

Figure 3-5. Comparison of MALDI-TOF-mass spectra of tryptic peptides obtained from WT-ZM*b*$_{561}$-H$_6$, Y71A-H$_6$, and Y71F-H$_6$. Mass spectra of WT-ZM*b*$_{561}$-H$_6$, Y71A-H$_6$, and Y71F-H$_6$ being aligned in the region from 2500 to 4500 m/z to visualize the site-specific substitution of the Tyr^{71} residue. The peptides containing the mutation site were indicated as underlined. Authentically-cleaved peptides by TPCK-treated trypsin are indicated in boldface. Peaks indicated by asterisk (*) are due to the K^+ ion form [M+K^+] of the molecular ion.

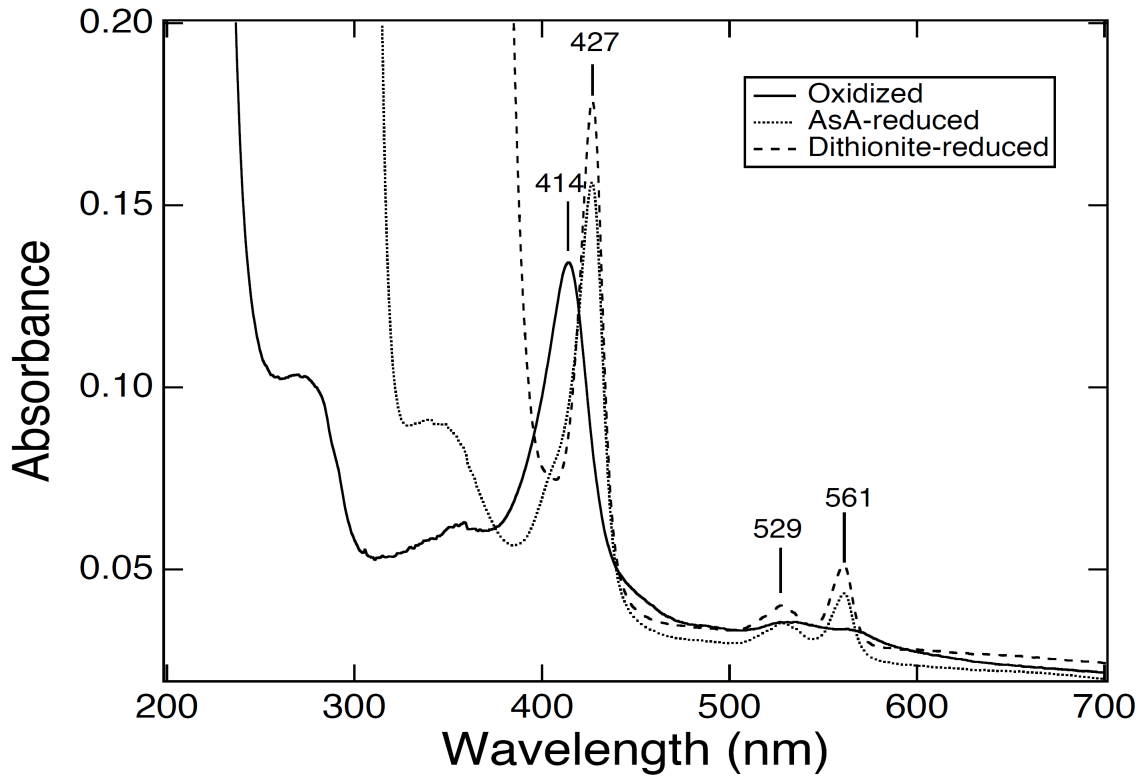

Figure 3-6. **Absorption spectra of oxidized, AsA-reduced and dithionite-reduced forms of R72A-H_6 at pH 7.0.** After 30 min of incubation of R72A-H_6 with AsA (10 mM) in 20 mM Na-phosphate buffer (pH 7.0), 1.0 % (w/v) β-octyl glucoside, its UV-visible absorption spectrum was recorded and was compared with those in oxidized and in dithionite-reduced states.

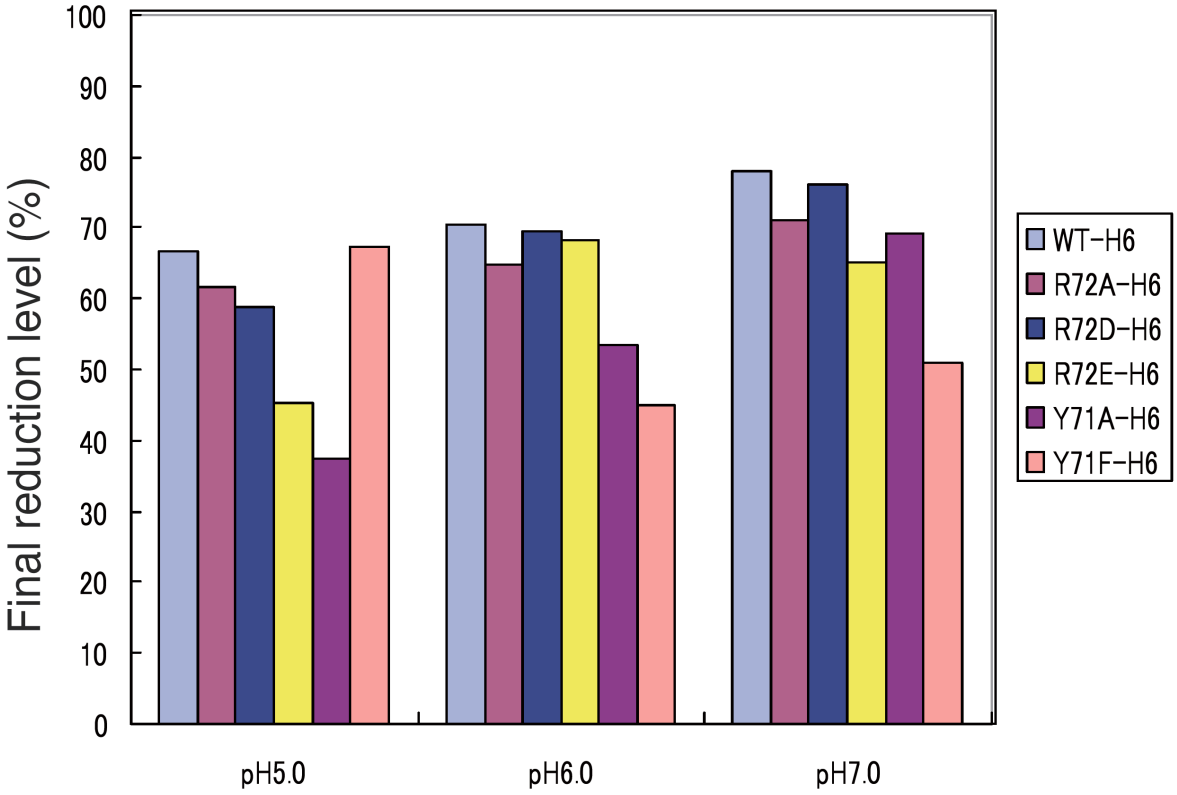

Figure 3-7. Effects of pH change on the final heme reduction levels of WT-ZMb_{561}-H_6 and its mutants using AsA as a reductant. After 30 min of incubation of WT-ZMb_{561}-H_6, R72A-H_6, R72D-H_6, R72E-H_6 and Y71A- H_6 with AsA (10 mM) in buffer containing 1.0 % (w/v) *n*-octyl-β-glucoside with three different pH (5.0, 6.0, and 7.0) at room temperature, their respective UV-visible absorption spectrum was recorded and was compared with those in oxidized and in the dithionite-reduced states. The final heme reduction levels with AsA as a reductant were calculated from the spectra based on the dithionite-reduced form as the 100 % level.

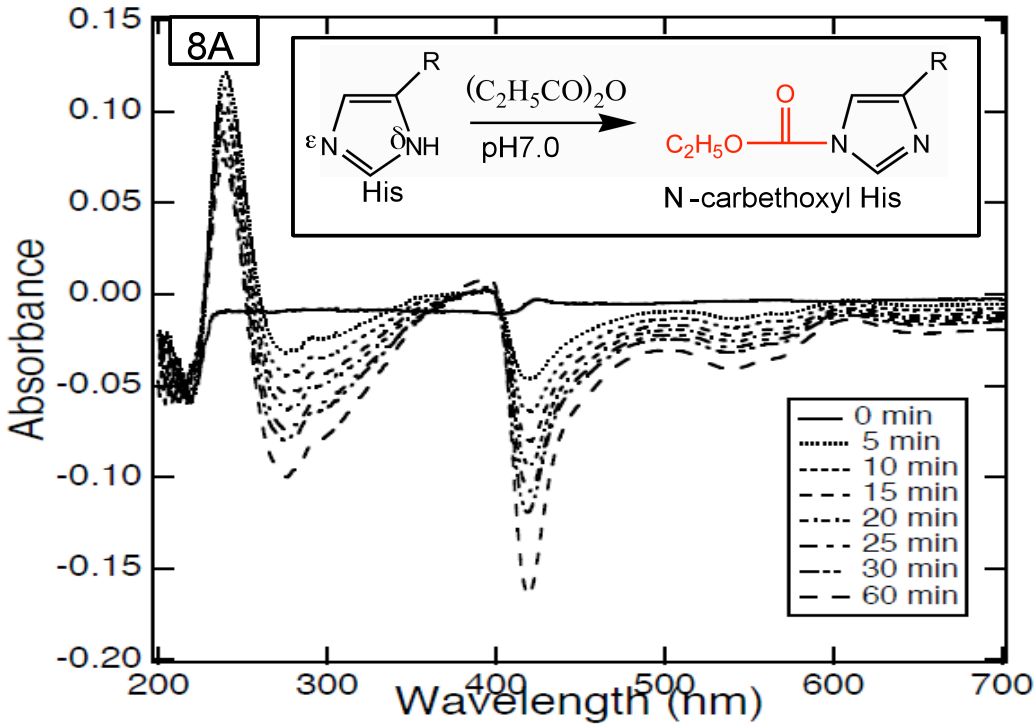
8A
R
$(C_2H_5CO)_2O$
pH7.0
His
N-carbethoxyl His
C_2H_5O
0 min
5 min
10 min
15 min
20 min
25 min
30 min
60 min
Absorbance
Wavelength (nm)

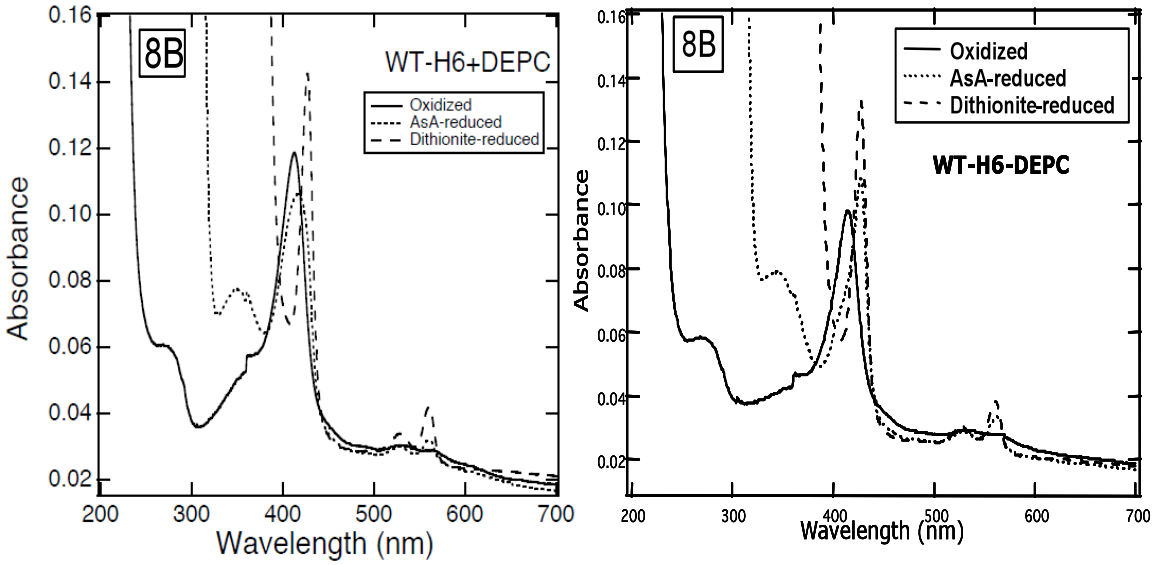
8B
WT-H6+DEPC
Oxidized
AsA-reduced
Dithionite-reduced
Absorbance
Wavelength (nm)
8B
Oxidized
AsA-reduced
Dithionite-reduced
WT-H6-DEPC
Absorbance
Wavelength (nm)

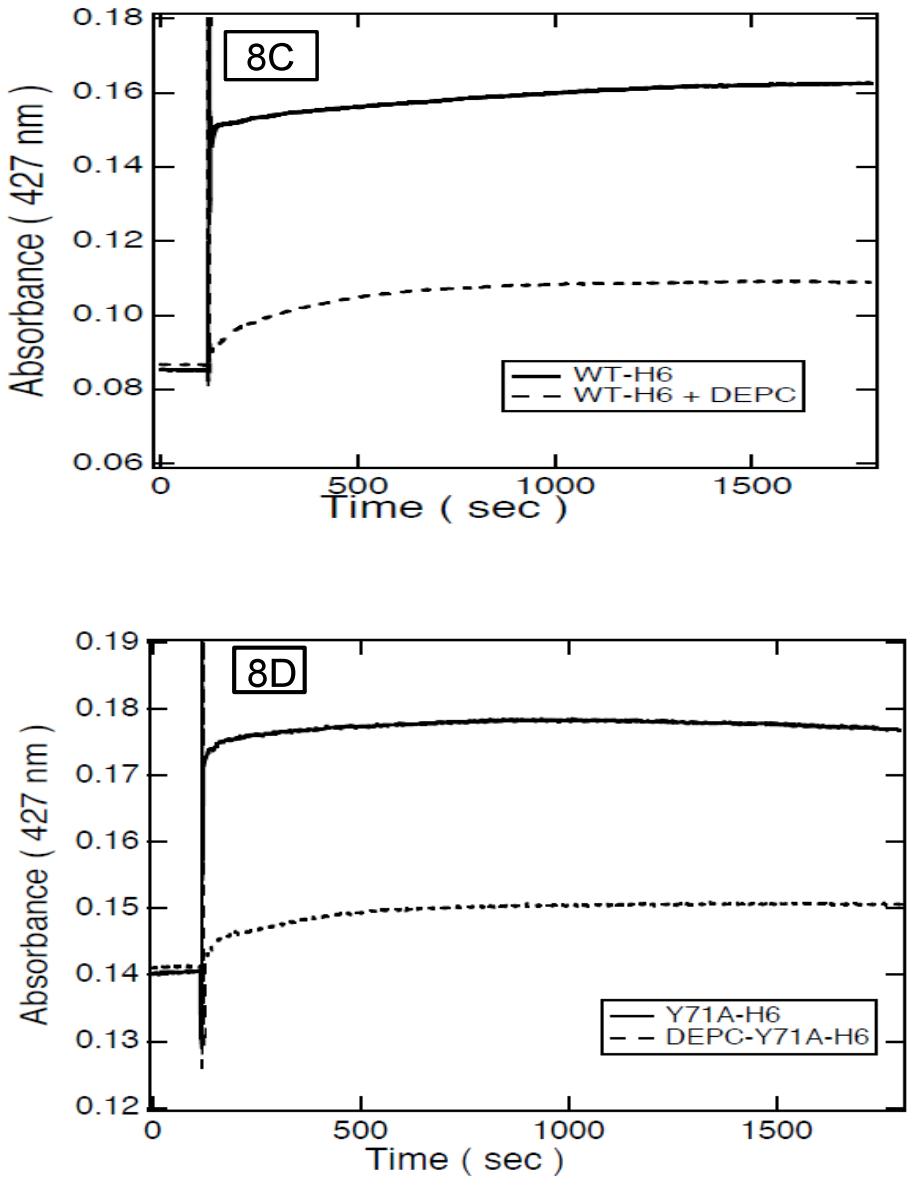

Figure 3-8. Effects of DEPC-treatment on the UV-visible absorption spectra of the purified WT-ZMb_{561}-H_6 and Y71A-H_6. (A) Difference spectral change during the DEPC reaction with the oxidized form of WT-ZMb_{561}-H_6. As the reaction proceeded, the increase in absorbance at 240 nm due to the formation of *N*-carbethoxyl histidine residues was observed. Inset shows a reaction scheme of

DEPC with histidine residue. (B) Absorption spectra of WT-ZMb_{561}-H_6 before and after the DEPC-treatment. Solid line, oxidized state; dotted line, AsA(10 mM)-reduced state; broken line,

dithionite-reduced state. (C) Time course of A_{427} of the DEPC-treated (or untreated) WT-ZMb_{561}-H_6 after mixing with AsA (final 10 mM). (D) Time course of A_{427} of the DEPC-treated (or untreated) Y71A-H_6 after mixing with AsA (final 10 mM).

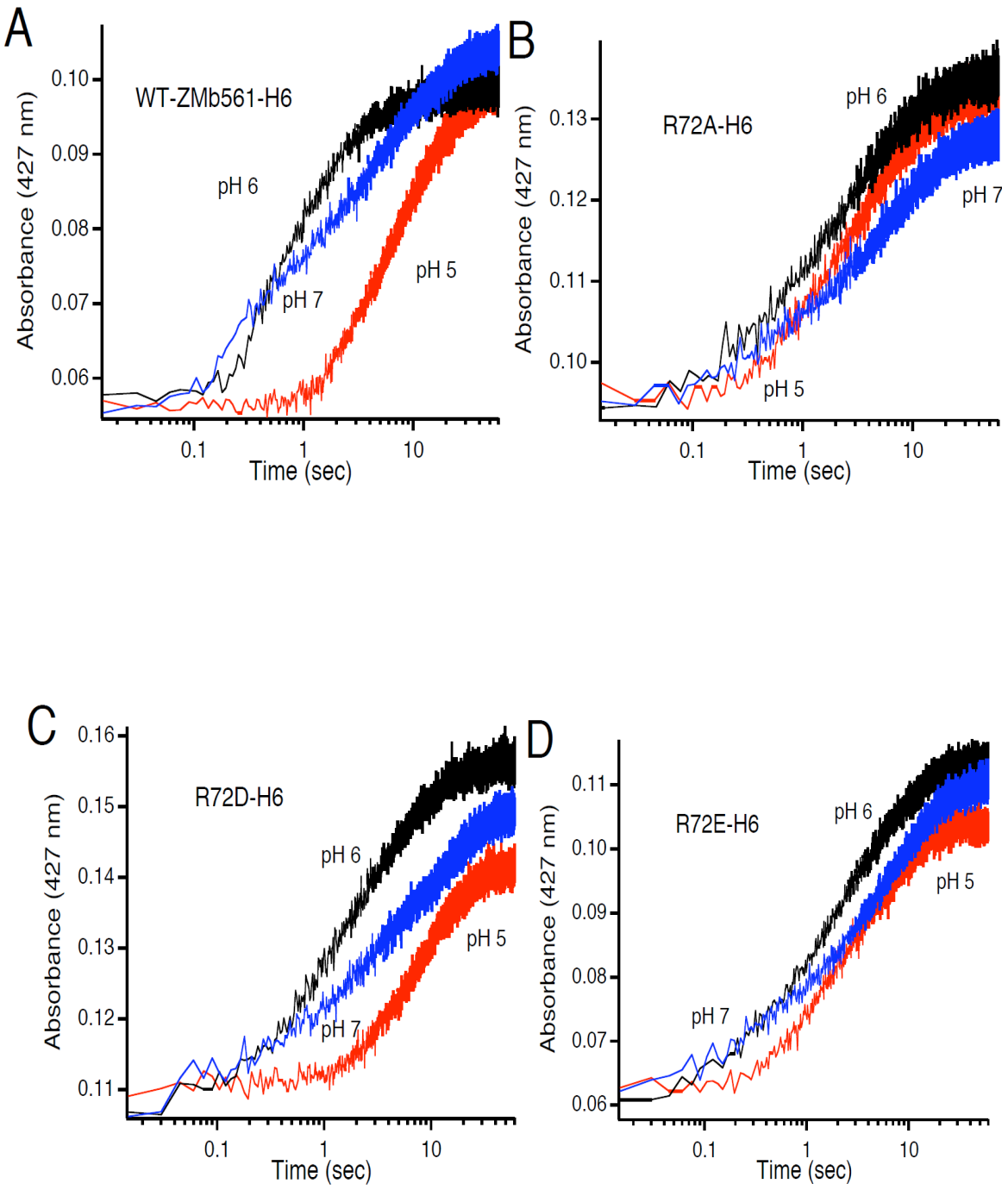

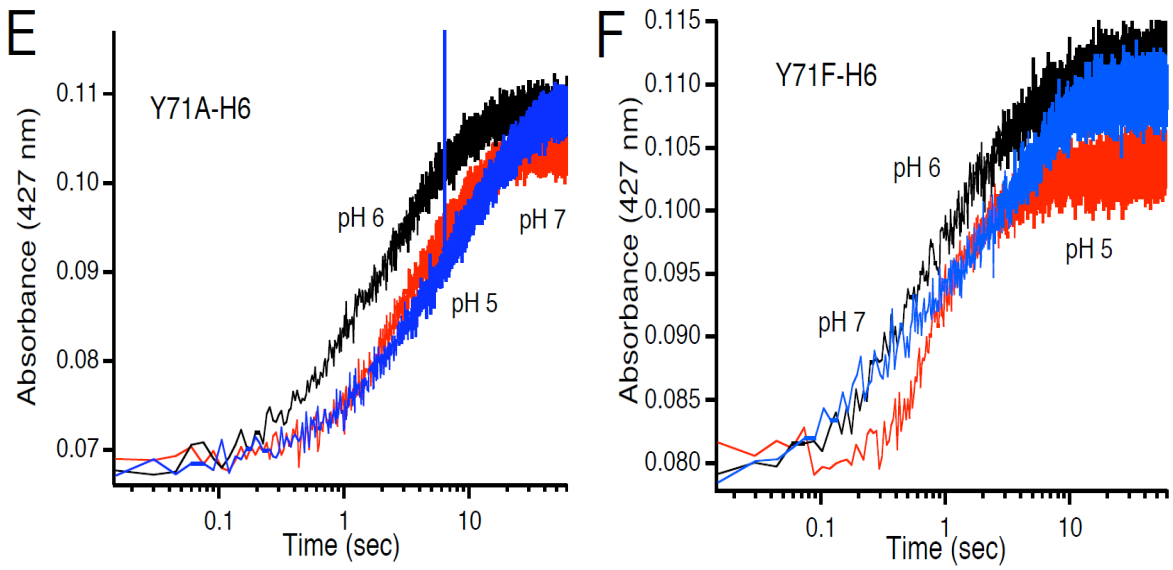

Figure 3-9. Stopped-flow analysis on the electron transfer from AsA for the purified WT-ZMb_{561}-H_6 (A), its R72 mutants (R72A-H_6 (B), R72D-H_6 (C), R72E-H_6 (D)), and its Y71 mutants (Y71A-H_6 (E), Y71F-H_6 (F)) at three different pH. The electron acceptance reactions of oxidized WT-ZMb_{561}-H_6 (and its site-directed mutants) (final, 1 μM) from AsA (final, 2 mM) were measured at 427 nm by stopped-flow spectrometry using two solution mixing system with a 1:1 volume ratio. The absorbance changes were plotted against time in a logarithmic scale. Other conditions including buffer conditions are described in the text.

Table 3-1. Primers used for site-directed mutagenesis of *Zea mays* cytochrome b_{561}

Mutants	Primers	Nucleotide sequences (5' to 3')
R72A-H_6	R72As	CGGTGAAGCTATAATGGTGTACGCGGTACTTCCAACATC
	R72Aa	GATGTTGGAAGTACCGCGTACACCATTATAGCTTCACCG
R72D-H_6	R72Ds	CGGTGAAGCTATAATGGTGTACGACGTACTTCCAACATCG
	R72Da	CGATGTTGGAAGTACGTCGTACACCATTATAGCTTCACCG
R72E-H_6	R72Es	CGGTGAAGCTATAATGGTGTACGAGGTACTTCCAACATC
	R72Ea	GATGTTGGAAGTACCTCGTACACCATTATAGCTTCACCG
Y71A-H_6	Y71As	GCGGTGAAGCTATAATGGTGGCCAGGGTACTTCCA
	Y71Aa	TGGAAGTACCCTGGCCACCATTATAGCTTCACCGC
Y71F-H_6	Y71Fs	GCGGTGAAGCTATAATGGTGTTCAGGGTACTTCCA
	Y71Fa	TGGAAGTACCCTGAACACCATTATAGCTTCACCGC

Underlines indicate the mutation sites.

Table 3-2. Theoretical tryptic fragments of the recombinant *Zea mays* cytochrome b_{561} and its site-directed mutants at Arg^{72} position

Num	From-To	MH^+	Sequence
1	1- 8	803.02	MGLGLGVR
2	9- 35	2848.39	AAPFTYAAHALAVAAAAMVLVWSIQFR
3	36- 45	990.10	GGLAIESTNK
4	46- 72	3046.76	NLIFNV**H**PVLMLIGYVIIGGEAIMVY**R**
(4+5'	46-83	4155.96	NLIFNV**H**PVLMLIGYVIIGGEAIMVYAVLPTSNHDTTK) (for R72A)
(4+5''	46-83	4199.97	NLIFNV**H**PVLMLIGYVIIGGEAIMVYDVLPTSNHDTTK) (for R72D)
(4+5'''	46-83	4213.99	NLIFNV**H**PVLMLIGYVIIGGEAIMVYEVLPTSNHDTTK) (for R72E)
5	73- 83	1213.33	VLPTSNHDTTK
6	84-106	2480.10	LI**H**LILHGIALVLGAVGIYFAFK
7	107-152	5066.82	NHNESGIANLYSL**H**SWIGIGTITLYGIQWIIGFVTFFFPGAAPNVK
8	153-153	147.20	K
9	154-181	3131.77	GVLPW**H**VLFGLFVYILALANAELGFLEK
10	182-192	1210.37	LTFLESSGLDK
11	193-223	3195.81	YGTEAFLVNFTALVVVLFGASVVVAAIAPVR
12	224-242	2324.44	LEEPQGYDPIPENHHHHHH

Theoretical tryptic peptides based on the deduced amino acid sequence of the recombinant *Zea mays* cytochrome b_{561} and its site-directed mutants at the Arg^{72} position are shown. Two pairs of the heme axial residues (His^{52} and His^{120}; His^{86} and His^{159}) are indicated in boldface and Arg^{72} is in boldface and underlined. The peptides 4+5', 4+5'', and 4+5''' are derived from R72A-H_6, R72D- H_6 and R72E- H_6, respectively.

Table 3-3. Theoretical V8-protease cleaved fragments of the recombinant *Zea mays* cytochromes b_{561} and its site-directed mutants at Arg^{72} position.

Num	From-To	MH^+	Sequence	
1	1- 41	4173.00	MGLGLGVRAAPFTYAAHALAVAAAAMVLVWSIQFRGGLAIE	
2	42- 66	2743.29	STNKNLIFNV**H**PVLMLIGYVIIGGE	
3	67- 80	1616.88	AIMVY**R**VLPTSNHD	
(3’	67-80	1531.77	AIMVYAVLPTSNHD)	(for R72A)
(3-1’	67-72	711.86	AIMVYD)	(for R72D)
(3-1’’	67-72	725.88	AIMVYE)	(for R72E)
(3-2’	73-80	882.95	VLPTSNHD)	(for R72D and R72E)
4	81-110	3304.95	TTKLI**H**LILHGIALVLGAVGIYFAFKNHNE	
5	111-175	7125.44	SGIANLYSL**H**SWIGIGTITLYGIQWIIGFVTFFFPGAAPNVKKGV LPW**H**VLFGLFVYILALANAE	
6	176-180	578.69	LGFLE	
7	181-186	750.91	KLTFLE	
8	187-191	478.48	SSGLD	
9	192-196	597.65	KYGTE	
10	197-235	4113.83	AFLVNFTALVVVLFGASVVVAAIAPVRLEEPQGYDPIPE	
11	236-242	955.97	NHHHHHH	

Theoretical V8 protease-digested peptides based on the deduced amino acid sequence of the recombinant *Zea mays* cytochrome b_{561} and its site-directed mutants are shown. Two pairs of the heme axial residues (His^{52} and His^{120}; His^{86} and His^{159}) are indicated in boldface and Arg^{72} is in boldface and underlined. The peptides 3’, 3-1’, and 3-1’’ are derived from R72A-H_6, R72D- H_6 and R72E- H_6, respectively. The peptide 3-2’ are derived from both R72D- H_6 and R72E- H_6.

Table 3-4. Theoretical tryptic fragments of the recombinant *Zea mays* cytochrome b_{561} and its site-directed mutants at Tyr^{71} position

Num	From-To	MH^+	Sequence	
1	1- 8	803.02	MGLGLGVR	
2	9- 35	2848.39	AAPFTYAAHALAVAAAAMVLVWSIQFR	
3	36- 45	990.10	GGLAIESTNK	
4	46- 72	3046.76	NLIFNV**H**PVLMLIGYVIIGGEAIMV**Y**R	
(4’	46-72	2954.66	NLIFNV**H**PVLMLIGYVIIGGEAIMVAR)	(for Y71A)
(4’’	46-72	3030.76	NLIFNV**H**PVLMLIGYVIIGGEAIMVFR)	(for Y71F)
5	73- 83	1213.33	VLPTSNHDTTK	
6	84-106	2480.10	LI**H**LILHGIALVLGAVGIYFAFK	
7	107-152	5066.82	NHNESGIANLYSL**H**SWIGIGTITLYGIQWIIGFVTFFFPGAAPNVK	
8	153-153	147.20	K	
9	154-181	3131.77	GVLPW**H**VLFGLFVYILALANAELGFLEK	
10	182-192	1210.37	LTFLESSGLDK	
11	193-223	3195.81	YGTEAFLVNFTALVVVLFGASVVVAAIAPVR	
12’	224-242	2324.44	LEEPQGYDPIPENHHHHHH	

Theoretical tryptic peptides based on the deduced amino acid sequence of the recombinant *Zea mays* cytochrome b_{561} and its site-directed mutants at the Tyr^{71} position are shown. Two pairs of the heme axial residues (His^{52} and His^{120}; His^{86} and His^{159}) are indicated in boldface and Tyr^{71} is in boldface and underlined. The peptides 4’ and 4’’ are derived from Y71A-H_6 and Y71F- H_6, respectively.

Table 3-5. Theoretical V8-protease cleaved fragments of the recombinant *Zea mays* cytochromes b_{561} and its site-directed mutants at Tyr^{71} position.

Num	From-To	MH^+	Sequence
1	1- 41	4173.00	MGLGLGVRAAPFTYAAHALAVAAAAMVLVWSIQFRGGLAIE
2	42- 66	2743.29	STNKNLIFNV**H**PVLMLIGYVIIGGE
3	67- 80	1616.88	AIMV**<u>Y</u>**RVLPTSNHD
(3'	67-80	1524.78	AIMVARVLPTSNHD) (for Y71A)
(3''	67-80	1600.88	AIMVFRVLPTSNHD) (for Y71F)
4	81-110	3304.95	TTKLI**H**LILHGIALVLGAVGIYFAFKNHNE
5	111-175	7125.44	SGIANLYSL**H**S<u>W</u>IGIGTITLYGIQWIIGFVTFFFPGAAPNVKKGV LPW**H**VLFGLFVYILALANAE
6	176-180	578.69	LGFLE
7	181-186	750.91	KLTFLE
8	187-191	478.48	SSGLD
9	192-196	597.65	KYGTE
10	197-235	4113.83	AFLVNFTALVVVLFGASVVVAAIAPVRLEEPQGYDPIPE
11	236-242	955.97	NHHHHHH

Theoretical V8 protease-digested peptides based on the deduced amino acid sequence of the recombinant *Zea mays* cytochrome b_{561} and its site-directed mutants at the Tyr^{71} position are shown. Two pairs of the heme axial residues (His^{52} and His^{120}; His^{86} and His^{159}) are indicated in boldface and Tyr^{71} is in boldface and underlined. The peptide 3' is derived from Y71A-H_6; whereas peptide 3'' is derived from Y71F-H_6.

Table 3-6. Apparent rate constants for the heme reduction of wild-type *Zea mays* cytochrome b_{561} and its site-directed mutants with ascorbate (AsA) as a reductant.

pH		WT-ZMb_{561}-H_6	R72A-H_6	R72D-H_6	R72E-H_6	Y71A-H_6	Y71F-H_6
5	10sec	0.137	0.357	0.146	0.355	0.285	1.009
		(0.002)	(0.003)	(0.003)	(0.002)	(0.002)	(0.001)
	60sec	0.109	0.194	0.108	0.203	0.205	0.739
		(0.001)	(0.001)	(0.001)	(0.001)	(0.001)	(0.011)
6	10sec	0.862	0.439	0.449	0.428	0.425	0.703
		(0.005)	(0.003)	(0.003)	(0.005)	(0.002)	(0.006)
	60sec	0.656	0.232	0.249	0.224	0.290	0.482
		(0.007)	(0.002)	(0.002)	(0.002)	(0.002)	(0.007)
7	10sec	0.438	0.284	0.230	0.280	0.213	0.395
		(0.004)	(0.003)	(0.002)	(0.003)	(0.002)	(0.004)
	60sec	0.140	0.132	0.099	0.135	0.105	0.289
		(0.001)	(0.001)	(0.001)	(0.001)	(0.001)	(0.003)

Apparent first order rate constants (k_{app} (sec^{-1})) and their standard deviations (σ, in parenthesis) at three different pH corresponding to the data represented in Figure 6 (final AsA concentration, 2.0 mM) are shown in two different time domains (10 and 60 sec). Both Igor Pro software (v. 6.03) and a built-in software of the stopped-flow apparatus were used for the calculation with assuming a single exponential decay for the initial 10 and 60 sec after the mixing. Both methods showed very similar values each other and the round values obtained from Igor Pro software were tabulated.

Chapter 4

Conclusions

My work during the last three years focused on the study of a family of transmembrane proteins, cytochrome b_{561}. Because of the high abundance of native chromaffin granule (CG) cytochrome b_{561} and the availability of its expression and purification techniques, the nature of CG cytochrome b_{561} has been characterized to some extent. The situation for the studies on plant cytochrome b_{561} was very different from that of CG cytochrome b_{561}. It was almost impossible to purify plant cytochrome b_{561} directly from plant tissues due to its lower expression level. To study their biochemical properties in details, heterologous expression of the recombinant cytochrome b_{561} might be essential. Therefore, we decided to exploit a heterologous expression system different from that using *Escherichia coli* cells to study the plant cytochrome b_{561}. The use of the methyltrophic yeast, *Pichia pastoris,* as a cellular host for the expression of recombinant proteins has become increasingly popular in recent days. *Pichia pastoris* is much easier to genetically manipulate and to culture than mammalian cells and can be grown to high cell densities under the control of alcohol oxidase (AOX1) promoter. Previously, our group had succeeded in molecular cloning of cytochrome b_{561} cDNA from corn *Zea mays*, its functional heterologous expression in *Pichia pastoris* cells, and its purification. The aims of my Ph.D. study were belonged in two different categories. The first one was to extend the heterologous expression system for a better yield in the expression level and a better purification method. The second one was, using such purified sample, to elucidate the molecular mechanism underlying the possible AsA-specific transmembrane electron transfer catalyzed by *Zea mays* cytochrome b_{561} using various molecular biological and biochemical techniques. The major findings in my Ph.D. study are summarized below.

In the first part of my study (as described in Chapter 2), I have succeeded in the

construction of heterologous expression system of recombinant *Zea mays* cytochrome b_{561}, in which the 6×His-tag moiety was introduced at the COOH-terminus of the full-length *Zea mays* cytochrome b_{561}. I have also succeeded in its purification to a highly homogenous state. The recombinant *Zea mays* cytochrome b_{561} (WTZMb_{561}-His_6) showed characteristics visible absorption spectra very similar to those of bovine cytochrome b_{561} and WTZMb_{561}. SDS-PAGE and Western blotting analyses of purified WTZMb_{561}-His_6 showed a single band at 26.2 kDa. Stopped-flow analyses suggested that wild-type *Zea mays* cytochrome b_{561} utilizes AsA as a physiological electron donor. Pre-treatment of the purified WTZMb_{561}-His_6 with dietylpyrocarbonate (DEPC) in the oxidized form caused a drastic inhibition of the electron transfer from AsA and such inhibition was protected by the presence of AsA during the treatment. These results suggested that plant cytochrome b_{561} might perform an AsA-related transmembrane electron transfer reaction by utilizing a similar molecular mechanism with that of bovine cytochrome b_{561}. Thus, our *Pichia pastoris* expression system offers an improvement in the yield and the quality and other advantages over the existing insect and yeast expression systems for producing membraneous cytochromes b_{561} for the detailed studies concerning their structures and functions.

In the second part of my study (as described in Chapter 3), I focused on the investigation using the site-directed mutagenesis techniques to clarify the roles of the highly conserved amino acid residues in a conserved motif of *Zea mays* cytochrome b_{561}. The conserved motif, located near the electron accepting (low potential) heme center, was suggested to play a role in the AsA-binding. Indeed, covalent modifications with DEPC and the site-directed mutations on the conserved Lys (K83) residue near this

motif resulted in a significant decrease of the electron accepting ability from AsA. Thus, we hypothesized that well-conserved residues (Y71 and R72) locating in this motif could play an important role in the AsA-binding and the electron transfer. Therefore, I generated several site-directed mutants (Y71A, Y71F, R72A, R72D, and R72E) at these sites. The visible absorption spectra of all these mutants were very similar to those of WTZMb_{561}-His_6, although the final reduction levels with AsA as a reductant were somewhat different each other. The effects of changing pH on the reduction processes with AsA of oxidized WTZMb_{561}-His_6 and of these mutants were examined by stopped-flow techniques. We found that the time course of the reduction of WTZMb_{561}-His_6 was very dependent on the medium pH. In a higher pH, the reduction process was very fast; whereas in a lower pH, the reduction process became very slow, as previously observed for bovine cytochrome b_{561}. This pH-dependent time-lag was almost completely lost for the R72A, R72E, and Y71A mutants. Further, for the Y71F mutant, there was a clear acceleration of the electron transfer from AsA. These results suggested that both Y71 and R72 residues have some important roles, but very different from that of K83 residue, upon the electron transfer event from AsA.

To verify our present proposal, however, a detailed crystallographic structural data on cytochrome b_{561} might be highly necessary. With such information including substrate binding site, interacting residues, and possible electron transfer pathways to the heme center and between the two heme centers, several important questions about the molecular mechanism working in *Zea mays* cytochrome b_{561}, which we postulated as "concerted H^+/e^- transfer mechanism" at the cytosolic heme center, will be solved.

Acknowledgements

Without the supports from many people, completion of my Ph.D. dissertation would not be possible. Above all, I would like to express my best regards, deep indebtedness and sincere gratitude to my reverend advisor, Dr. Motonari Tsubaki, Professor of Department of Chemistry, Graduate School of Science, Kobe University, for his close and constant supervision of the research, excellent guidance, continuous encouragements and various supports during my study and research. Throughout my three years' research in his lab, he encouraged me to develop independent thinking and research skills. I deeply appreciate his valuable advices, discussions and revisions on my papers and dissertation.

My coworkers in the lab provided a helpful and stimulating atmosphere. I especially want to thank my good friend Dr. Nobuyuki Nakanishi, for teaching me about cell culture, microsomes preparation, protein purification, and furthermore patiently listening to my day to day minutiae occurred during my research. I am really grateful to him forever.

My warmest appreciation to the students who were already a member of the Tsubaki lab and help me to get started: Mr. Jun Hamada, Ms. Maiko Shibuya, Ms. Yuka Nishimura, Ms. Yoshimi Mushika, and Mr. Qu Peng. The students who joined later were also helpful: Ms. Aya Muraki, Ms. Mariko Yoshida, Mr. Masamitsu Fujito, Ms. Mariam Recuenco, Mr. Masahiro Shimazaki, Mr. Takaaki Murakami, Mr. Masahiro Miura, Ms. Tomomi Aono, Ms. Mina Kamei, and Mr. Youichi Sakamoto.

Finally, I would like to acknowledge the help of a postdoctoral fellow, Dr.

Fusako Takeuchi. I especially want to thank her for teaching me repeatedly about basic lab techniques and for her cooperation's.

I am very grateful to the additional members of my thesis committee, Professor Keisuke Tominaga and Professor Tetsuro Mimura, Graduate School of Science and Technology, Kobe University for their time spent reviewing my thesis and providing me with many valuable suggestions.

My acknowledgement is extended to the Ministry of Education, Science, Sports and Culture (Monbukagakusho) of Japan for the Scholarship contributed to my study in Japan and this research work as well.

I am greatly indebted to my late mother who passed away last year and my sisters for their love, support and continued encouragement throughout my life. Most especially I would like to thank my wife, Lipi. Without her understanding, patience, encouragement, and I could not have completed this work.